The Construction and Characterization of a Synthetic SARS VLP Comprised of Betacoronavirus Consensus Sequence-Encoded Viral Components

by

Andrew Ng

A thesis
presented to the University of Waterloo
in fulfillment of the
thesis requirement for the degree of
Master of Science
in
Pharmacy

Waterloo, Ontario, Canada, 2022

© Andrew Ng 2022

Author's Declaration

I hereby declare that I am the sole author of this thesis. This is a true copy of the thesis, including any required final revisions, as accepted by my examiners.

I understand that my thesis may be made electronically available to the public.

Abstract

In 2019, a novel coronavirus called severe acute respiratory syndrome coronavirus 2 (SARS-CoV-2) emerged from Wuhan, China leading to the COVID-19 pandemic. Although there was an outbreak of severe acute respiratory syndrome coronavirus (SARS-CoV) and Middle Eastern respiratory syndrome coronavirus (MERS-CoV) in 2003 and 2012, respectively, a vaccine against the two SARS viruses were not given high priority due to low interest. The lack of investment into a SARS vaccine in the past has placed researchers in the position to race against time to produce a COVID-19 vaccine in a span of several months. The three coronavirus outbreaks and the emergence of several strains of COVID-19 suggests that future outbreaks are inevitable. Although the COVID-19 pandemic is still a concern, the time to start preparing for the next pandemic-causing coronavirus is now. A "universal vaccine", which may provide cross-protective abilities, may be a highly effective approach in the protection against current and future coronaviruses, removing the need to generate new vaccines to address each emerging strain or variant. Universal vaccines function by relying on viral components that are highly conserved among various strains. A consensus sequence, which is a single sequence that represents several related sequences, may function to confer universal protection. Virus-like particles (VLPs) have been shown to be a highly safe and promising vaccine platform that can mimic the native virus and activate an immune response comparable to natural infections. This project will explore whether a consensus sequence based on the similarities of SARS-CoV, MERS-CoV and SARS-CoV-2, including its emerging variants, can produce a viable VLP that assembles to serve as a potential cross-protective vaccine candidate.

Acknowledgements

I would like to express my gratitude to my supervisors, Dr. Roderick Slavcev and Dr. Marc Aucoin for giving me the opportunity to pursue this degree in their lab. I was extremely fortunate to receive guidance and advice from the both of you. Thank you for all of the comments and support.

I am grateful to have been a part of two amazing labs. I would like to thank all of my lab mates in the Slavcev Lab (Dr. Shirley Wong, Debbie Pushparajah, Rohini Prakash, Jesse St. Jean, Heba Alattas, Merium Fernando, and Harika Nagireddy) and the Aucoin lab (Dr. Mark Bruder, Dr. Faranak Mavandadnejad, Madhuja Chakraborty, Scott Boegel, Lisa Nielsen, Dr. Chris Nogueira, Jacqueline Powichrowski, Aaron Yip, and Sara Haghayegh Khorasani) for making the lab such a great and friendly environment. I have learned a lot from all of you and appreciate all the knowledge, insights, and advice I have received.

I would also like to thank the Dixon Lab (Tania Rodriguez Ramos) for allowing me to conduct experiments in this lab and Doxey Lab (Jennifer Aguiar) for providing me with the consensus sequences needed to conduct this work.

Lastly, I would like to thank my family and friends who have given me constant encouragement and support.

Table of Contents

List of Figures x

List of Tables xii

List of Abbreviations xiii

Chapter 1: Introduction 1

1.1 Rationale of the work 3

1.1.1 Hypothesis 5

1.1.2 Objectives 5

Chapter 2: Literature Review 6

2.1 Coronaviruses 6

2.2 SARS-CoV-2 7

2.2.1 SARS CoV-2 Variants 11

2.3 SARS-CoV, MERS-CoV and SARS-CoV-2 14

2.4 Vaccines against SARS Betacoronaviruses 16

2.4.1 Routes of Administration 18

2.4.2 Adjuvants 19

2.4.3 Antibody-Dependant Enhancement 22

2.5 Universal Vaccines 23

2.6 Virus-Like Particles as a Vaccine Candidate 25

2.6.1 SARS VLPs 30

2.6.2 VLP Production Platforms 32

2.7 Baculovirus 33

2.7.1 IC-BEVS 36

2.7.2 IC-BEVS for VLP Production 37

2.7.3 Bac-to-Bac BEVS 38

Chapter 3: Materials and Methods 40

3.1 Cell Culture Maintenance 40

3.2 Construction of SARS-CoV-2 and Universal S, E and M plasmids for IC-BEVS 40

3.3 Production and Amplification of Recombinant Baculoviruses 41

3.3.1 Production of Competent DH10Bac *E. coli* Cells 41

3.3.2 Transformation of *E. coli* 41

3.3.3 Isolation of Recombinant Bacmid....42

3.3.4 Transfection of *Sf9* Cells and P0 Baculovirus Production....43

3.3.5 Amplification of P0 to P1 Baculovirus Stock....44

3.4 Determination of Baculovirus Titers using End-point Dilution Assay....44

3.5 Production of SARS VLPs....44

3.6 Tracking Cell Infection....45

3.6.1 Cell Density and Viability....45

3.6.2 Flow Cytometry Analysis....45

3.7 Semi-purification of SARS-CoV-2 VLPs....46

3.7.1 Sucrose Cushion Ultracentrifugation....46

3.7.2 Iodixanol Density Gradient Ultracentrifugation....46

3.8 Characterization and Visualization of SARS VLPs and Baculoviruses....47

3.8.1 Sodium Dodecyl Sulfate – Polyacrylamide Gel Electrophoresis (SDS-PAGE)/Western Blot Analysis...47

3.8.2 Sandwich Enzyme-Linked Immunosorbent Assay (ELISA)....48

3.8.3 Detection of Baculoviruses via Infectious Assay....49

3.8.4 Quantification of Baculovirus Particles using Flow Cytometry....49

3.8.5 Visualization of SARS-CoV-2 VLPs via Transmission Electron Microscopy 50

Chapter 4: Results 51

4.1 Tracking Cell Infection 51

4.2 Detection of SARS-CoV-2 VLPs 55

4.3 Detection of SARS-CoV-2 VLPs and Baculoviruses after Semi-Purification 58

4.4 Visualization of SARS-CoV-2 VLPs 66

4.5 Detection of Universal SARS Betacoronavirus VLPs 67

Chapter 5: Discussion 70

5.1 Simple glycosylation patterns from insect cells did not affect SARS-CoV-2 S protein trimerization 70

5.2 SARS-CoV-2 E and M protein can be simultaneously expressed under one promoter using a 2A self-cleaving peptide in *Sf9* insect cells 70

5.3 Baculovirus Expression of SARS-CoV-2 S, E, and M Proteins form VLPs 73

5.4 Purifying and characterizing SARS-CoV-2 VLPs is challenging due to contaminating baculoviruses 75

5.5 Structural proteins (S, E, M) produced from SARS betacoronavirus consensus sequences form universal VLPs 76

Chapter 6: Conclusions and Future Steps 78

6.1 Production and Detection of SARS-CoV-2 VLPs 78

6.2 Downstream Processing of SARS-CoV-2 VLPs 78

6.3 Production and Detection of Universal SARS Betacoronavirus VLPs 79

6.4 Future Steps 80

References 82

Appendices 110

Appendix A: *Sf9* Cell Infection Preliminary Data 110

Appendix B: VLP Constructs 112

Appendix C: Recombinant Bacmid Production 114

Appendix D: VLP Production 116

List of Figures

Figure 1: Genetic layout of SARS-CoV-2. 7

Figure 2: SARS-CoV-2 Virus Morphology 8

Figure 3: Schematic of S protein binding to a host receptor (ACE2) and fusion between host and viral membrane 9

Figure 4: Five SARS-CoV-2 variants of concern (Omicron, Alpha, Beta, Delta, and Gamma) containing spike protein mutations 12

Figure 5: Genomic Structure of SARS-CoV, MERS-CoV, and SARS-CoV-2. 14

Figure 6: Comparison between native SARS-CoV-2 virus particle and SARS-CoV-2 VLP. 26

Figure 7: Schematic of the adaptive immune response stimulated by VLP-based vaccines. ..... .27

Figure 8: Schematic of SARS VLP formation 29

Figure 9: TEM image of SARS-CoV-2 VLPs produced in Sf9 insect cells 32

Figure 10: Morphology of baculoviruses 34

Figure 11: Baculovirus gene expression occurring in the early and late phases 35

Figure 12: Bac-to-Bac BEVS Schematic 39

Figure 13: Iodixanol Density Gradient 47

Figure 14: Sf9 cell density at 24, 48, and 72 hpi 52

Figure 15: Sf9 cell viability at 24, 48, and 72 hpi 53

Figure 16: Flow cytometry analysis of Sf9 cells at 24, 48, and 72 hpi 54

Figure 17: Western blot analysis to detect for SARS-CoV-2 VLPs 57

Figure 18: Western blot analysis to detect for SARS-CoV-2 VLPs and baculoviruses from purified fractions 1-12 59

Figure 19: Schematic of sandwich ELISA 60

Figure 20: Detection of viral particles containing GP64 protein and SARS-CoV-2 spike protein via sandwich ELISA 62

Figure 21: Baculovirus titers calculated for fractions 1-12 based on infectious assay. 63

Figure 22: Quantification of Baculoviruses via SYBR green staining 65

Figure 23: TEM images of purified fraction 4 67

Figure 24: Western blot analysis to detect for universal SARS VLPs 69

List of Tables

Table 1: Function, advantages, and disadvantages of various vaccine platforms. 18

Table 2: Characteristics of various cell lines used for VLP production 33

List of Abbreviations

ACE2	Angiotensin-converting enzyme 2
ADE	Antibody-dependent enhancement
Alum	Aluminum salt-based adjuvants
APCs	Antigen presenting cells
BCRs	B cell receptors
Bp	Base pairs
BVs	Budded virions
CsCl	Cesium chloride
CTLs	Cytotoxic T lymphocytes
D614G	Aspartic acid to glycine point mutation at position 614
DCs	Dendritic cells
DPP4	Dipeptidyl-peptidase 4
E protein	Envelope protein
E. coli	*Escherichia coli*
E484K	Glutamic acid to lysine point mutation at position 484
EPDA	End-point dilution assay
FDA	Food and Drug Administration
FP	Fusion peptide
GSG	Glycine-serine-glycine
HA	Hemagglutinin

hCoV	Human coronavirus
Hpi	Hours post-infection
HIV	Human immunodeficiency virus
IC-BEVS	Insect cell baculovirus expression vector system
IgG	Immunoglobulin G
IgA	Immunoglobulin A
IPTG	Isopropyl beta-d-1-thiogalactopyranoside
IRES	Internal ribosome entry site
K417N	Lysine to asparagine point mutation at position 417
K417T	Lysine to threonine point mutation at position 417
kDa	kiloDalton
M protein	Membrane protein
M1 protein	Matrix 1 protein
M2e	Matrix 2 ectodomain
MERS-CoV	Middle Eastern respiratory syndrome coronavirus
MHC	Major histocompatibility complex
mKOk	Red fluorescent protein-expressing baculovirus
MOI	Multiplicity of infection
NA	Neuraminidase
NAbs	Neutralizing antibodies
N protein	Nucleocapsid protein

NP	Nucleoprotein
Nsp	Non-structural protein
NTA	Nanoparticle tracking analysis
N501Y	Asparagine to tyrosine point mutation at position 501
OB	Occlusion body
OD	Optical density
ODNs	Oligodeoxynucleotides
ODVs	Occlusion derived virions
ORF	Open reading frame
P2A	Porcine teschovirus-1 2A self-cleaving peptide
P6.9mAG	P6.9 monomeric Azami-Green *Sf9* insect cells
PAMPs	Pathogen-associated molecular patterns
PBS	Phosphate-buffered saline
PBS-T	PBS with 0.1% Tween20 detergent
Polh	Polyhedrin
PRRs	Pattern recognition receptors
PTMS	Post-translational modifications
PVDF	Polyvinylidene difluoride
RBD	Receptor binding domain
RBM	Receptor binding motif
RPM	Revolutions per minute

S protein	Spike protein
SARS-CoV	Severe acute respiratory syndrome coronavirus
SARS-CoV-2	Severe acute respiratory syndrome coronavirus 2
SDS-PAGE	Sodium dodecyl-sulfate polyacrylamide gel electrophoresis
Sf9	*Spodoptera frugiperda* clonal isolate 9
Sf21	*Spodoptera frugiperda* clonal isolate 21
TCRs	T cell receptors
TEM	Transmission electron microscopy
Th cells	T helper cells
Th1 cells	Type 1 T helper cells
Th2 cells	Type 2 T helper cells
TLRs	Toll-like receptors
TMD	Transmembrane domain
VLPs	Virus-like particles

Chapter 1: Introduction

Severe acute respiratory syndrome coronavirus 2 (SARS-CoV-2) is a novel coronavirus first identified in Wuhan, China in 2019 and the cause of COVID-19 (World Health Organization, 2021a). This is not the first time an outbreak involving a highly pathogenic coronavirus has occurred, as demonstrated by the severe acute respiratory syndrome coronavirus (SARS-CoV) outbreak in 2003 and the Middle Eastern respiratory syndrome coronavirus (MERS-CoV) outbreak in 2012. SARS-CoV affected over 8,000 individuals and resulted in 774 deaths while MERS-CoV has caused a total of 858 deaths to date (Z. Wu & McGoogan, 2020). As of early November 2022, SARS-CoV-2 has already infected over 630 million individuals and caused over 6.5 million deaths (World Health Organization, 2021b). Unlike the disappearance of SARS-CoV, SARS-CoV-2 is unlikely to undergo the same fate due to its high transmission rate and long incubation periods (Petersen et al., 2020).

The emergence of three highly pathogenic coronaviruses (SARS-CoV, MERS-CoV and SARS-CoV-2) in the last two decades suggests that future outbreaks may be inevitable. As evidenced by the rapid mutations leading to multiple SARS-CoV-2 variants (refer to 2.2.1), it is likely just a matter of time before a new strain with high pandemic potential emerges (CDC, 2021). In fact, a study from the University of Toronto found that antibodies generated from current vaccines against SARS-CoV-2 offer zero protection against the new omicron strains (Kim et al., 2022), suggesting that future variants can potentially emerge and recreate the original disaster. The COVID-19 pandemic, along with those of SARS-CoV and MERS-CoV

have shown us that without an effective vaccine, the global death toll is high, and the economic impact is astronomical as it affects primary, secondary, and tertiary sectors (Nicola et al., 2020).

To date, there are no commercially available vaccines for SARS-CoV and MERS-CoV despite the severity of their associated diseases. The fact that SARS-CoV ceased to exist in 2004 and that MERS was mainly localized to a certain geographical region resulted in a low interest to invest in a vaccine (Padron-Regalado, 2020). In contrast, the COVID-19 pandemic created a sense of urgency to spur on and fund vaccine development due to its global and persistent spread. To date, several vaccines have been authorized for use against SARS-CoV-2 by the Food and Drug Administration in the United States and Health Canada (FDA, 2021; Health Canada, 2021). These include mRNA vaccines developed by Pfizer-BioNTech and Moderna, viral vector vaccines developed by AstraZeneca and Johnson & Johnson, a protein-based vaccine produced by Novavax, and a plant-based VLP vaccine developed by Medicago (Health Canada, 2021). However, now is also the time to prepare for future outbreaks and the answer to preventing future outbreaks lies with the creation of a "universal vaccine" to combat different strains and variants of the same virus.

Universal vaccines have been a topic of interest for many years, with influenza being one of the most studied candidate infectious agents. Promising results have been achieved by using highly conserved regions to provide broad-based protection (Pica & Palese, 2013) – yet no universal vaccine has been brought to market to date. Like influenza, highly conserved regions among coronaviruses can be used to develop cross-protective immunity. Since SARS-CoV, MERS-CoV and SARS-CoV-2 consist of the same structural proteins, genomic analyses have been conducted to determine the similarities between the sequences (Abdelrahman et al., 2020;

Maldonado et al., 2021). These similarities may allow for the development of broad sequences that are representative of all three viruses. However, a potential limitation is that the three viruses infect different cells which could drastically limit cross-reactivity of spike proteins.

Virus-like particles (VLPs) are synthetic structures formed from multiple proteins in the absence of any nucleic acid material and offer the ability to imitate authentic virus particles without the ability to infect (Roldão et al., 2010). This project will focus on the production and characterization of a SARS-CoV-2 VLP and a VLP based on consensus sequences that was determined from a conservation analysis of SARS-CoV, MERS-CoV and SARS-CoV-2 and its associated variants. Although studies have explored the production of VLPs for SARS-CoV, MERS-CoV and SARS-CoV-2, the production of a VLP relying on the similarities of all three has not been explored thus far.

1.1 Rationale of the work

Since the outbreak of SARS-CoV in 2003 and MERS-CoV in 2012, the immunogenicity of SARS antigens has been significantly studied – yet a vaccine did not exist to date against those 2 viruses. The eventual outbreak of yet another coronavirus, SARS-CoV-2, would ultimately require researchers to develop a vaccine to contain the pandemic. The past three SARS outbreaks prove that more needs to be done to handle outbreaks. Currently, a reactive approach is taken, where effort in creating a vaccine does not seem to exist until a serious outbreak requires it. Dealing with individual strains and variants as they arise is an ineffective approach because the time it takes to research and develop a vaccine only provides the virus with more opportunity to spread. Although various vaccines against SARS-CoV-2 exist to date, the

emergence of many strains and variants have researchers questioning whether current vaccines are effective against them. In fact, a study had shown that current SARS-CoV-2 vaccines are ineffective against the newest omicron variant. To solve these issues, we need to approach SARS outbreaks in a more proactive manner, by creating a universal vaccine that would prevent the next outbreak from occurring. This project will explore a universal vaccine approach by creating a synthetic SARS VLP based on consensus sequences that contains genetic information from SARS-CoV, MERS-CoV, and SARS-CoV-2. The formation of a 'universal' SARS VLP and assessment of its cross-reactive and cross-protective properties will determine whether it can potentially be used as a universal vaccin in the future.

VLPs are safe and attractive vaccine candidates that can resemble the native virus and, when administered intranasally, can closely resemble the natural infection process and stimulate humoral and cellular immune responses both systemically and at the most relevant mucosal surfaces (Bachmann & Zinkernagel, 1997; Brun et al., 2011). Moreover, VLP-based vaccines have been produced against Hepatitis B and human papillomavirus, in addition to those that are currently in preclinical and clinical trials to treat other diseases such as HIV, influenza and Ebola (Mohsen et al., 2017; Roldão et al., 2010; Contreras-Gómez et al., 2014).

This research will also provide a platform that may be applicable to universal vaccine development against other viruses such as influenza. Viral mutations are inevitable, and vaccines are often short-lived and require modifications to continue to confer efficacy across epidemic or pandemic variations. This is the case for viruses such as influenza, where a yearly shot is required. The rise of new strains means that the development of one vaccine to protect us against all strains is sensible. Overall, this research will provide knowledge on a VLP candidate that may

be used to protect against past and future CoV strains, and possibly other viruses such as influenza and HIV.

1.1.1 Hypothesis

Consensus sequences generated for the spike (S), envelope (E) and membrane (M) proteins based on SARS-CoV, MERS-CoV and SARS-CoV-2 can produce S, E and M 'synthetic consensus' proteins using the insect cell-baculovirus expression vector system (IC-BEVS) and form into VLPs.

1.1.2 Objectives

The main objective of this work is to produce a universal coronavirus VLP which can be used as a potential vaccine candidate against SARS betacoronaviruses. Specific objectives for this research are:

1. To produce recombinant baculoviruses expressing SARS-CoV-2 S, E and M proteins and recombinant baculoviruses expressing SARS betacoronavirus consensus sequence-based S, E, and M proteins
2. To produce SARS-CoV-2 VLPs and universal SARS VLPs
3. To perform semi-purification of the SARS-CoV-2 VLPs
4. To characterize SARS-CoV-2 VLPs and universal SARS VLPs

Chapter 2: Literature Review

2.1 Coronaviruses

Coronaviruses belong to the family *Coronaviridae* that are enveloped positive-strand RNA viruses that infect mammals and birds (Fehr & Perlman, 2015; Raoult et al., 2020). The genomes of coronaviruses range between 27 to 32 kilobases (kb), the largest among RNA viruses (Hartenian et al., 2020). The term "coronavirus" is based on the spherical shape of the virus and the projections of spike proteins from the virion surface resembling a crown-like structure (Ashour et al., 2020). These viruses are divided into four subgroups: *Alphacoronavirus*, *Betacoronavirus*, *Deltacoronavirus* and *Gammacoronavirus* (To et al., 2013). Alphacoronaviruses and betacoronaviruses are known to infect mammals while deltacoronavirus and gammacoronavirus infect birds and have not been reported to cause human disease (Bassetti et al., 2020; Satarker & Nampoothiri, 2020). Currently, seven coronaviruses are known to infect humans including human coronavirus (hCoV)-229E, hCoV-NL63, hCoV-OC43, hCoV-HKU1, SARS-CoV, MERS-CoV and most recently, SARS-CoV-2. Between 15-30% of "common cold" cases are caused by hCoV-229E, hCoV-NL63, hCoV-OC43, hCoV-HKU1, all of which are endemic. On the other hand, SARS-CoV, MERS-CoV and SARS-CoV-2 can infect both upper and lower respiratory tract, leading to potentially life-threatening diseases (To et al., 2013). Although coronaviruses infect the respiratory tract, other organs, and tissues such as the brain, thyroid, heart, gastrointestinal tract, spleen, lymph nodes and skeletal muscles may also be damaged (Abdelrahman et al., 2020).

2.2 SARS-CoV-2

SARS-CoV-2 is highly transmissible from human-to-human through direct and indirect contact. Common modes of spreading include coughing, sneezing, inhalation of droplets and contact with either the oral, nasal or eye mucous membranes (Umakanthan et al., 2020). The SARS-CoV-2 genome consists of 30,000 base pairs (bp) with a total of 10 open reading frames (ORFs) that encode for 16 non-structural proteins (nsp1-16), accessory proteins and four structural proteins (**Figure 1A**).

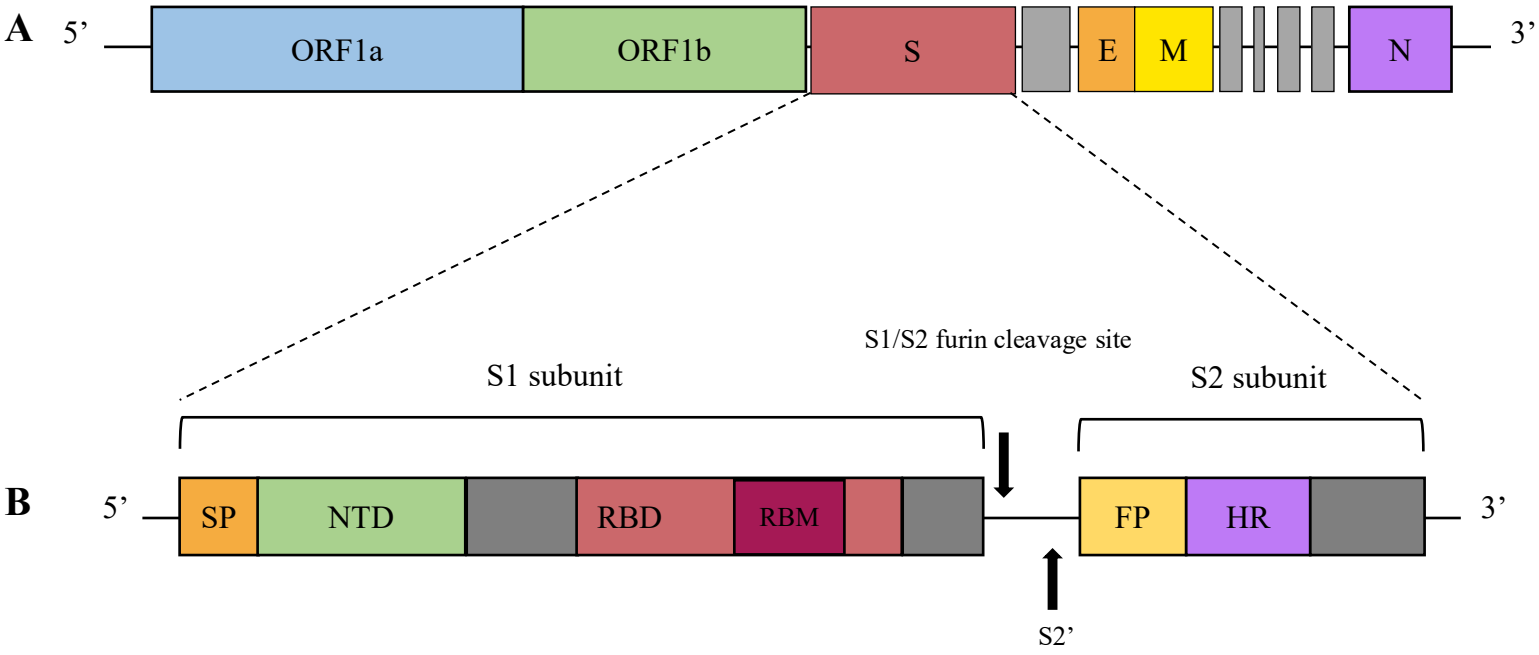

Figure 1: Genetic layout of SARS-CoV-2. (A) Overall genome including the 4 major structural proteins (S, E, M, N). (B) Enlarged view of the S protein sequence displaying the S1 and S2 subunits. NTD: N-terminal domain. RBD: Receptor Binding Domain. RBM: Receptor Binding Motif. FP: Fusion Peptide. HR: Heptapeptide Repeat Sequence.

SARS-CoV-2 is comprised of four essential structural proteins including the spike (S) protein, envelope (E) protein, membrane (M) protein, and nucleocapsid (N) protein **(Figure 2)** (Satarker & Nampoothiri, 2020).

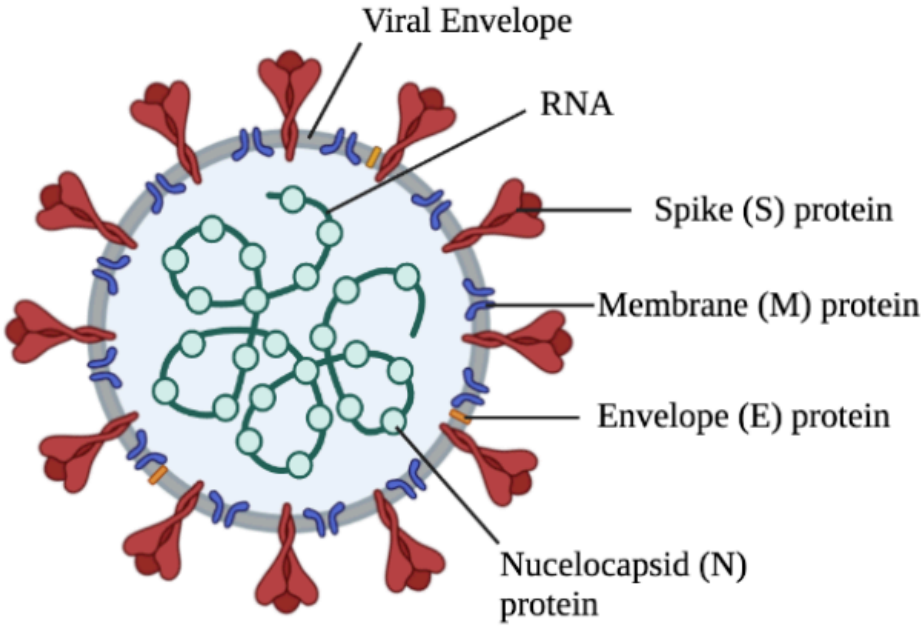

Figure 2: SARS-CoV-2 Virus Morphology

The S protein is a glycoprotein protruding from the virus' surface existing in a trimeric form. It is responsible for recognizing and binding to a host receptor and is classified as a class I viral fusion protein. Each S protein monomer is approximately 140-180 kDa in size and contains two subunits 1) S1, responsible for the recognition and attachment of the host receptor and 2) S2,

responsible for facilitating the fusion between the virus and host membrane **(Figure 3)** (Satarker & Nampoothiri, 2020; Jaimes et al., 2020b).

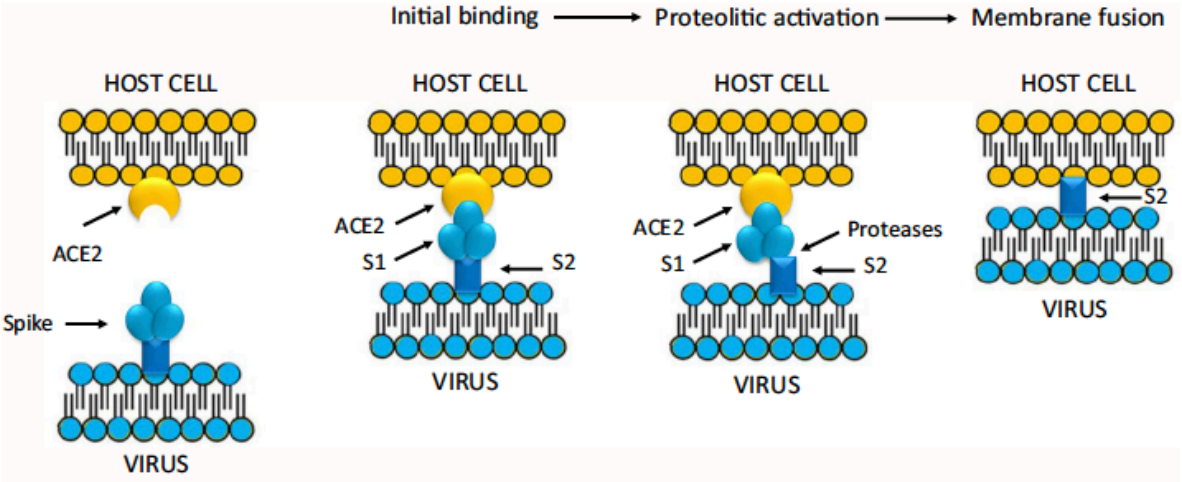

Figure 3: Schematic of S protein binding to a host receptor (ACE2) and fusion between host and viral membrane.

The S1 subunit contains the receptor binding domain (RBD), which is responsible for recognizing and binding to the host receptor and the receptor binding motif (RBM), which mediates contact with the host receptor **(Figure 1B)** (Hu et al., 2020). The angiotensin-converting enzyme 2 (ACE2) receptor, found on lung cells of the lower respiratory tract of humans, is the functional receptor for SARS-CoV-2 and SARS-CoV (Ou et al., 2016; Ou et al., 2020). Binding of the RBD to the host cell receptor leads to proteolytic cleavage by host cell proteases, namely TMPRSS2. This cleavage takes place at the S2' cleavage site **(Figure 1B)** which exposes the fusion peptide (FP) located within the S2 subunit (M.-Y. Wang et al., 2020). Unlike SARS-CoV and MERS-CoV, SARS-CoV-2 also contains the underlined four amino acid

insertion (SPRRARS) between the S1 and S2 subunit, resulting in a furin cleavage site (Örd et al., 2020). Furin is a proteolytic enzyme expressed in the human body and recognizes the binding motif RxxR, where x represents any amino acid. (Y. Wu & Zhao, 2021). The S1/S2 furin cleavage site is used for S protein activation and allows for cell-to-cell fusion and viral entry (Jaimes et al., 2020a; Hoffmann et al., 2020). Furthermore, it allows a higher proportion of S proteins to bind to the ACE2 receptor and a study showed that a SARS-CoV-2 mutant lacking the furin cleavage site had an impact on its infectivity and reduced viral pathogenesis in hamsters and mice expressing human ACE2 receptors (Johnson et al., 2021).

Upon viral entry into the host cell, the positive-strand RNA template is then released, and the translation of non-structural proteins occur. One of these non-structural proteins, Nsp12, is an RNA-dependent RNA polymerase that will transcribe a negative-strand RNA sequence which can be used as a template to replicate new positive-strand RNAs. Afterwards, the structural proteins are translated and self-assemble with the positive-strand RNAs before exiting the cell and forming new SARS-CoV-2 virions (Y.-D. Li et al., 2020).

The E protein is a small integral membrane protein ranging from 8-12 kDa in size (Schoeman & Fielding, 2019). Although it is abundantly expressed, very few proteins are incorporated into the virion envelope (Schoeman & Fielding, 2019). The E protein is involved in virus assembly, budding and maturation (Nieto-Torres et al., 2011; Schoeman & Fielding, 2019). The M protein is the most abundant protein and interacts with the other three structural proteins to regulate the shape of the viral envelope (Neuman et al., 2011). The N protein is the only structural protein that interacts with the RNA genome. This interaction aids in genomic processes following the fusion between virus and host cell (Satarker & Nampoothiri, 2020).

2.2.1 SARS CoV-2 Variants

The World Health Organization (WHO) has grouped SARS-CoV-2 variants into 2 categories: variants of concern (VOC) and variants of interest (VOI). VOC are those that have increased transmissibility, virulence and are resistant to current vaccines or acquired immunity from previous infection (Mistry et al., 2022). Several variants of SARS-CoV-2 containing mutations in the S protein have been reported including the D614G, alpha variant (B.1.1.7), beta variant (B.1.351), gamma variant (P.1), delta variant (B.1.617) and omicron variant (B.1.1.529) **(Figure 4)** (CDC, 2021; Cherian et al., 2021; BCCDC, 2021; Mistry et al., 2022).

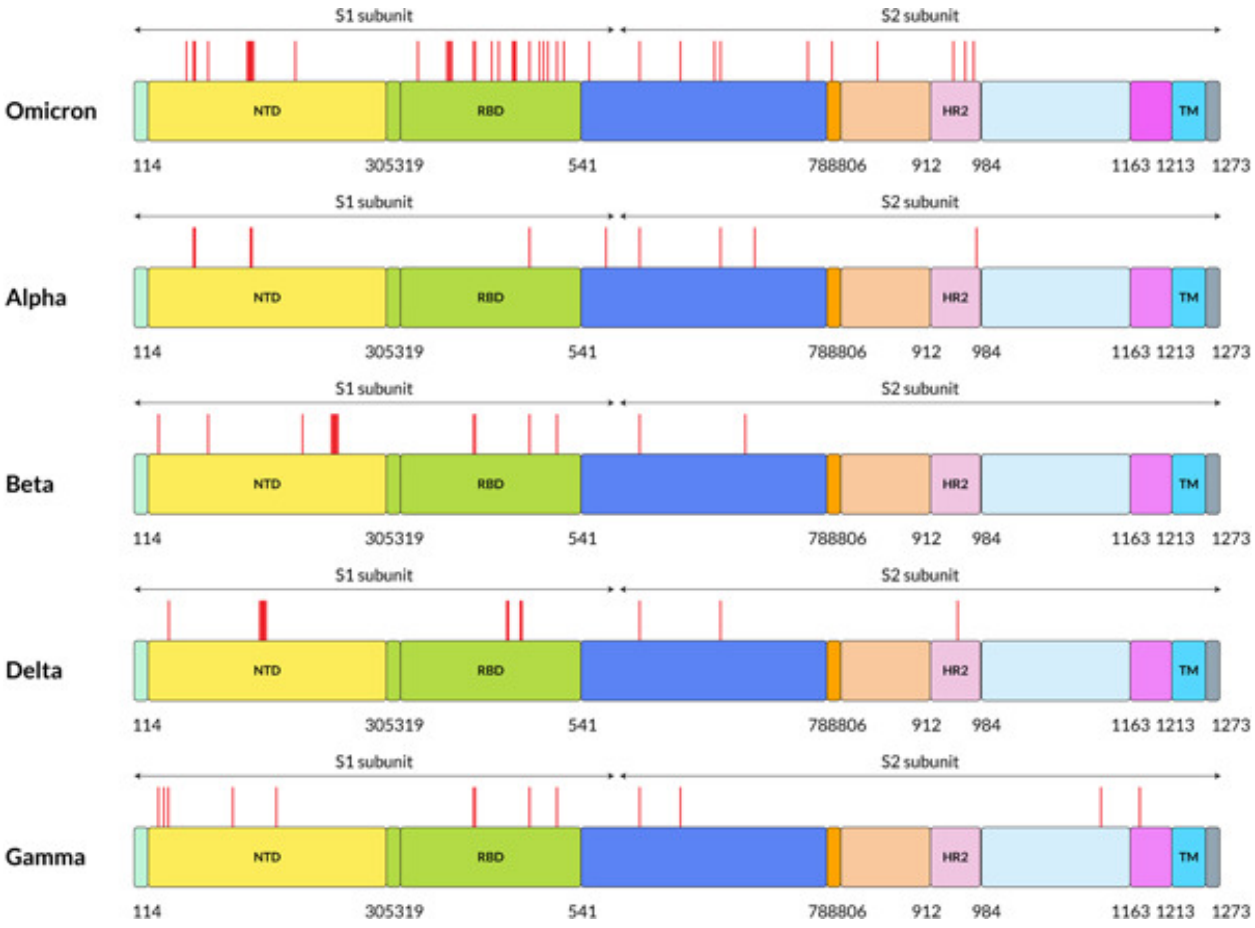

Figure 4: Five SARS-CoV-2 variants of concern (Omicron, Alpha, Beta, Delta, and Gamma) containing spike protein mutations. Red lines indicate the location of the mutation. NTD: N-Terminal Domain. RBD: Receptor Binding Domain. HR2: Heptapeptide Repeat Sequence. TM: Transmembrane Domain. (Image obtained from Araf et al., 2022)

The D614G variant contains an aspartic acid to glycine mutation at aa position 614 and has been reported to increase proteolytic cleavage and enhance the infectivity of SARS-CoV-2 (Hou et al., 2020). This mutation affects the RBD, where the RBD is reoriented to a "standing up" conformation (Hou et al., 2020). Normally, the RBD can alternate between a "standing-up"

and “lying-down” conformation, where the “lying down” conformation is associated with less efficient binding and acts as a conformational masking strategy to favor immune evasion (Rossi et al., 2020). However, the D614G mutation causes the RBD to spend most of its time in the “standing up” conformation, resulting in a higher binding affinity to the ACE2 receptor (Hou et al., 2020). The Alpha variant first emerged in the United Kingdom and contains an N501Y (asparagine substituted with tyrosine at position 501) mutation in the RBD. Population genetic modelling suggests that these variant spreads 56% more quickly (Galloway et al., 2021; Lauring & Hodcroft, 2021). The Beta variant, however, was first detected in South Africa and contains three mutations in the RBD including K417N, E484K and N501Y. Despite these substitutions, there has been no definitive evidence suggesting an increase in the severity of the disease (Tang et al., 2021). The Gamma variant which emerged in Brazil also contains three RBD mutations, two of which are the same as the Beta variant (E484K and N501Y) and a K417T mutation (CDC, 2021). Unlike the Beta variant, however, the Gamma variant has been associated with increased transmissibility (Firestone et al., 2021). The Delta variant was first detected in India and contains a L452R and E484Q mutation in the RBD, as well as a P681R mutation in the furin cleavage site. Based on current evidence, the Delta variant is estimated to be 40-60% more transmissible than the Alpha variant (Kumar et al., 2022A). The most recent variant, Omicron, was first detected in South Africa and contains double the number of mutations compared to the Delta variant, bringing concerns over the efficacy of current vaccines (Mistry et al., 2022). Omicron is split into three lineages, namely BA.1, BA.2 and BA.3 (Fan et al., 2022). BA.1 was the most prevalent strain in the world and 39 mutations in the S protein have been identified in this lineage. The BA.2 lineage, however, is beginning to replace BA.1 as the most prevalent strain

while the number of cases belonging in the BA.3 lineage is relatively low (Fan et al., 2022). The BA.2 and BA.3 lineage contains 31 and 34 mutations in the S protein, respectively (Kumar et al., 2022B). Twenty-one of these mutations are shared among all three lineages (Kumar et al., 2022B).

2.3 SARS-CoV, MERS-CoV and SARS-CoV-2

SARS-CoV and MERS-CoV are both believed to have originated from bats. Although SARS-CoV-2 has been reported to be genetically similar to a Bat-CoV known as RaTG13, there have also been reports that indicate pangolins may be the natural reservoir instead (Zhu et al., 2020). Since SARS-CoV, MERS-CoV and SARS-CoV-2 are all classified as betacoronaviruses, their overall genomic structure is quite similar. Generally, the structure of the betacoronavirus genome consists of a 5' methylated cap and a 3' polyadenylated tail. One-third of the genome encodes for the four structural proteins (S, E, M and N) while the remaining two-thirds are responsible for encoding non-structural proteins **(Figure 5)** (Zhu et al., 2020).

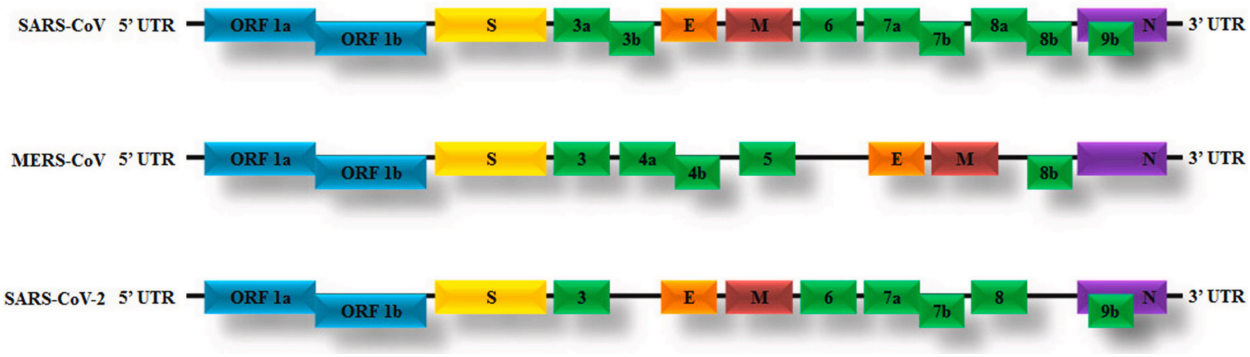

Figure 5: Genomic Structure of SARS-CoV, MERS-CoV, and SARS-CoV-2.

Genomic analyses reveal that the overall genome of SARS-CoV-2 shares an 80% and 50% similarity with SARS-CoV and MERS, respectively (Jaimes et al., 2020b). SARS-CoV and SARS-CoV-2 share a common receptor, ACE2 receptor, while MERS-CoV binds to dipeptidyl-peptidase 4 (DPP4) (Ou et al., 2016; Ou et al., 2020; Walls et al., 2020). The ACE2 receptor is expressed ubiquitously including the lung, stomach, liver, small intestine, etc. However, those expressed in alveolar epithelial cells and endothelial cells in the lungs are the main targets for infection (Hamming et al., 2004; Valencia et al., 2020). Similarly, DPP4 is also ubiquitously expressed and found on epithelial and endothelial cells located on several organs including the lung, kidney, liver, etc. (Y. Li et al., 2020). More importantly, DPP4 is also found on leukocytes making them natural hosts of the virus (Y. Li et al., 2020). As a result, the implications of antibody-dependent enhancement (ADE) are extremely important for MERS-CoV (See 2.4.3).

The S protein nucleotide sequence for SARS-CoV-2 is 76% similar to SARS-CoV versus a much lower similarity of 29% to MERS-CoV (Ahmed et al., 2020). Differences in S protein sequence between SARS-CoV-2 and SARS-CoV may also explain the difference in affinities that SARS-CoV-2 and SARS-CoV have for the ACE2 receptor (Yan et al., 2020). The S2 subunit is highly conserved among SARS-CoV and SARS-CoV-2, ranging from 88-99% in sequence similarity (Chan et al., 2020; Walls et al., 2020). In particular, the highly conserved S2' FP can elicit highly cross-reactive antibodies, making it a key component in the development of a universal vaccine (Khan et al., 2020; N. Wang et al., 2020). The S1 subunit, however, does not show the same level of conservation with the RBD and RBM only showing 73-76% and 50-53% similarity, respectively (Wan et al., 2020). These differences likely explain why the SARS-CoV-2 RBD has a higher binding affinity to ACE2 than SARS-CoV, even though it has been reported

to spend most of its time in the "lying-down" conformation and is less exposed than the SARS-CoV RBD (Rossi et al., 2020; J. Shang et al., 2020). As for the other structural proteins (E, M and N), the sequence identities are all greater than 90% between SARS-CoV-2 and SARS-CoV, while MERS-CoV only share a similarity of 30-45% with SARS-CoV-2. The E protein, however, is the most conserved in both comparisons (Ahmed et al., 2020).

MERS-CoV is the largest among the three betacoronaviruses, with a genomic size of approximately 30.11 kb compared to 20.9 kb for SARS-CoV-2 and 29.75 kb for SARS-CoV (Al-Qahtani, 2020). However, SARS-CoV-2 has the highest transmissibility with a basic reproductive number of 2-3.58, while SARS-CoV and MERS-CoV have basic reproductive numbers of 1.7-1.9 and less than 1, respectively (P. Wu et al., 2020; Zhu et al., 2020). In addition, the mean incubation period for SARS-CoV-2 was reported to be 5.2 days compared to 4 days and 5.2 days for SARS-CoV and MERS-CoV, respectively (Zhu et al., 2020), although the difference in incubation periods among the three were not found to be statistically significant (Jiang et al., 2020). Common symptoms among all three viruses include fever, cough, fatigue, and myalgia (Hu et al., 2020).

2.4 Vaccines against SARS Betacoronaviruses

Currently, no vaccines are available for SARS-CoV and MERS-CoV. However, multiple vaccines against SARS-CoV-2 have been authorized for public use including two mRNA vaccines produced by Pfizer-BioNTech and Moderna, two viral vector vaccines produced by Johnson & Johnson and AstraZeneca, a protein-based vaccine produced by Novavax, and a plant-based VLP vaccine produced by Medicago (Health Canada, 2021). In fact, there were over

180 vaccine candidates in development against SARS-CoV-2 (World Health Organization, 2020).

The different vaccine platforms include live attenuated, inactivated, subunit, viral vector, nucleic acid (DNA and mRNA) and virus-like particles (VLPs) **(Table 1)** (Iwasaki & Omer, 2020). Live attenuated vaccines are based on weakened versions of a virus that are able to induce an immune response, but only replicate minimally so as to not cause disease. Inactivated virus vaccines are inactivated before use and thus, are incapable of replicating (N.-H. Lee et al., 2012). In contrast, subunit vaccines only use antigenic components from a virus (García-Sastre & Mena, 2013). Viral vector vaccines use a modified virus that is able to encode the antigen(s) of interest of a different virus (Y.-D. Li et al., 2020). These vectored vaccines may be able to replicate or may serve only to deliver genetic cargo. Similarly, DNA vaccines also utilize the host cellular system to transcribe genes that encode antigens of interest; however, delivery of the DNA is not through the use of a virus. DNA vaccines typically rely on synthetic means for delivering DNA (eg. Micelles). Note, although DNA is more stable than its RNA counterpart, DNA typically requires transport to the nucleus, which can be more challenging. RNA vaccines also rely on a synthetic delivery system; however, mRNA-based sequences do not need to be shuttled to the nucleus before translation occurs (Krammer, 2020). VLP vaccines are multiprotein structures assembled from structural proteins originating from a virus (Roldão et al., 2010). VLPs will be further explored in section 2.6.

Table 1: Function, advantages, and disadvantages of various vaccine platforms.

Vaccine Platform	Function	Advantages	Disadvantages
Live attenuated	Weakened version of the virus	Can be administered intranasally No adjuvants required	Risk of reversion back to pathogenic form
Inactivated	Inactivation/killing of the virus	Easy production	Risk of not fully being inactivated
Viral vector	Uses a harmless virus as a delivery vehicle to deliver viral genes	Strong innate and adaptive immune responses Do not require adjuvants	May be pre-existing immunity towards the vector
Subunit	Uses specific components of the virus	Non-infectious Strong humoral response	Potential risk for infection
DNA	Uses DNA sequences of the viral gene(s)	High stability of plasmid DNA	Low immunogenicity DNA needs to be transported past two cell membranes
RNA	Uses RNA sequences of the viral gene(s)	mRNA does not have to be integrated into the host genome and is translated in the cytosol	Problems with instability leading to low immunogenicity
VLP	Uses structural proteins that self-assemble into particles that mimic that native virus	Non-infectious and safe Induce strong immune responses	Long-term stability is a concern

2.4.1 Routes of Administration

When natural infection with the native virus occurs, a systemic and mucosal immune response is induced. The systemic immune response is comprised of mainly immunoglobulin G (IgG) antibodies with a high prevalence in the lower respiratory tract. Meanwhile, the mucosal immune response mainly involves immunoglobulin A (IgA) antibodies with a high prevalence in the upper respiratory tract and mucosal linings (Krammer, 2020). In the case for vaccines, the type of immunity stimulated is dependent on the route of administration. Vaccines can be

delivered intramuscularly, intradermally, or intranasally. Intramuscular/intradermal injection leads to strong IgG responses with minimal IgA response, while intranasal delivery leads to strong IgA responses and minimal IgG responses (Krammer, 2020). Vaccines that are currently available for SARS-CoV-2 are all delivered intramuscularly. Intramuscular injections rely on systemic immunity and since it leads to strong IgG responses and minimal IgA responses, there may be an insufficient activation of immunity in the upper respiratory tract necessary to neutralize mucosal infection. However, it is important to note that the local immunity in the upper respiratory provided by IgA responses is important in preventing viral entry into the body. These drawbacks indicate that although current SARS-CoV-2 vaccines may protect individuals from symptomatic disease, there is still a possibility that viral entry into the upper respiratory tract will occur and continue to be transmitted (Mohsen et al., 2017). In contrast, mucosal administration can induce strong humoral and cell-mediated immunity through the activation of CD8+ CTLs and production of IgA (Hellfritzsch & Scherließ, 2019). For vaccines to work at mucosal sites, they must penetrate the mucous and epithelial layers to reach the underlying immune cells and are therefore favorable when using certain delivery vehicles such as nanoparticles (Farris et al., 2016). For SARS-CoV-2, mucosal administration may be more effective than intradermal or intramuscular administration since natural infection occurs through respiratory droplets.

2.4.2 Adjuvants

Adjuvants are substances that are delivered along with vaccines to boost the immune response (Grunwald & Ulbert, 2015). Depending on the vaccine platform, adjuvants may or may

not need to be administered as well. DNA vaccines, for example, generally lead to low immunogenicity in large animal models and humans and adjuvants are often required (Rauch et al., 2018). VLP-based vaccines may also be formulated with adjuvants to enhance their stability (Cimica & Galarza, 2017). In contrast, RNA vaccines have shown to induce strong T cell and humoral immune responses without adjuvants (C. Zhang et al., 2019; Rauch et al., 2018). Live-attenuated, inactivated, and viral vector vaccines also do not require adjuvants as they are normally capable of eliciting an adequate immune response for protection (Lee & Nguyen, 2015; Rauch et al., 2018). One of the most commonly used adjuvants is aluminum salt-based adjuvants (alum). When alum is formulated with the S protein or RBD in coronavirus vaccines, it was shown to enhance humoral immune responses (Liang et al., 2020). In addition, alum is capable of strongly inducing IgG production and neutralizing antibody titers in VLPs and inactivated vaccines containing the E, M and N proteins (Liang et al., 2020). However, alum is mainly involved in the promotion of type 2 T helper (Th2) immune responses and stimulation of type 1 T helper (Th1) cells is limited (Cimica & Galarza, 2017; Liang et al., 2020). Some adjuvants such as delta inulin, however, can induce a balanced Th1/Th2 immune response which can lower the risk of Th2 immunopathology (Honda-Okubo et al., 2015). Alpha-tocopherol is another adjuvant used to supplement immunity in humans and is found in emulsion adjuvants such as AS03 (Liang et al., 2020). In comparison to alum adjuvant, AS03 can elicit humoral and cellular immune responses which leads to a more balanced immunity. The presence of alpha-tocopherol in this adjuvant allows it to improve antigen uptake, recruit immune cells, and promote the migration of activated antigen-presenting cells (Liang et al., 2020).

As mentioned by alum and delta inulin, adjuvants are capable of enhancing T cell responses such as Th1 and Th2 cells. Th1 cells are involved in the stimulation of a cell-mediated immune response through the production of proinflammatory cytokines. Th2 cells, however, stimulate humoral immune responses by promoting B cell proliferation and antibody production (Eden et al., 2002). Adjuvants have been widely studied including ligands that can stimulate Toll-like receptors (TLRs). TLRs are a type of pattern recognition receptor (PRR) which detect pathogen-associated molecular patterns (PAMPs) from microbes. They are found on cell and endosomal surfaces of APCs and upon recognition and activation, will cause the release of proinflammatory cytokines and type 1 interferons (IFNs) to help further enhance the innate and adaptive immune responses (Gupta & Gupta, 2020). RNA vaccines are able to stimulate TLR7 and TLR8, resulting in cytokine secretion, higher antigen presentation, B cell stimulation and elicit strong innate immune responses (C. Zhang et al., 2019). Past studies have adjuvanted DNA vaccines with alum which showed to be ineffective in humans and larger animals (Grunwald & Ulbert, 2015). However, CpG oligodeoxynucleotides (ODNs), another type of adjuvant that are primarily found in prokaryotic DNA, can induce both cell-mediated and humoral immune responses (Bode et al., 2011; Liang et al., 2020). CpG ODNs are capable of eliciting Th1 responses and cytokine production through the stimulation of TLR9 (Gupta & Gupta, 2020). DNA plasmids, which are normally produced in prokaryotic cells such as bacteria, will contain the CpG motifs that allow them to self-adjuvant and can lead to a potent IFN gamma response (A. Zhang et al., 2005). IFN-gamma is a cytokine that is important for innate and adaptive immune responses as it plays a role in the activation of macrophages and the stimulation of natural killer cells and neutrophils (Tau & Rothman, 1999). Another notable adjuvant is

Protollin, which is capable of inducing antigen-specific IgG and IgA antibodies and increasing IFN and cytokine production through the stimulation of TLR2 and TLR4 (Gupta & Gupta, 2020).

2.4.3 Antibody-Dependant Enhancement

Although the production of antibodies against SARS-CoV-2 antigens is the main objective of vaccines, there is also a concern for ADE. ADE occurs when suboptimal or non-neutralizing antibodies enhance viral entry into the host cell and increase the severity of the disease (Arvin et al., 2020). Currently, there are no evidence proving that ADE occurs in SARS-CoV-2 infection (Karthik et al., 2020), however, it is still a cause for concern as ADE has been observed for many viruses including dengue virus, feline infectious peritonitis virus, SARS-CoV and MERS-CoV (W.S. Lee et al., 2020). The potential for MERS-CoV to demonstrate ADE is very likely due to Fc gamma receptor-mediated uptake which can lead to the infection of leukocytes (W.S. Lee et al., 2020). As a result, vaccine development for SARS-CoV-2 should target epitopes that elicit NAbs, such as those targeting the RBD (Karthik et al., 2020).

ADE can occur through two mechanisms: i) infection of monocytes and macrophages and ii) the formation of immune complexes (W.S. Lee et al., 2020). The first scenario occurs when non-neutralizing antibodies attach to viral antigens, followed by viral entry and infection of phagocytic cells via antibody-dependent endocytosis. In contrast, the second scenario occurs when the interaction between non-neutralizing antibodies and viral antigens lead to the formation of immune complexes inside airway tissues. The immune complexes lead to a cascade of events (cytokine secretion, recruitment of immune cells), which cause pathological effects in the lungs

(W.S. Lee et al., 2020). This is evident in a study where inactivated and viral vector vaccines for SARS-CoV and MERS-CoV led to enhanced inflammation and immunopathology linked to Th2 cytokine responses, also known as Th2 immunopathology (W.S. Lee et al., 2020). Furthermore, another study demonstrated that macaques given a SARS-CoV vaccine expressing the full-length S protein led to the production of anti-S protein IgG that resulted in more severe lung injury (L. Liu et al., 2019).

2.5 Universal Vaccines

Universal vaccines are based on the idea that antigens common to multiple strains and variants of viruses can be used to develop cross-protective adaptive immunity (Hamad, 2011). This can be achieved through several approaches such as determining highly conserved sequences that do not change significantly over time and using them to induce broadly neutralizing antibodies (NAbs) or by using epitopes from different strains (Nachbagauer & Krammer, 2017; Nabel, 2013; Sautto et al., 2018). Influenza virus is a prime example of a virus that has been long researched and currently being researched to develop a universal vaccine. Studies have identified major surface proteins on influenza virus that may serve as potential targets for universal vaccines including the matrix 2 ectodomain (M2e) and two surface proteins, hemagglutinin (HA) and neuraminidase (NA). Furthermore, other conserved protein sequences such as the matrix 1 (M1) and nucleoprotein (NP) are also possible targets since they contain many T cell epitopes (Sun et al., 2020). The M2e is the exposed region on the M2 protein that has been reported to be highly conserved among all influenza subtypes, making it a highly promising target (Pica & Palese, 2013; Vogel & Manicassamy, 2020). The HA protein is the

receptor binding protein for influenza which consists of a stem and a globular head (Estrada & Schultz-Cherry, 2019).

Different approaches have been taken in the development of a universal influenza vaccine such as targeting the stem region of HA, using chimeric HA and targeting the NA protein. The HA head varies between different subtypes of influenza and is prone to antigenic drift, making it a difficult region to target. However, the stem of HA is relatively conserved among many subtypes of influenza and have a much lower mutation frequency compared to the HA head. The HA stem has also been reported to activate T-cell immunity and stimulate the production of CD8+ cytotoxic lymphocytes (CTLs) (Sun et al., 2020). A drawback of this approach is that the immunogenicity of the stem is much lower than the head, and multiple immunizations are required in order to induce a sufficient antibody response (Jang & Seong, 2019). The chimeric HA approach involves a combination of the stem domain from one influenza subtype and the head domain from other subtypes (McMillan et al., 2021). The idea behind this approach is that immunizations with various vaccines containing the same HA stem and a different head domain will lead to the production of stem-specific antibodies and allow for broader protection (Sun et al., 2020; McMillan et al., 2021). Unlike the HA and M2 protein which play a role in viral entry and maturation, the NA protein is responsible for the virus to exit host cells and continue to replicate. By targeting the NA protein, viral replication and spread can be limited (Estrada & Schultz-Cherry, 2019). Recently, a multivalent DNA vaccine has been in the works which combines multiple antigens such as the M2e and HA gene from the H1N1 virus. Delivery of this DNA vaccine into mice led to antibody responses against the HA and M2e proteins. After viral

challenge with a different subtype, H5N2, the mice had a 100% survival rate (McMillan et al., 2021).

2.6 Virus-Like Particles as a Vaccine Candidate

Attenuated and inactivated vaccines are among the most common licensed vaccines; however, a common concern is that they run the risk of either reverting to their pathogenic form or that they are not fully inactivated (Comas-Garcia et al., 2020). VLPs are promising and safe vaccine candidates that can overcome this limitation. VLPs mimic the conformation, structure, and antigenicity of naturally occurring virus particles without containing the genetic content that enables replication of the virus and exponential growth **(Figure 6)**. Therefore, VLPs may stimulate B-cells and activate T-lymphocytes to elicit immune responses in the same way as the native virus (Roldão et al., 2010; Kumar et al., 2018). Several studies have shown that VLPs may effectively stimulate the immune system, activating B cells, T cells and producing high titer antibodies (Bachmann & Zinkernagel, 1997; Brun et al., 2011).

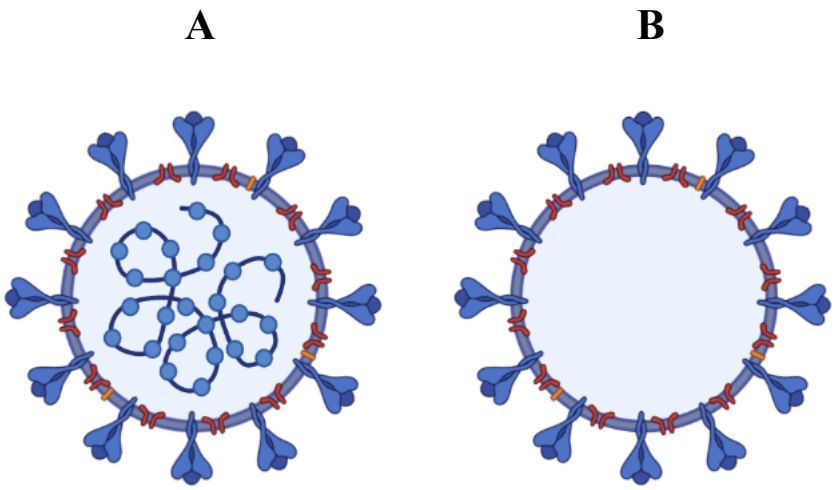

Figure 6: Comparison between native SARS-CoV-2 virus particle and SARS-CoV-2 VLP. (A) SARS-CoV-2 virus particle. (B) SARS-CoV-2 VLP containing S, E and M proteins.

An innate immune response is stimulated when VLPs are phagocytosed by innate immune cells such as macrophages and dendritic cells (DCs). VLPs can be packaged with TLR ligands such as RNA which can stimulate TLR7/8 or DNA containing non-methylated CpG motifs to stimulate TLR9 (Klimek et al., 2018). These TLR ligands can elicit an immune response similar to RNA vaccines and the CpG motif adjuvant effects in DNA vaccines described in section 1.5.2 (Klimek et al., 2018). Recognition of these ligands by their associated TLRs will stimulate a downstream cascade of events that lead to cytokine secretion and proinflammatory responses (Bender et al., 2020).

Adaptive immune responses are stimulated when VLPs are recognized and internalized by antigen presenting cells (APCs), followed by the presentation of the resulting antigen peptides

on major histocompatibility complex (MHC) I and MHC II molecules, which are recognized by CD8+ CTLs and CD4+ T helper (Th) cells, respectively **(Figure 7)**.

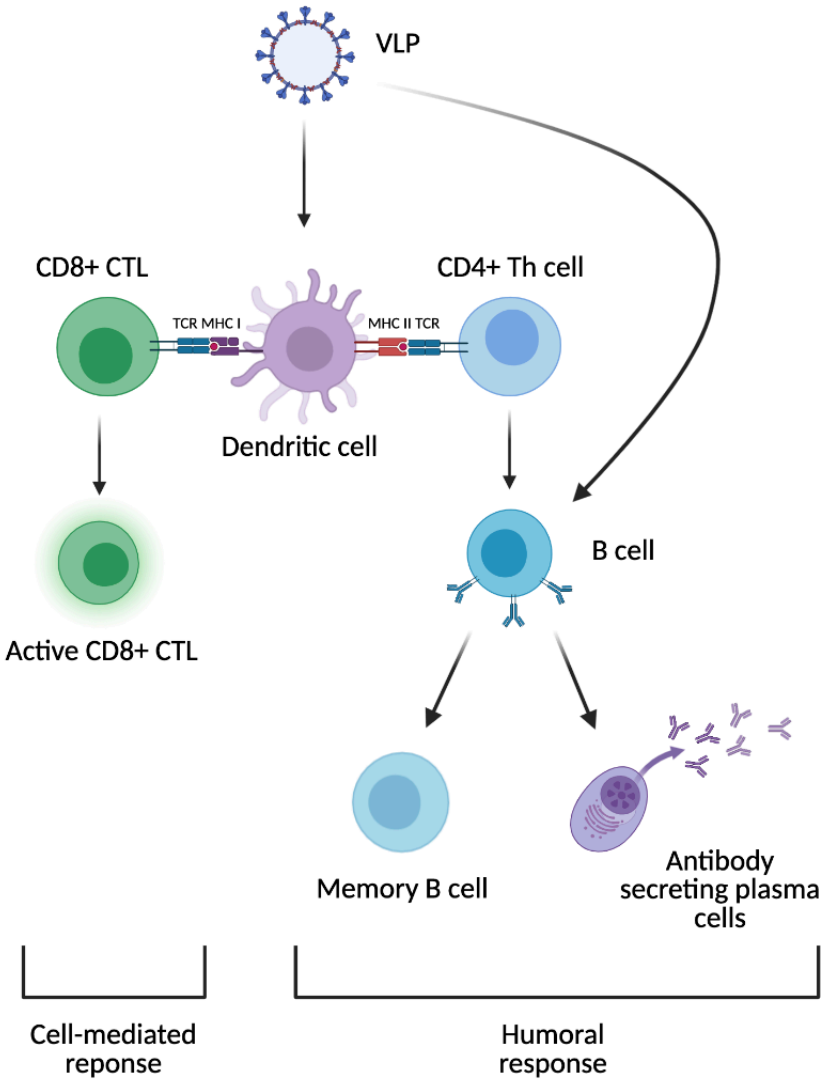

Figure 7: Schematic of the adaptive immune response stimulated by VLP-based vaccines.

A cell-mediated immune response occurs when antigens presented by MHC-I is recognized by T cell receptors (TCRs) located on naive CD8+ CTLs, promoting the release of cytokines and cytotoxic activity of CD8+ CTLs (Shah et al., 2020). Along with the help of other costimulatory molecules and cytokines provided by the APC, and possible help from Th cells, the effector CD8+ CTLs mature and become activated to kill virus-infected target cells (Nooraei et al., 2021). The humoral immune response is induced when CD4+ Th cells recognize the antigens presented on MHC II through TCRs which stimulates the transcription of cytokine genes, resulting in proinflammatory responses and B cell activation, where B cells differentiate into antibody-secreting plasma cells or memory B cells. B cells can also act as an APC and present the antigens on MHC II (Donaldson et al., 2018; Nooraei et al., 2021). In some cases, B cells can recognize VLPs through their B cell receptors (BCRs) and internalize them to stimulate a humoral immune response in the absence of Th cells (Nooraei et al., 2021).

The size of VLPs can range from 20 to 200 nm (Mohsen et al., 2017) and they can be non-enveloped or enveloped. Non-enveloped VLPs are much easier to produce, simple in structure, and contain either one or more structural proteins of a virus. In contrast, enveloped VLPs are much more complex as they carry a host cell-derived membrane. Enveloped VLPs form the membrane structure inside the cell and either bud out of the cell or exit the cell via exocytosis (Lu et al., 2022***;*** Qian et al., 2020) **(Figure 8)**.

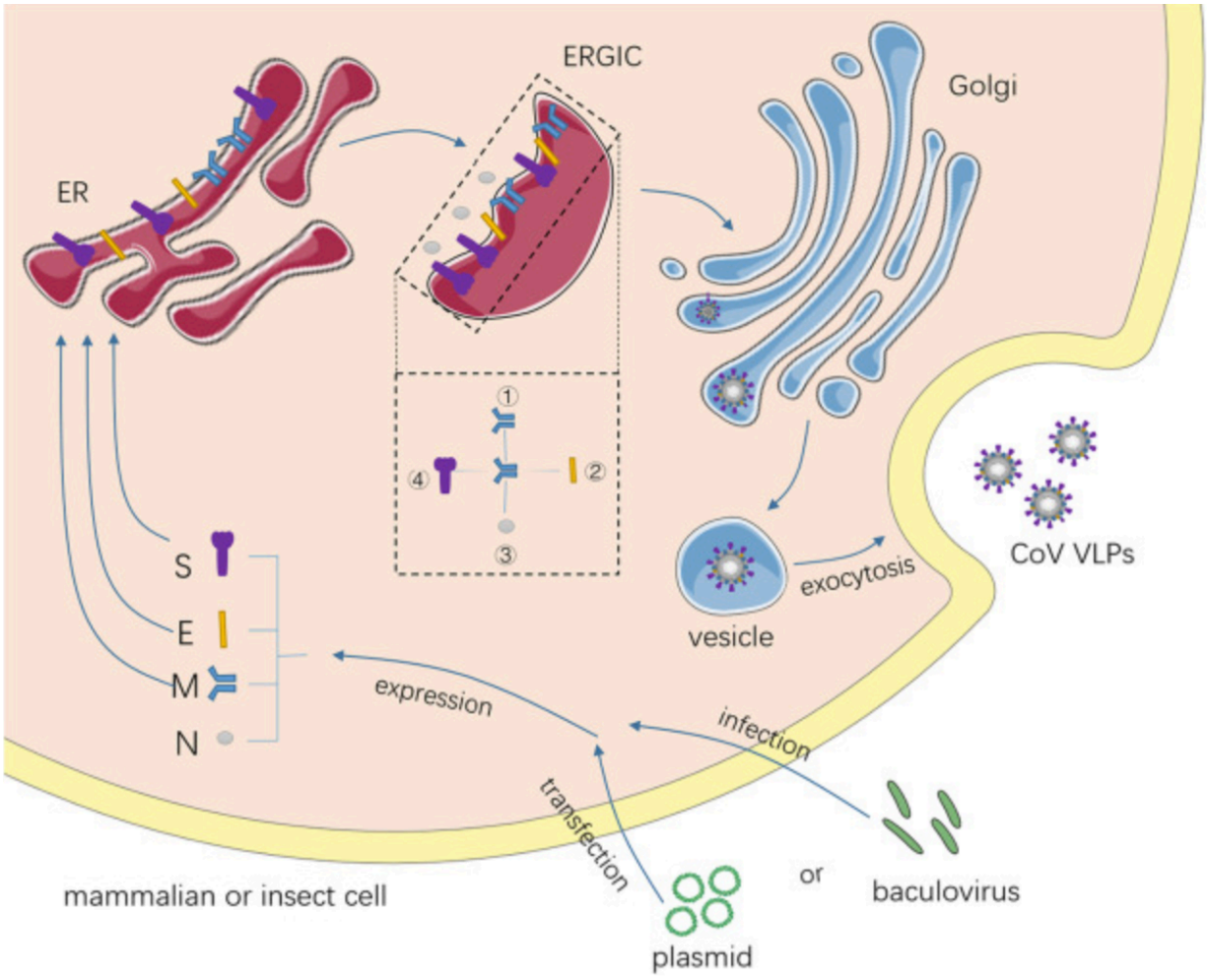

Figure 8: Schematic of SARS VLP formation. Image obtained from Lu et al., 2022.

VLP vaccine candidates are currently undergoing preclinical or clinical trials to combat influenza virus, parvovirus, Norwalk virus, Ebola virus, human immunodeficiency virus (HIV) and rotavirus (Roldão et al., 2010; Contreras-Gómez et al., 2014). In addition, several VLP-based vaccines have been successfully developed against Hepatitis B, human papillomavirus, and malaria (Mohsen et al., 2017). Malaria is the first parasitic disease to have a VLP-based vaccine, marketed as *Mosquirix*. This vaccine involves the use of a Hepatitis B VLP to present

components of circumsporozoite, a protein secreted from the malaria-causing parasite (Fuenmayor et al., 2017).

2.6.1 SARS VLPs

VLPs have been successfully produced for SARS-CoV, MERS-CoV and SARS-CoV-2 (Mortola & Roy, 2004; C. Wang et al., 2016; Swann et al., 2020). The minimal requirement for SARS-CoV VLP formation remains uncertain as several studies have shown different results. Some studies suggest that efficient SARS-CoV VLP production required the expression of M and E (Hsieh et al., 2005; DeDiego et al., 2007). In contrast, Siu et al. (2008) showed that the minimal requirements for SARS-CoV and MERS-CoV VLP formation is M+N and M+E, respectively. The controversy over the minimal requirements for SARS-CoV VLP formation has brought uncertainty over the minimal requirements for SARS-CoV-2 VLPs as well. While early findings suggested that M and E are the minimal requirements for SARS-CoV-2 VLP formation (Xu et al., 2020), new studies have shown that the co-expression of M with S or N was the minimal requirement (Plescia et al., 2021).

The effectiveness of SARS-CoV-like particles has been tested on animal models before, as seen in a study conducted by Coleman et al. (2004), which demonstrated that MERS-CoV and SARS-CoV VLPs are able to induce NAbs and successfully mount an immune response in mice following a single injection (Coleman et al., 2014). The E, M and N proteins can elicit an increased immune response but not strongly enough to provide adequate protection against subsequent SARS infection. The S protein is reported to be the main inducer of NAbs and is the main neutralization antigen used for many vaccine candidates (Mousavizadeh & Ghasemi,

2020). Therefore, co-expression of the S protein with either M or E protein, prompted a much greater immune response capable of providing protection (Buchholz et al., 2004). While the S protein is highly immunogenic, vaccine research on SARS-CoV and MERS-CoV found that the use of the entire S protein sequence could potentially lead to antibody-dependent enhancement (ADE) (See 2.4.3) (Karthik et al., 2020). An effective way to overcome this complication is to only use regions of the sequence that induce NAbs such as the RBD (Y.-D. Li et al., 2020).

The size of the S, E and M proteins detected in SARS-CoV VLPs were reported to be approximately 180, 10 and 30 kiloDalton (kDa) which corresponds to the size of the native proteins (Mortola & Roy, 2004). Furthermore, the size of the SARS VLPs produced in numerous studies are approximately 100 nm, which is consistent with the size of the native viruses. MERS-CoV, SARS-CoV and SARS-CoV-2 VLPs characterized with transmission electron microscopy (TEM) and cryotomography have also been shown to have a similar diameter of approximately 100 nm, 79-224 and 100-200 nm, respectively (C. Wang et al., 2016; Swann et al., 2020). SARS-CoV-2 VLPs produced in insect cells can be seen as vesicle-like structures clumped together and contains “fringe-like projections” on the outer surface that are indicative of the presence of spike proteins (Sullivan et al., 2022) **(Figure 9)**.

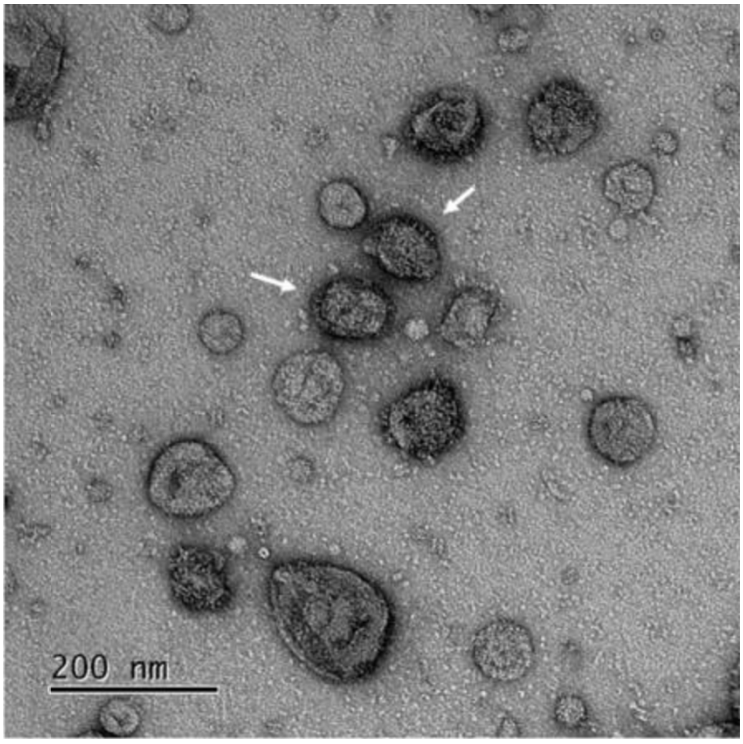

Figure 9: TEM image of SARS-CoV-2 VLPs produced in *Sf9* insect cells. White arrows point towards two SARS-CoV-2 VLPs out of many nanoparticles. Image obtained from Sullivan et al., 2022.

2.6.2 VLP Production Platforms

The production of VLPs can be accomplished using a diverse number of systems including bacteria, yeast, mammalian cells and insect cells (Fuenmayor et al., 2017) **(Table 2)**. Bacteria and yeast are quick and easy systems that can produce a high yield of proteins. However, bacteria such as *E. coli* are unable to perform complex post-translational modifications (PTMs) while yeast do not perform the same PTMs as humans. In contrast, mammalian cells can perform complex PTMs, but offer much lower production yields compared to those of other

systems. These drawbacks can be eliminated by using the insect cell baculovirus expression vector system (IC-BEVS) which can produce an abundant number of proteins that are comparable with bacteria and yeast while being able to perform complex PTMs (Fuenmayor et al., 2017). A study showed that the number of influenza VLPs produced in *Sf9* cells were 35 times more than the amount produced in HEK293 mammalian cells (Thompson et al., 2015). Baculoviruses will be further explored in section 2.7.

Table 2: Characteristics of various cell lines used for VLP production. -, no successful cases reported; +, low; ++, medium; +++, high. (Recreated from Dai et al., 2018).

	Bacteria	**Yeast**	**Insect cells**	**Mammalian cells**	**Plants**
VLP type	**Non-enveloped**	**Non-enveloped, enveloped**	**Non-enveloped, enveloped**	**Non-enveloped, enveloped**	**Non-enveloped, enveloped**
Secretory expression	-	+	++	++	+
Speed	+++	+++	++	++	++
Cost	+	+	++	+++	++
Scalability	+++	+++	++	++	++
Yield	+++	++	++	+	++
VLP complexity	+	++	+++	++	++

2.7 Baculovirus

Baculoviruses are enveloped, rod-shaped viruses that infect and replicate in insect cells. The genome consists of double-stranded circular DNA ranging from 80 to 180 kb in size, while the diameter and length of the viral particles are 30 to 60 nm and 250 to 300 nm, respectively. (Contreras-Gómez et al., 2014). Baculoviruses exist in two phenotypes, occlusion derived virions

(ODVs) and budded virions (BVs). ODVs are packaged into a crystalline protein matrix known as an occlusion body (OB), made from the polyhedrin protein and mostly exist in the external environment **(Figure 10)** (Jehle et al., 2006). ODVs are responsible for spreading the virus from one host to another. BVs, however, allow the virus to spread within host cells to produce more viruses (Jehle et al., 2006).

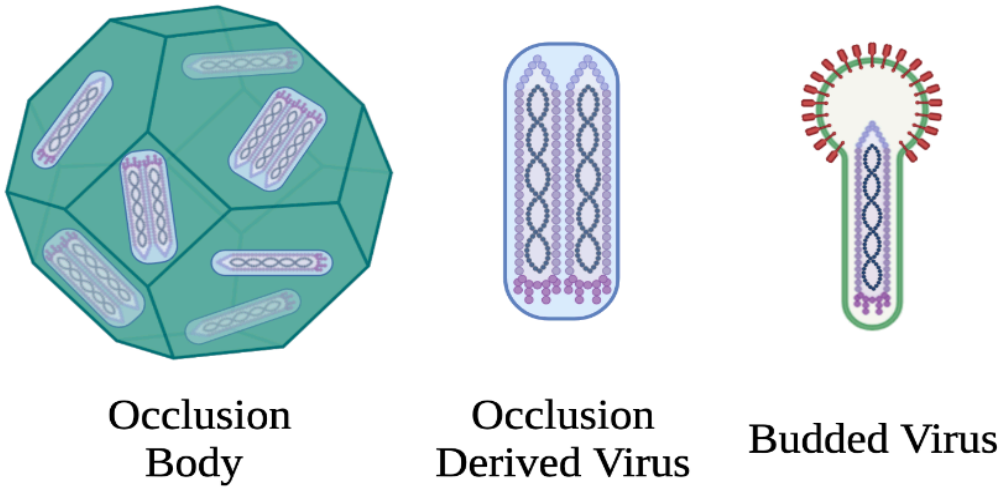

Figure 10: Morphology of baculoviruses. Two phenotypes of baculovirus: 1) occlusion derived virus infects different hosts. 2) Budded virus spreads virus between host cells.

The baculovirus infection cycle is biphasic, consisting of a primary and secondary infection. The primary infection is initiated when OBs are ingested by insects, followed by the release of ODVs and infection of the midgut epithelial cells. Replicated viruses are subsequently formed and bud out of the host cell to form the BVs that initiate secondary infections in nearby cells (Kelly et al., 2007). Upon infection, the baculovirus gene expression occurs in four phases:

immediate-early phase, delayed-early phase, late phase, and very-late phase (Contreras-Gómez et al., 2014). The immediate-early and delayed-early phases include the expression of transcriptional activators and other factors that are required for DNA replication. During the late phase, the production of nucleocapsids occurs. The very-late phase involves the expression of two essential proteins for the formation and release of OBs called polyhedrin and p10, respectively **(Figure 11)** (Ikeda et al., 2015; Contreras-Gómez et al., 2014).

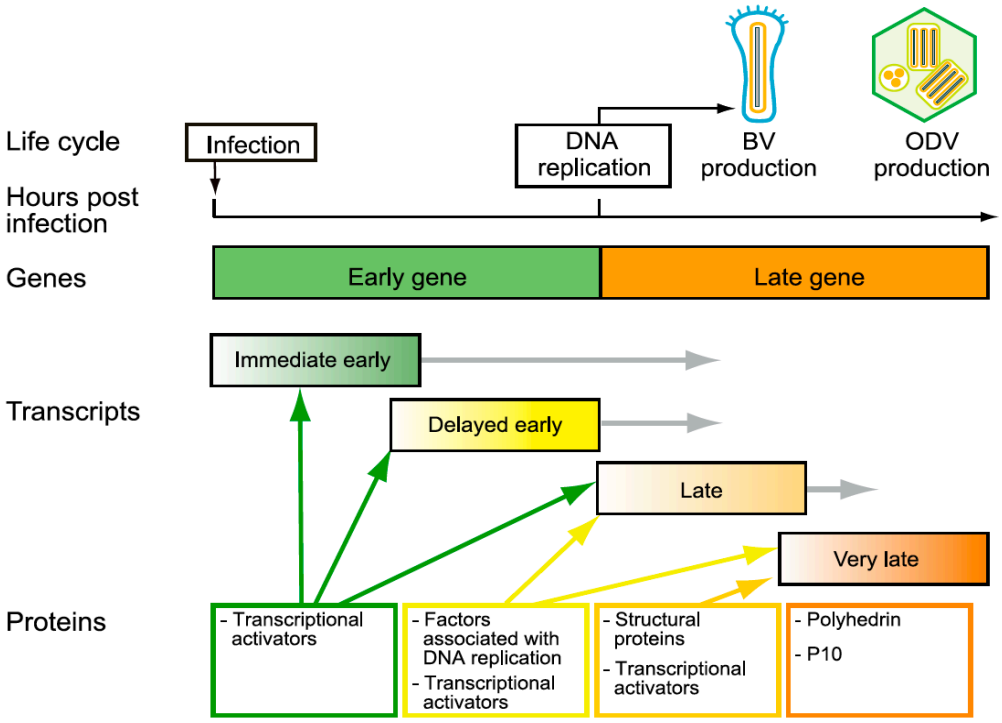

Figure 11: Baculovirus gene expression occurring in the early and late phases. Early phase is divided into immediate, early and delayed early. Late phase is divided into late and very late phases.

2.7.1 IC-BEVS

The IC-BEVS is a system used to express large quantities of recombinant proteins using baculoviruses. The IC-BEVS consists of three parts: i) a donor plasmid containing the gene(s) of interest; ii) baculovirus vector; iii) insect host line (Hitchman et al., 2011). *Spodoptera frugiperda* clonal isolate 21 (Sf21) and *Spodoptera frugiperda* clonal isolate 9 (*Sf9*) are commonly used insect cell lines derived from ovarian tissue of fall armyworms (Vaughn et al., 1977; Jarvis, 2009). A frequently used baculovirus is *Autographa californica multinucleopolyhedrovirus* (AcMNPV) (Hitchman et al., 2019). AcMNPV along with other baculoviruses, produce large amounts of OBs during viral infection. The formation of OBs and transmission of baculoviruses from insect-to-insect require polyhedrin and p10, which are produced in copious amounts during the very late stage of infection under the very strong, very late polyhedrin (polh) promoter and p10 promoter, respectively (van Oers, 2011). In fact, more than half of the total protein content found inside cells during the end of the infectious cycle is polyhedrin (Jarvis, 2009). Smith et al. (1983), however, demonstrated that the polyhedrin protein is not essential for baculovirus replication. The IC-BEVS exploits this by removing the polyhedrin and p10 gene and replacing it with a gene(s) of interest to generate large amounts of the desired protein(s). In addition, since BVs do not require the polyhedrin or p10 protein, replacing the polyhedrin and p10 gene does not affect BV synthesis (Hitchman et al., 2009).

2.7.2 IC-BEVS for VLP Production

There has been success in the production of VLP-based vaccines using the IC-BEVS such as the human papillomavirus VLP vaccine, Cervarix (Deschuyteneer et al., 2010). Furthermore, VLP-based vaccine candidates for several diseases including HIV, influenza virus, Chikungunya virus, Ebola virus, dengue fever virus, Norwalk virus and more, have been successfully produced using the IC-BEVS (Nooraei et al., 2021). VLP production using the IC-BEVS is advantageous compared to a yeast or bacterial system since insect cells undergo similar PTMs as mammalian cells such as protein folding, oligomerization, phosphorylation, glycosylation, etc. (F. Liu et al., 2013). Glycosylation is critical because the release of enveloped VLPs is dependent on the expression of glycoproteins and play a role in stabilizing the VLPs (Nooraei et al., 2021). In addition, PTMs such as glycosylation and phosphorylation are crucial because they are often necessary for an appropriate immune response to be stimulated (Nooraei et al., 2021). Glycosylation in the IC-BEVS however, is much simpler than the glycosylation patterns in mammalian cells (Nooraei et al., 2021). The main disadvantage of the IC-BEVS is that the production of VLPs occur concurrently with enveloped baculoviruses, which requires a purification step upon VLP formation (Fuenmayor et al., 2017).

VLP production using the IC-BEVS can be accomplished using two strategies: co-infection or co-expression. The co-infection approach (or monocistronic) involves the infection of insect cells using multiple baculoviruses, each carrying a different gene. In contrast, the co-expression approach (or polycistronic) uses a single baculovirus carrying multiple genes (Sokolenko et al., 2012). The co-expression strategy ensures that each infected cell contains all the necessary structural proteins to form VLPs (F. Liu et al., 2013). A study conducted by Vieira

et al. (2005) explored the production of triple layered rotavirus VLPs where the co-expression method was used in comparison to co-infection. The study demonstrated that co-expression resulted in higher DNA replication rates, higher stability among the three mRNAs and an equal ratio between the proteins which resulted in a more efficient production of rotavirus VLPs (Vieira et al., 2005). Furthermore, studies have been conducted demonstrating that the infection of insect cells using a single recombinant baculovirus containing the S, E and M genes for SARS-CoV resulted in high expression of all three proteins and the formation of SARS-CoV VLPs (Mortola & Roy, 2004; Ho et al., 2004). The self-assembly of enveloped VLPs can be explained in two steps: i) formation of the capsid and ii) budding out of the cell or release via exocytosis. The lipid membrane that coats enveloped VLPs are derived from the cell membrane of the insect cells. Non-enveloped VLPs, however, are only formed by the structural proteins expressed inside the insect cells (F. Liu et al., 2013).

2.7.3 Bac-to-Bac BEVS

The Bac-to-Bac BEVS is an approach that involves genetic transposition of a gene(s) of interest from a donor plasmid into a copy of the AcMNPV genome, also referred to as the 'bacmid'. This system was developed in the 1990s and is now marketed by Invitrogen (Carlsbad, CA) (Luckow et al., 1993). Five different donor plasmids can be used in the Bac-to-Bac system including pFastBac1, pFastBac Dual, pFastBacHT-A, pFastBacHT-B and pFastBacHT-C (H. Shang et al., 2017). All of these plasmids contain one polyhedrin promoter except for pFastBac Dual, which includes an additional p10 promoter. These plasmids all contain a left and right transposon element (Tn7L and Tn7R) that flanks the promoter and gene(s) of interest. This

system also uses DH10Bac competent *Escherichia coli* (*E. coli*) cells containing the bacmid and a helper plasmid that aids in the transposition process (Jarvis, 2009). The system begins with the transformation of a donor plasmid containing a gene(s) of interest into the DH10Bac *E. coli* cells. Upon transformation, the promoter, and gene(s) of interest are transposed into a specific site on the plasmid known as 'attTn7' to form a recombinant bacmid. The recombinant bacmid is further transfected into insect cells, which leads to the production of recombinant baculoviruses **(Figure 12)** (Jarvis, 2009). The recombinant baculoviruses can be used to infect insect cells to produce recombinant proteins.

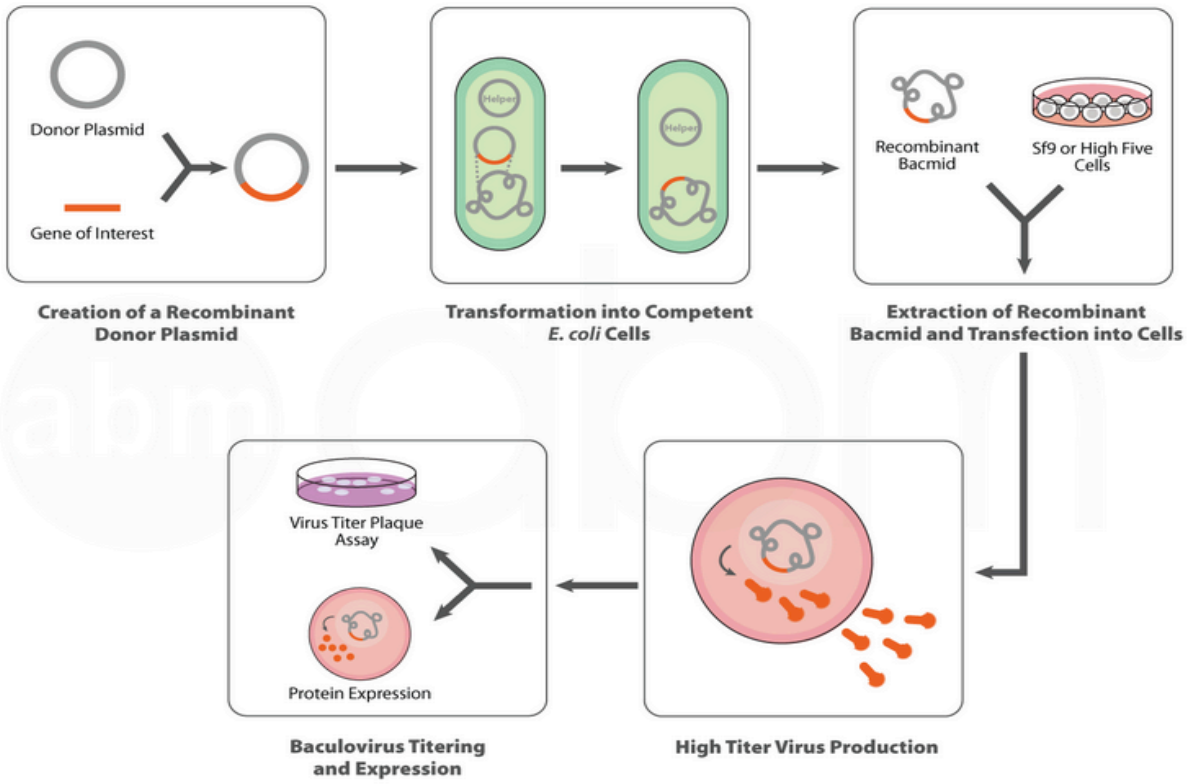

Figure 12: Bac-to-Bac BEVS Schematic.

Chapter 3: Materials and Methods

3.1 Cell Culture Maintenance

Spodoptera frugiperda isolate 9 (*Sf9*) cells were maintained in SF900-III Serum-free media (Gibco) and kept in suspension at 37ºC at 130 revolutions per minute (RPM). The cells were passaged at a density of $0.4x10^6$ to $0.6x10^6$ cells/mL in 125 mL shaker flasks with a total working volume of 30 mL. The cell density and viability were measured using trypan blue dye exclusion and analyzed with Countess II automated cell counter (ThermoFisher Scientific).

3.2 Construction of SARS-CoV-2 and Universal S, E and M plasmids for IC-BEVS

The construction of plasmids containing the S, E, and M protein sequences for SARS-CoV-2 and consensus sequences for SARS betacoronavirus S, E and M proteins were performed *in silico* using the SnapGene software (Insightful Science). The consensus sequences were provided by the Doxey Lab and were based on SARS-CoV, MERS-CoV and SARS-CoV-2. The sequences were codon optimized for insect cells and cloned into the pFastBac Dual plasmid.

The S protein sequences were inserted downstream of the p10 promoter. The E and M protein sequences were connected by a porcine teschovirus-1 2A (P2A) self-cleaving peptide sequence and inserted downstream of the polyhedrin (polh) promoter. The final constructs containing the S, E and M protein sequences for SARS-CoV-2 and universal SARS betacoronaviruses were ordered from GenScript (GenScript Biotech) and stored at -20ºC.

3.3 Production and Amplification of Recombinant Baculoviruses

3.3.1 Production of Competent DH10Bac *E. coli* Cells

A glycerol stock of DH10Bac *E. coli* cells were streaked onto an LB plate and grown overnight at 37ºC. A single colony of *E. coli* cells was inoculated to a 5 mL starter culture of LB and grown on a shaker at 37ºC overnight. Twenty-five mL of LB media was inoculated with 250 µL of starter culture and the optical density (OD) was measured until it reached 0.35-0.4, in which the cells were immediately placed on ice for 20-30 min. The culture was transferred to ice cold centrifuge bottles and spun at 3000xg for 15 min at 4ºC to harvest the cells. The supernatant was removed, and the pellet was resuspended in 25 mL of ice cold $MgCl_2$ before being spun down at 2000xg for 15 min at 4ºC. The supernatant was removed, and the pellet was resuspended in 50 mL of ice cold $CaCl_2$ and placed on ice for 20 min. The culture was centrifuged at 2000xg for 15 min at 4ºC again, and the supernatant was removed before resuspending the pellet in 50 mL of ice cold 85 mM $CaCl_2$, 15% glycerol. The culture was transferred to a new centrifuge tube and spun down at 1000xg for 15 min at 4ºC. The supernatant was removed, and the pellet was resuspended in 2 mL of ice cold 85 nM $CaCl_2$, 15% glycerol. One hundred µL aliquots of the suspended cells were transferred to 1.5 mL microfuge tubes and snap frozen with liquid nitrogen and stored in -80ºC.

3.3.2 Transformation of *E. coli*

Competent DH10Bac *E. coli* cells were thawed, and 100 ng of the SEM plasmid was added to 100 µL of the cells before incubation on ice for 30 min. The tube containing the cells and plasmid was heat shocked in a water bath at 42ºC for 45 s and immediately transferred to ice

for 2 min. Nine hundred μL of room temperature Super Optimal broth with Catabolite repression (SOC) media was added to the tube and placed on shaker at 37ºC at 225 rpm for 4 hr. One hundred μL of the transformed cells were added and spread on a LB agar plate containing 7 μg/mL carbenicillin, 10 μg/mL tetracycline, 50 μg/mL kanamycin, 40 μg/mL IPTG and 100 μg/mL of x-gal before incubation at 37ºC for 48 hr. Blue-white screening was performed, and white colonies were isolated by restreaking them on a different LB agar plate.

3.3.3 Isolation of Recombinant Bacmid

A single white colony was used to inoculate 4 mL of LB media containing 50 μg/mL kanamycin, 50 μg/mL carbenicillin, and 50 μg/mL tetracycline in a 15 mL Falcon tube. The tube was placed on a shaker set at 220 rpm and grown at 37ºC overnight. One point five mL of the culture was transferred into a 1.7 mL microcentrifuge tube and centrifuged at 14,000xg for 1 min. The supernatant was removed and 300 μL of Qiagen buffer P1 was used to resuspend the pellet. Then, 300 μL of Qiagen buffer P2 was added to the tube and incubated at room temperature for 5 min. Next, 300 μL of Qiagen buffer P3 was slowly added to the tube and gently mixed before placing it on ice for 5-10 min. The tube was centrifuged for 10 min at 14,000xg. The supernatant was transferred to a different 1.7 mL microcentrifuge tube containing 800 μL of isopropanol, gently mixed by inverting the tube, and placed on ice for 5-10 min. The tube was centrifuged at 14,000xg for 15 min. The supernatant was removed and 500 μL of 70% ethanol was added to wash the pellet. The tube was centrifuged at 14,000xg for 5 min and the

washing step was repeated. The supernatant was removed, and the pellet was air dried for 5-10 min before resuspending it in 40 μL of sterile milliQ H_2O. The sample was stored at 4ºC.

3.3.4 Transfection of *Sf9* Cells and P0 Baculovirus Production

Sf9 cells were prepared for transfection by diluting them with pre-warmed SF900-III Serum-free media (Gibco) to a cell density of $0.4x10^6$. Two mL was aliquoted to each well of a 6-well plate. The plate was rocked side-to-side and front-to-back to distribute the cell culture on the surface evenly. The plate was left at room temperature for 20-30 min to allow for cell attachment before transfection. To prepare the bacmid DNA and transfection reagent, 1 μg of the bacmid DNA was diluted with tissue grade sterile water to a final volume of 100 μL. Two μL of Escort IV Transfection Reagent was diluted with 97 μL of SF900-III Serum-free media (Gibco). The diluted Escort IV and diluted DNA mixture was mixed (1:1) by gentle pipetting and incubated for 15-30 min at room temperature. To transfect the *Sf9* cells, the medium in each well was aspirated with a serological pipette and 800 μL of fresh, pre-warmed SF900-III media (Gibco) was added to the cells. Then, 0.2 mL of the DNA/Escort IV lipid complex was added dropwise to each well and the plate was swirled gently for even distribution. The plate was incubated at 27ºC for 4-6 d under non-humified conditions. The passage 0 (P0) baculovirus stock was harvested and centrifuged at 1000xg for 10 min to pellet the cells and debris. The supernatant was transferred to a fresh tube and stored at 4ºC in the dark.

3.3.5 Amplification of P0 to P1 Baculovirus Stock

Sf9 cell culture was diluted with SF900-III media (Gibco) to a cell density of $1.5x10^6$ cells/mL and 25 mL was aliquoted into a 125 mL shaker flask. Next, 250 µL of the P0 baculovirus stock was added to the flask and placed onto a shaker platform and incubated at 27ºC at 130 rpm for 3-4 d. The cells were harvested and transferred into a 50 mL falcon tube and centrifuged at 1200xg for 10 min at room temperature. The supernatant was transferred into a new 50 mL falcon tube and stored at 4ºC in the dark.

3.4 Determination of Baculovirus Titers using End-point Dilution Assay

Baculovirus titers were determined by performing an end-point dilution assay using p6.9 monomeric Azami-Green (mAG) *Sf9* cells. Briefly, the virus stock was serially diluted from 10^{-4} to 10^{-10} and 100 µL of each virus dilution was inoculated into 12 replicate cell cultures on a 96-well plate. The plates were then analyzed for green fluorescence using a fluorescence microscope at 7 d post-infection. The number of infected and uninfected wells were recorded and used to calculate the virus titer. The assay was performed in duplicates and the two calculated titers were used to calculate an average titer.

3.5 Production of SARS VLPs

Sf9 cells were passaged at a density of $2x10^6$ cells/mL and infected with the recombinant baculovirus stock at a multiplicity of infection (MOI) of 5. The volume of virus added to the cell culture was calculated based on the desired MOI and virus titer **(Appendix D)**. At 72 hours post-infection (hpi), the infected cell culture was transferred to a 50 mL falcon tube and spun at 500xg

for 10 min in a centrifuge (Eppendorf). The supernatant was collected and stored at 4ºC for further experiments. Next, 2.4 mL of CytoBuster™ protein extraction reagent (ThermoFisher Scientific) was added to the cell pellet and spun at 4000xg for 20 min using a centrifuge (Eppendorf). The resulting cell lysate was collected and stored at 4ºC for further experiments.

3.6 Tracking Cell Infection

3.6.1 Cell Density and Viability

To track the density and viability of the infected *Sf9* cells, a sample of the infected cell culture was analyzed at 24, 48 and 72 hpi. Briefly, 50 µL of the infected cell culture was mixed with a trypan blue solution and placed into a hemocytometer upon analysis using the Countess II automated cell counter (ThermoFisher Scientific).

3.6.2 Flow Cytometry Analysis

The infected *Sf9* cells were analyzed at 24, 48 and 72 hpi using the BD FACS Calibur Flow Cytometer (BD Biosciences). The sample was prepared by transferring 1 mL of the infected cell culture into a 1.7 mL microcentrifuge tube and centrifuged at 300xg for 10 min. The supernatant was discarded, and the cell pellet was resuspended using 1 mL of 2% paraformaldehyde solution and incubated in the dark at 4ºC for 30 min. The sample was then transferred to a cytometer tube and diluted using 2 mL of PBS. The BD FACS Calibur Flow Cytometer (BD Biosciences) was used to measure the forward scatter (FSC) and side scatter (SSC) to indicate the relative size and complexity/granularity of the cells, respectively. The results were analyzed using the FlowJo software (BD Biosciences).

3.7 Semi-purification of SARS-CoV-2 VLPs

3.7.1 Sucrose Cushion Ultracentrifugation

The sample was filtered using a 0.22 um filter and a 10 mL syringe before being ultracentrifuged using a 25% sucrose cushion. Briefly, 5 mL of the sample was added to a polyallomer (PA) tube (Beckman Coulter), followed by 1.5 mL of 25% sucrose solution and the remaining 5 mL of the sample. The samples were ultracentrifuged at 4ºC for 90 min at 26,000 rpm in a SW41 TI rotor using the Beckman Coulter Optima XPN-100 ultracentrifuge (Beckman Coulter). The supernatant was aspirated and 2 mL of 1X NTC solution was added to the PA tube to resuspend the pellet. The tube was placed in ice and placed on a shaker for 30 min before being further purified through an iodixanol density gradient.

3.7.2 Iodixanol Density Gradient Ultracentrifugation

The OptiPrep density gradient medium (Sigma-Aldrich) was diluted in 1X NTC solution (1M NaCl, 0.2M Tris-HCl pH 7.4, 50 mM $CaCl_2$) to prepare 10%-60% iodixanol solutions. An iodixanol gradient was prepared by layering 1.5 mL of each iodixanol solution to a thin wall PA tube (Beckman Coulter), starting with the most concentrated solution **(Figure 13)**. Next, 1 mL of 1X NTC solution was added to the gradient, followed by 2 mL of the resuspended virus pellet from the previous experiment. The sample was ultracentrifuged in a SW41 TI rotor using the Beckman Coulter Optima XPN-100 ultracentrifuge (Beckman Coulter) at 4ºC for 2.5 hr at 35,000 rpm. The tube was removed, and 1 mL fractions were collected by piercing the side of the tube using a 10 mL syringe. A total of 12 fractions were collected where fractions 1 to 12 were

ordered from top to bottom of the tube **(Figure 13)**. The fractions were stored at 4ºC for further analysis.

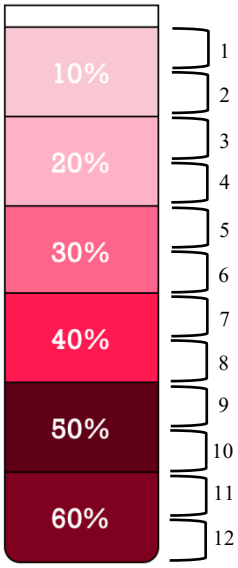

Figure 13: Iodixanol Density Gradient. Twelve fractions were obtained from top to bottom.

3.8 Characterization and Visualization of SARS VLPs and Baculoviruses

3.8.1 Sodium Dodecyl Sulfate – Polyacrylamide Gel Electrophoresis (SDS-PAGE)/Western Blot Analysis

Mini polyacrylamide gels were casted using the Tris-Glycine eXtended (TGX) Stain-Free FastCast Acrylamide Kit, 12% (Bio-Rad) according to the manufacturer's instructions. To prepare the sample buffer, 100 µL of b-mercaptoethanol was added to 900 µL of 4x laemmli sample buffer (BioRad). The 4x laemmli sample buffer (BioRad) was added to the samples at a 1:4 ratio and heated at 95ºC for 10 min. The samples were then loaded into separate wells and

the gel was run at 200 V for approximately 1-1.5 hr. The Trans-Blot Turbo Transfer System (Bio-Rad) was used to transfer the proteins from the TGX gels to a polyvinylidene difluoride (PVDF) membrane. Briefly, the membrane was blocked using 5% skim milk and washed with tris-buffered saline with 0.1% Tween20 detergent (TBS-T) (Sigma-Aldrich). The primary and secondary antibodies used to detect GP64 proteins were mouse anti-GP64 monoclonal (AcV5, ThermoFisher Scientific) and goat anti-mouse IgG HRP conjugate (BioRad), respectively. To detect the SARS-CoV-2 S, E and M proteins, the following primary antibodies were used: rabbit anti-spike S1, rabbit anti-envelope, and rabbit anti-membrane polyclonal (Novus Biologicals). The secondary antibody used for all 3 primary antibodies was goat anti-rabbit IgG HRP conjugate (Sigma-Aldrich). Enhanced chemiluminescence (ECL) imaging was performed using the Clarity Western ECL Substrate by Bio-Rad (contains peroxide reagent and luminol/enhancer reagent) and the ChemiDoc MP imager (Bio-Rad). The results were then analyzed using Image Lab Software (Bio-Rad).

3.8.2 Sandwich Enzyme-Linked Immunosorbent Assay (ELISA)

Mouse anti-GP64 monoclonal antibody (AcV5, ThermoFisher Scientific) was diluted in phosphate-buffered saline (PBS) as a coating buffer and added to each well on a 96-well plate and used as the capture antibody. PBS with 0.1% Tween20 detergent (PBS-T) (Sigma-Aldrich) and 5% skim milk were used as a washing and blocking buffer, respectively. The samples were prepared in 5% skim milk and added to each well for incubation at room temperature for 1 h. The plate was washed 3 times with PBS-T using a microplate washer (BioTek) and SARS-CoV-2 anti-spike S1 polyclonal antibody was used as the primary antibody and added to each well.

The plate was incubated at room temperature for 2 h. Goat anti-rabbit IgG secondary antibody, HRP conjugate (Sigma-Aldrich) was added to each well, incubated for 30 min and washed 3 times with PBS-T. The 3,3',5,5'-Tetramethylbenzidine (TMB) substrate was added to each well and incubated at room temperature for 30 min for colorimetric detection. Sulfuric acid (H_2SO_4) was used as a stop solution and added to each well before analyzing the plate at 450 nm using a plate reader (BioTek).

3.8.3 Detection of Baculoviruses via Infectious Assay

To determine whether fractions 1-12 contain infectious baculovirus particles, an end-point dilution assay (EPDA) was performed. Briefly, each fraction was serially diluted from 10^{-4} to 10^{-10} and 100 μL of each fraction dilution was inoculated into 12 replicate cell cultures (p6.9mAG *Sf9* cells) on a 96-well plate. The plates were analyzed using a fluorescence microscope at 7 d post-infection to detect for green fluorescence. The number of infected and uninfected wells were recorded to calculate virus titer.

3.8.4 Quantification of Baculovirus Particles using Flow Cytometry

Samples were prepared by diluting them to 10^{-1} and 10^{-2} in PBS buffer (without calcium and magnesium) and fixed with 2% paraformaldehyde at 4ºC for 1 hour. The samples were then freeze-thawed at -80ºC for 30 min before being permeabilized with 10% Triton X-100 for 5 min. The SYBR Green I Nucleic Acid stain was then added to the samples and heated in a water bath in the dark at 80ºC for 10 min. Flow-Set Fluorospheres (Beckman Coulter) were used for calibration and the samples were then placed in ice before being analyzed in triplicates using the BD Accuri C6 Plus Flow Cytometer (BD Biosciences). The flow cytometer was set to analyze

the samples at a flow rate of 35 μL/min with a 30 s run limit. The results were analyzed using the FlowJo software (BD Biosciences).

3.8.5 Visualization of SARS-CoV-2 VLPs via Transmission Electron Microscopy

Fractions that contained the S and M proteins (F4-F7) were visualized via transmission electron microscopy (TEM). Twenty μL of the samples were added onto Electron Microscopy Sciences carbon-coated copper grids (ThermoFisher Scientific) and incubated for 1-2 min. Whatman® Cellulose Filter Paper was used to filter the sample solution from the grid. The samples were then washed by adding 40 μL of MilliQ water and left for 1 min before being removed with the filter paper. The grids were then stained by adding 20 μL of 2% phosphotungstic acid (PTA) and left for 1 min at room temperature before being removed using the filter paper. To remove the stain, 40 μL of MilliQ water was used to wash the stain off and repeated 5 times. The samples were left to air dry overnight before being imaged using the Philips CM10 transmission electron microscope at a magnification of 64 000X.

Chapter 4: Results

4.1 Tracking Cell Infection

To produce the SARS-CoV-2 VLPs, recombinant baculoviruses expressing the SARS-CoV-2 S, E, and M proteins were used to infect *Sf9* insect cells. The cell densities and viabilities were measured at 24, 48, and 72 hpi in order to track the infection. cell densities and viabilities were determined at 24, 48, and 72 hpi. The cell density of uninfected cells approximately doubled every 24 h, whereas the density of infected cells remained relatively stable at approximately $2x10^6$ cells/mL at 24, 48, and 72 hpi **(Figure 14)**. This data shows that infection of cells had occurred, and cell replication had halted as the infection progressed.

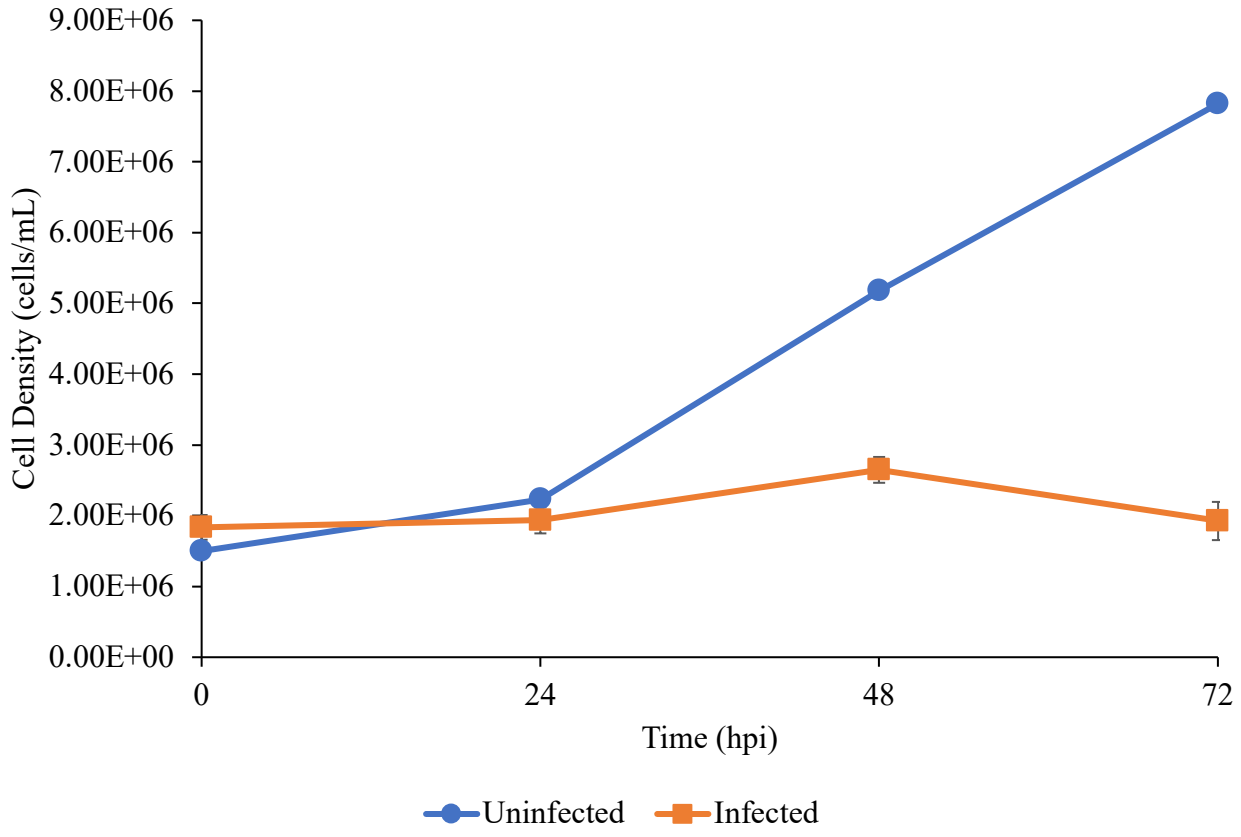

Figure 14: *Sf9* cell density at 24, 48, and 72 hpi. *Sf9* cells were infected with rBEV containing SARS-CoV-2 S, E and M protein sequences. Error bars represent the range of duplicate flasks.

In contrast, the trend for cell viability is opposite to the trend for cell density. The cell viability for uninfected cells remained at approximately 99%, however, the viability of infected cells decreased starting at 24 hpi **(Figure 15)**. This data indicates that cell infection had occurred which resulted in cell death as the infection progressed overtime.

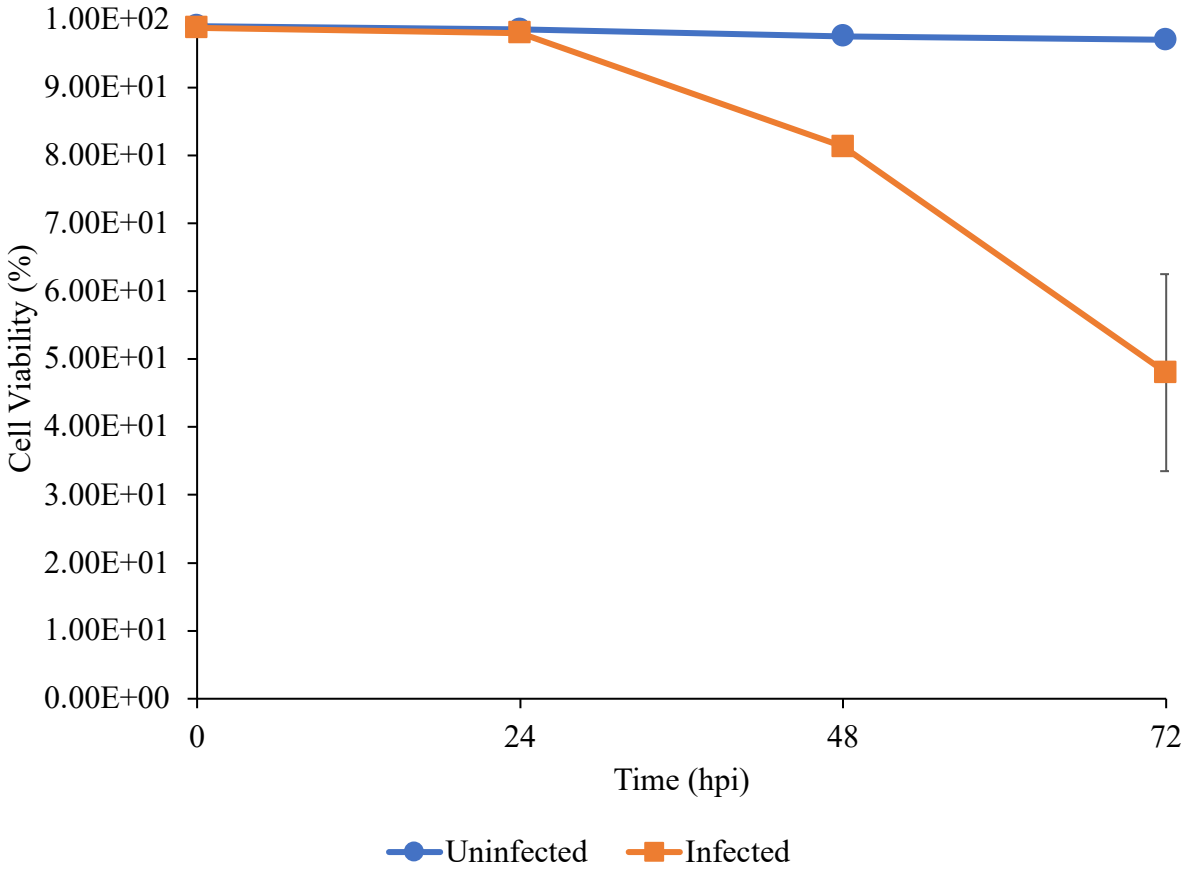

Figure 15: *Sf9* cell viability at 24, 48, and 72 hpi. *Sf9* cells were infected with rBEV expressing SARS-CoV-2 S, E and M proteins. Error bars represent the range of duplicate flasks.

Flow cytometry analysis was done to track cell infection at 24, 48, and 72 hpi. The x-axis represents forward scatter (FSC) which is a measure of cell size **(Figure 16)**. FSC detects light as it scatters through the cell, which measures the diameter of the cell. The y-axis represents side scatter (SSC), which measures cell complexity. SSC detects light that is refracted or reflected off of internal structures inside the cell, which measures the internal complexity of the cell. The

population of infected cells shown in blue in **Figure 16** can be seen shifting towards the right and higher up on the y-axis, indicating an increase in cell size and complexity, respectively. These results were expected as cell size and complexity generally increase as the cell becomes infected over time. The cell size and internal complexity increased over the course of the infection as the virus replicated inside the cell and took over the cell's machinery. Viral replication takes place inside the cell and leads to the swelling of the cell and eventual lysis as the replicated viruses are released from the cell. The increase in cell size and internal complexity suggested that cell infection by the recombinant baculoviruses had occurred.

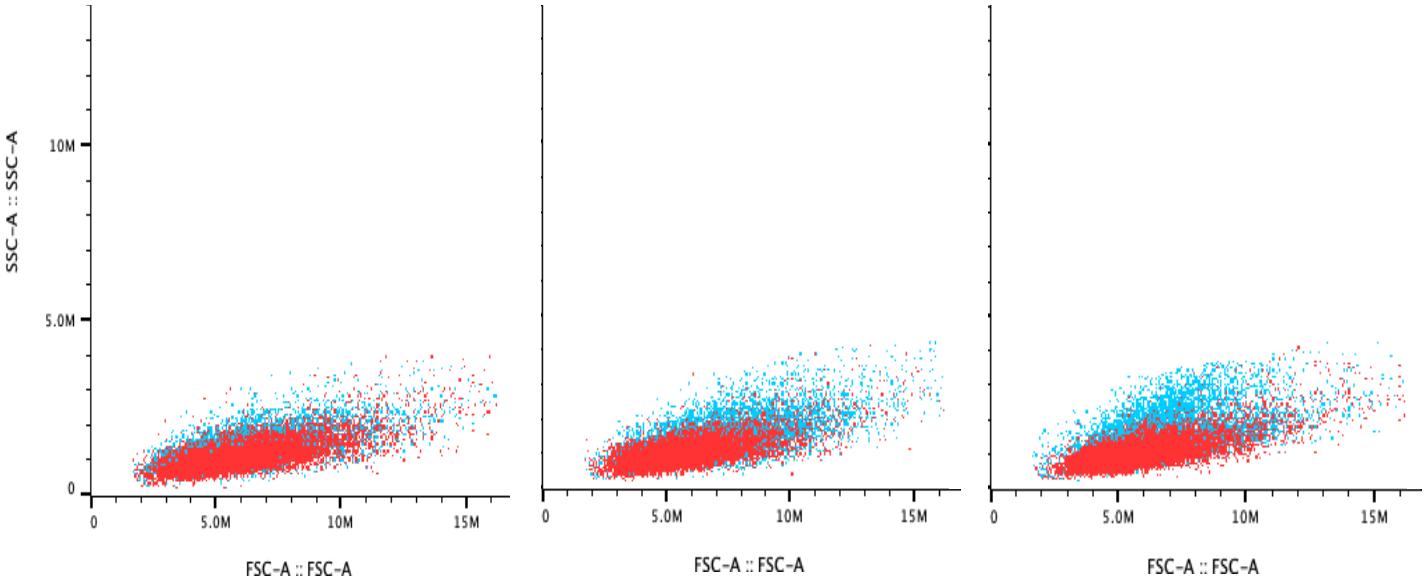

Figure 16: Flow cytometry analysis of *Sf9* cells at 24, 48, and 72 hpi. Red population represents uninfected *Sf9* cells. Blue population represents *Sf9* cells infected with rBEV expressing SARS-CoV-2 S, E and M proteins.

4.2 Detection of SARS-CoV-2 VLPs

The SARS-CoV-2 S, E, and M protein was detected in the supernatant and *Sf9* cell lystate via western blot analysis **(Figure 17)**. S protein trimers were detected in the supernatant as seen from the band above 250 kDa. This indicates that the generated S proteins are functional as they are able to trimerize. The molecular weight of S protein monomers are approximately 140 kDa, which was detected in the cell lysate **(Figure 17A)**. The presence of S protein trimers in the supernatant was expected since the VLPs secreted into the supernatant carry S protein trimers on its outer surface. However, since baculoviruses are also produced inside the cell, it is possible that the S proteins seen in the supernatant are being carried by contaminating baculoviruses instead. The absence of trimers in the cell lysate was also expected since a denaturing agent was used for SDS-PAGE. Meanwhile, S protein monomers were expected to be in the cell lysate since they are produced inside the cell before trimerization. The absence of monomers in the supernatant, however, was not expected. Since a denaturing agent was used during SDS-PAGE, the trimers should have been broken down into its monomeric form. This may be due to insufficient use of denaturing agent or a short heating time during SDS-PAGE which were unable to break down the trimers.

Bands at approximately 55 kDa in the supernatant and cell lysate were detected, which may have been a result of E protein oligomerization **(Figure 17B)**. Specifically, these bands may potentially indicate pentamers, as 55 kDa is the approximate size of five E protein monomers. Alternatively, this band could be uncleaved E and M proteins as they interact with each other during VLP formation. Additional bands around 20 and 22 kDa were detected in the cell lysate, which corresponds to the size of E protein dimers **(Figure 17B)**. The E protein band in the cell

lysate is significantly more concentrated than the band seen in the supernatant. This is expected because E proteins are produced in high amounts in the cell, however, only a small amount is included in the VLPs. The SARS-CoV-2 M protein was also detected in the supernatant and cell lysate at approximately 22 kDa **(Figure 17C)**. The size of these bands corresponds to the M protein, which is approximately 20-25 kDa in size.

The presence of S, E, and M protein in the cell lysate suggests that all three proteins are being generated inside the host cell. In addition, the presence of S, E, and M proteins in the supernatant suggests that SARS-CoV-2 VLP formation may have occurred since VLP assembly and release via exocytosis is required for these proteins to be present in the supernatant.

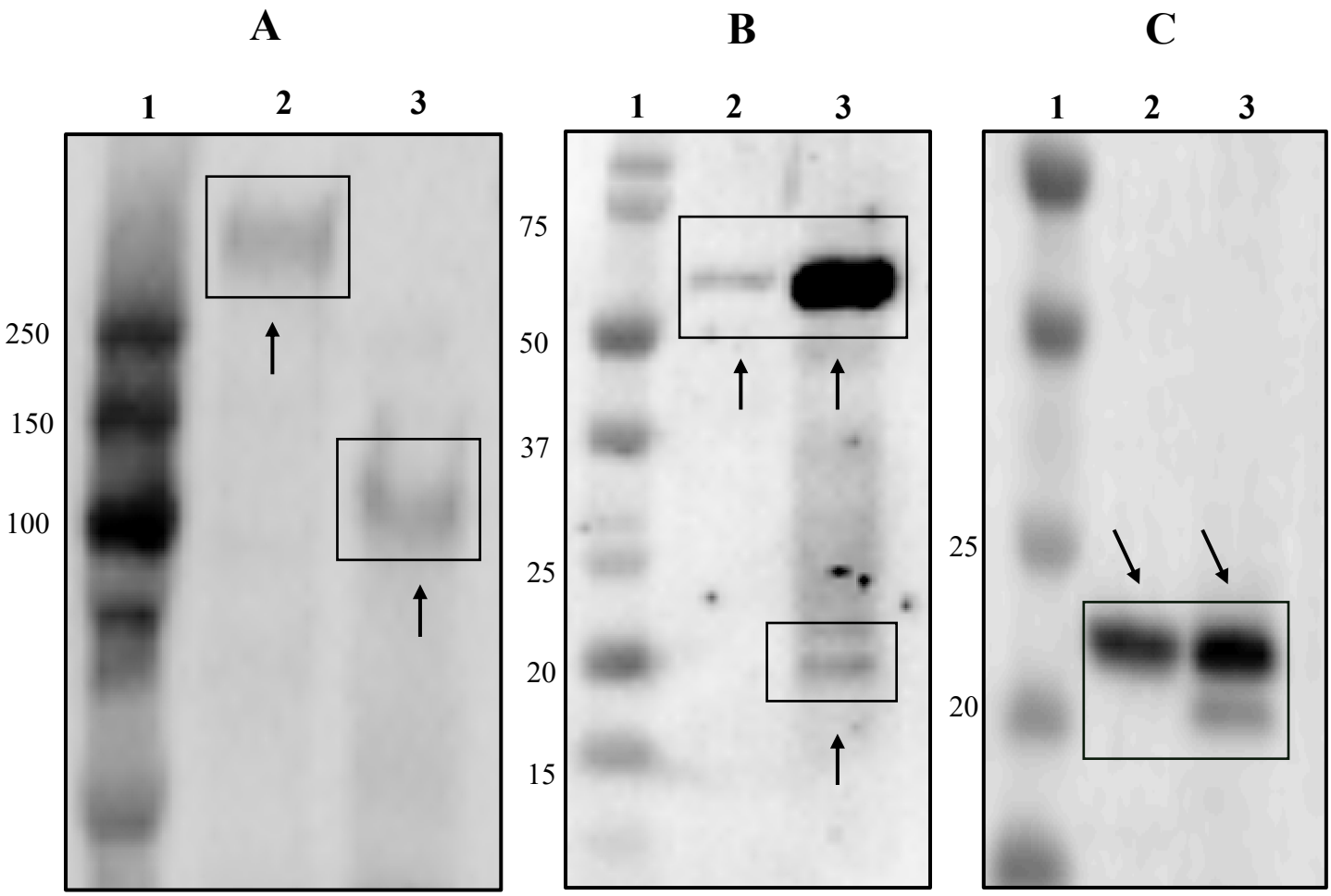

Figure 17: Western blot analysis to detect for SARS-CoV-2 VLPs. (A) Spike protein. (B) Envelope protein. (C) Membrane protein. Lane 1, protein ladder; lane 2, supernatant; lane 3, cell lysate.

4.3 Detection of SARS-CoV-2 VLPs and Baculoviruses after Semi-Purification

After semi-purification of VLPs using iodixanol gradient ultracentrifugation, 12 fractions were obtained. However, due to baculovirus contamination when VLPs are produced using the IC-BEVS, a western blot analysis was performed to detect for the major envelope protein of baculoviruses, GP64. GP64 is produced during baculovirus infection of *Sf9* cells.

Western blot analysis of GP64 proteins reveals the separation of GP64 proteins. GP64, approximately 64 kDa, are shown by the bands in fractions 4, 5, 6 and 7 **(Figure 18A)**. This data suggests that fractions 4, 5, 6, and 7 may contain baculovirus particles. However, since enveloped VLPs and baculoviruses both carry host cell-derived membranes, VLPs carrying GP64 proteins are also possible. For a more accurate testing of baculovirus presence, an infectious assay was performed to determine the presence of infectious baculovirus particles.

The detection for SARS-CoV-2 S protein was conducted via Western blot analysis. The results displayed bands at different molecular weights for fractions 3, 4, 5 and 6. Fractions 3 and 4 displayed bands greater than 250 kDa, most likely representing S protein trimers **(Figure 18B)**. Bands at approximately 140 kDa was observed for fractions 4 and 6, which corresponds to the size of S protein monomers. Fractions 4, 5 and 6 also displayed a band between 50 and 75 kDa, which corresponds to the size of the S1 subunit **(Figure 18B)**. The presence of these bands in fractions 3-6 indicate that VLPs have migrated to those fractions and are separated from other impurities.

A western blot analysis of SARS-CoV-2 membrane proteins was conducted to identify which fractions could potentially be a carrier of SARS-CoV-2 VLPs. The WB analysis resulted in bands seen in fractions 4, 5 and 6 at approximately 25 kDa **(Figure 18C)**, corresponding to the

approximate size of SARS-CoV-2 M protein. This evidence suggests that SARS-CoV-2 VLPs may be present in fractions 4, 5 and 6.

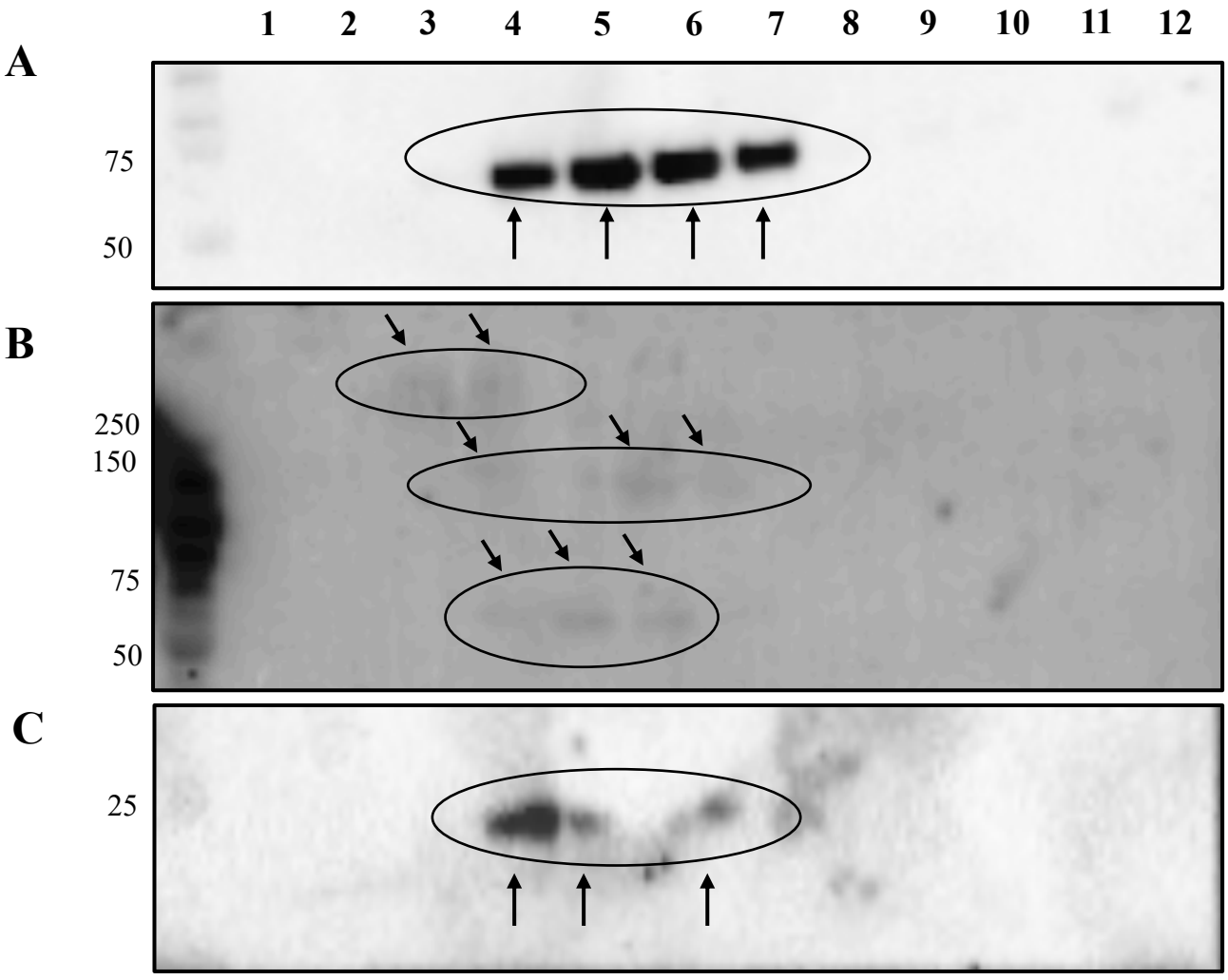

Figure 18: Western blot analysis to detect for SARS-CoV-2 VLPs and baculoviruses from purified fractions 1-12. (A) GP64 proteins. (B) SARS-CoV-2 spike proteins. (C) SARS-CoV-2 membrane proteins.

Although the GP64, S and M proteins was detected via western blot analysis, it was important to identify whether the proteins were actually carried by a viral particle or whether they were only free-floating proteins. To determine this, a sandwich ELISA was performed using anti-GP64 antibodies as the capture antibody and SARS-CoV-2 anti-spike antibodies as the detection antibody **(Figure 19)**. Samples taken from fractions 4-7 resulted in a signal being detected via colorimetric detection.

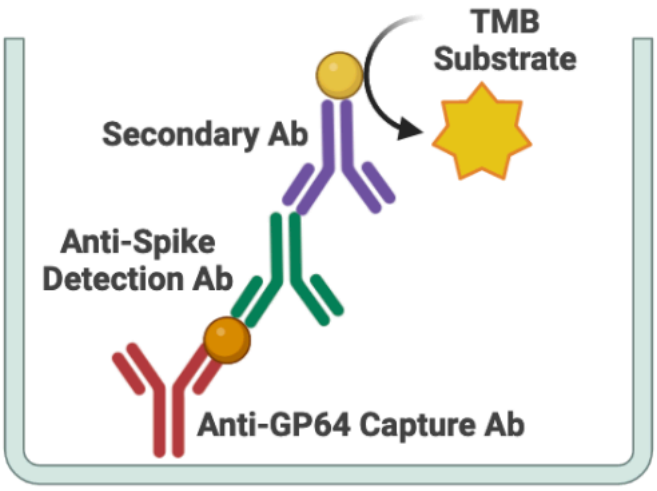

Figure 19: Schematic of sandwich ELISA. Red antibody represents the anti-GP64 capture antibody. Orange sphere represents the antigen. Green antibody represents the anti-spike detection antibody. Purple antibody represents the secondary antibody. Yellow sphere represents the HRP conjugate.

A sandwich ELISA was performed to identify whether the fractions containing GP64, and SARS-CoV-2 S proteins (F4-7) contain viral particles carrying the two proteins on its outer surface. Colorimetric detection was used in this experiment, and a color change was seen for fractions 4, 5, 6, 7 and the negative control as well (data not shown). The results indicated that the negative control resulted in an optical density (OD) of approximately 0.34, meanwhile fractions 4, 5, 6 and 7 resulted in an OD value of approximately 0.72, 0.49, 0.50 and 0.54, respectively **(Figure 20)**. In comparison to each other, fraction 4 resulted in the most intense signal meanwhile fractions 5, 6 and 7 showed similar signal intensities. This suggests that fraction 4 may be the fraction that contains the most viral particles containing either GP64 or SARS-CoV-2 S proteins.

Out of the four fractions that were tested (fractions 4-7), the OD value measured for fraction 4 was the highest at approximately 0.72, which was nearly double the OD value for the negative control at approximately 0.35 **(Figure 20)**. Fractions 5-7, however, displayed similar OD values to each other at approximately 0.50.

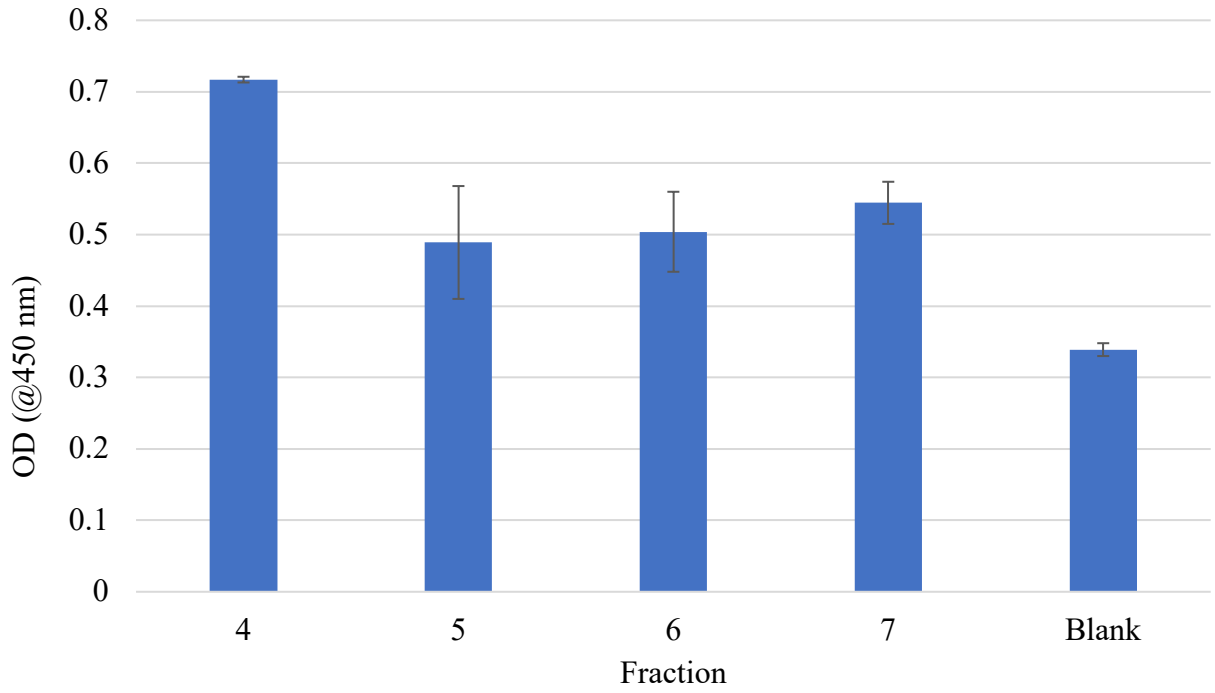

Figure 20: Detection of viral particles containing GP64 protein and SARS-CoV-2 spike protein via sandwich ELISA. Error bars indicate the range of duplicate readings.

To identify whether infectious baculovirus particles are present in fractions 1-12, an infectious assay was performed via EPDA. P6.9mAg *Sf9* cells were infected with each fraction and green fluoresence was seen in wells infected with fraction 5, 6 and 7, indicating those fractions contain infectious baculovirus particles. Fractions 1, 2, 3, 4, 8, 9, 10, 11 and 12 did not cause cell infection as no green fluoresence was detected, indicating that infectious baculoviruses are not present in those fractions. Baculovirus titers for fractions 5 and 7 were both approximately 2.6×10^4 pfu/mL, whereas fraction 6 resulted in a much lower baculovirus titer at approximately 7.9×10^3 pfu/mL **(Figure 21)**, suggesting a lower number of infectious baculovirus

particles. Typically, a high baculoivirus titer is expected (~ 10^7 or 10^8), however, the low titers detected in this experiment may indicate that majority of the baculovirus particles in these fractions are defective. No virus titer was calculated for fractions 1, 2, 3, 4, 8, 9, 10, 11 and 12 as a result of no cell infection.

Fractions 5-7 appeared to cause cell infection and contained low titer baculovirus particles **(Figure 21)**. Fraction 4 became the major focus since it contained GP64 proteins, S proteins and M proteins **(Figure 18)** but no infectious baculovirus particles **(Figure 21)**. To further determine whether baculovirus contamination exists in fraction 4, a SYBR green assay was performed to detect for any defective baculovirus particles.

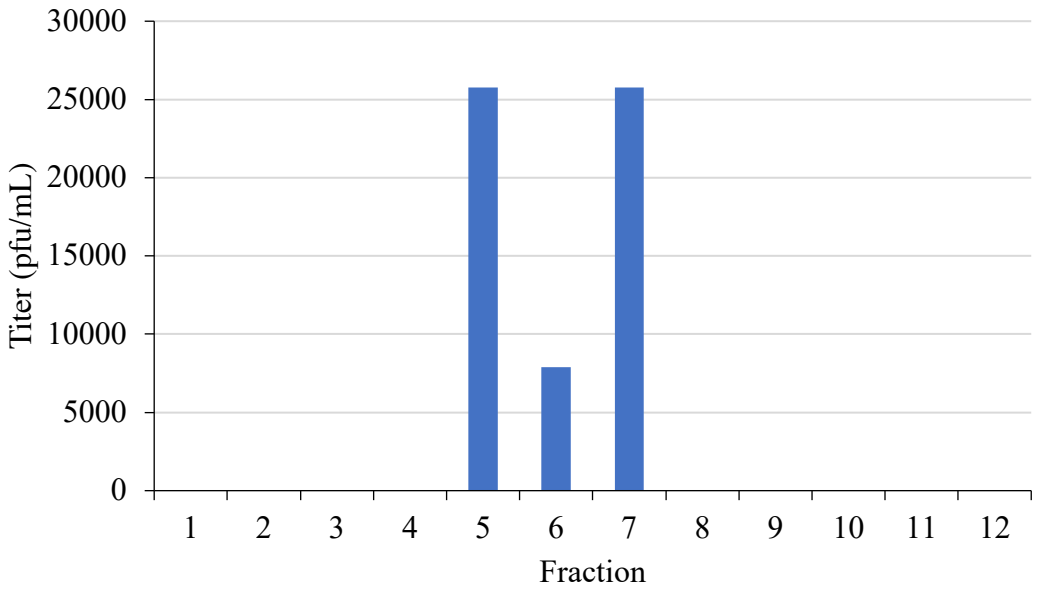

Figure 21: Baculovirus titers calculated for fractions 1-12 based on infectious assay.

A SYBR green assay was performed to quantify defective baculoviruses that were not detectable using an infectious assay. SYBR green I is a highly fluorescent nucleic acid specific dye that can stain baculovirus DNA and could therefore be used as a direct count of baculovirus particles (Shen et al., 2002). Fraction 4 was of particular interest since it contained GP64 proteins and SARS-CoV-2 S and M proteins, however, did not contain any infectious baculoviruses based on the infectious assay. A negative control containing no baculoviruses was included to determine background noise in the baculovirus gate **(Figure 22A)** and a positive control containing high titer (~1.5 x 10^8 pfu/mL) baculoviruses **(Figure 22B)** was included to compare it to fraction 4. The number of baculovirus events in the negative control was 0.099 compared to 0.41 in the positive control. The results for fraction 4 showed that the number of baculovirus events was 0.066 **(Figure 22C).** In comparison to the negative and positive control, the number of events in the baculovirus gate for fraction 4 was similar to the negative control, suggesting that no baculovirus particles may be present.

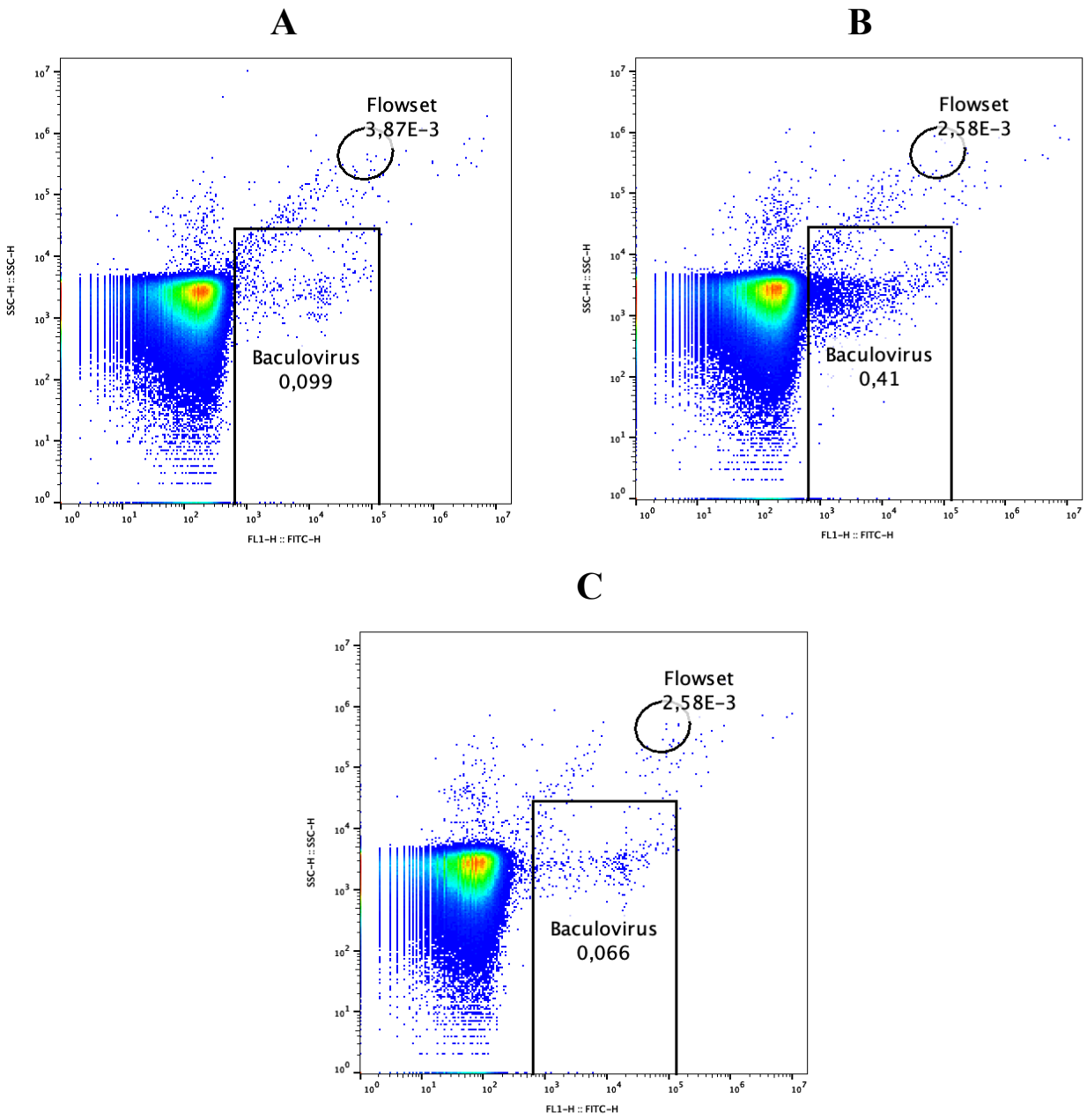

Figure 22: Quantification of Baculoviruses via SYBR green staining. (A) Negative control. (B) Positive control. (C) Fraction 4. Flowset gate was set to calibrate the flow cytometer and a baculovirus gate was set to determine the number of baculovirus events.

Based on the discussed experiments, fraction 4 was the purified fraction that was the main focus. To summarize, fraction 4 was found to contain GP64, S, and M proteins **(Figure 18)** and contained no infectious or defective baculovirus particles based on the infectious assay **(Figure 21)** and SYBR green assay **(Figure 22)**, respectively. In addition, the high OD value detected based on the sandwich ELISA **(Figure 20)** suggests there may be viral particles carrying GP64 and S proteins. If no baculovirus particles are present, fraction 4 may potentially contain VLPs carrying GP64 proteins, S proteins or a combination of both.

4.4 Visualization of SARS-CoV-2 VLPs

The separation of baculoviruses and VLPs in fraction 4 was further examined by visualization via TEM **(Figure 23)**. Vesicle-like structures with projections protruding on the outer surface are observed **(Figure 23A, 23B)**, indicating that SARS-CoV-2 VLPs may be present. The images obtained appeared to show no signs of baculovirus particles, which is consistent with the findings that no infectious and defective baculoviruses are present in fraction 4 based on an infectious assay and SYBR green assay, respectively. A TEM image of a negative control was also obtained **(Figure 23C)**, showing no vesicle-like structures or baculovirus particles.

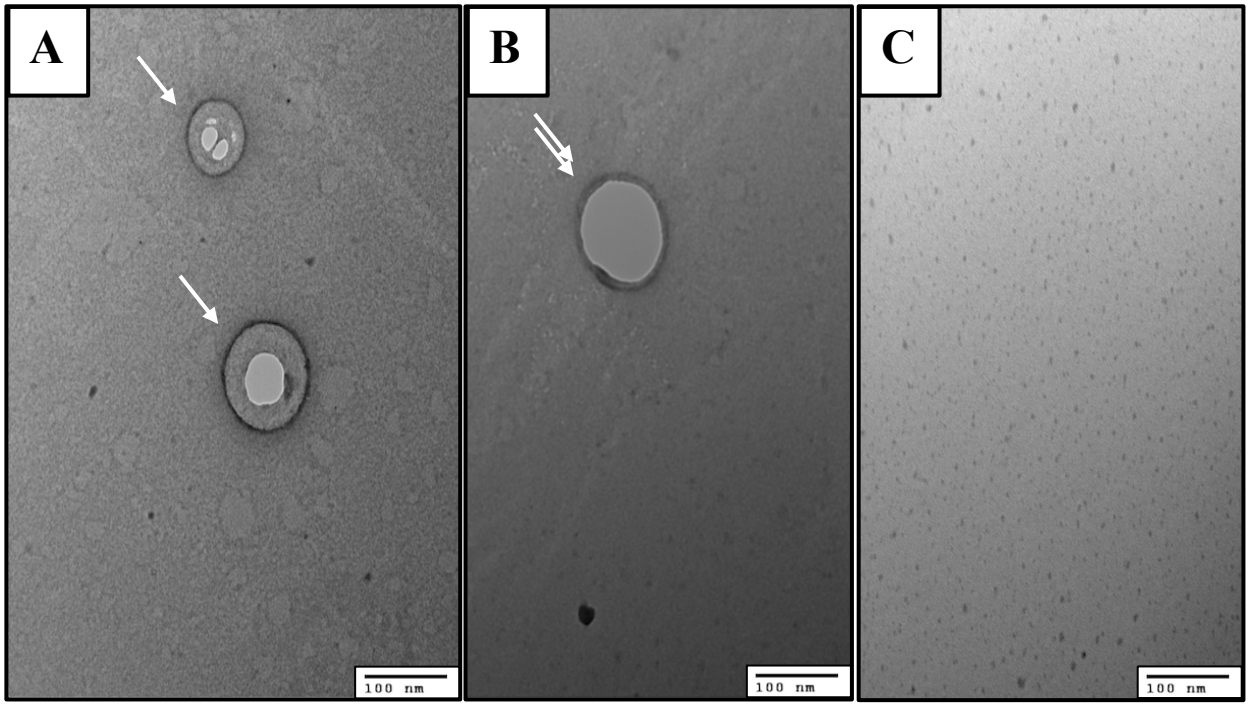

Figure 23: TEM images of purified fraction 4. (A) Image 1 from fraction 4. (B) Image 2 from fraction 4. (C) Negative control. White arrows point towards VLP-like structures. Scale bar = 100 nm.

4.5 Detection of Universal SARS Betacoronavirus VLPs

The universal SARS betacoronavirus S, E, and M protein was detected in the supernatant and *Sf9* cell lystate via western blot analysis **(Figure 24)**. Anti-S, anti-E, and anti-M antibodies against SARS-CoV-2 were used to detect the universal S, E, and M proteins, respectively. Trimeric universal S proteins were detected in the supernatant at a molecular weight that was greater than 250 kDa. Meanwhile, the cell lysate contained monomeric universal S proteins at approxamtely 140 kDa **(Figure 24A)**. The universal E and M proteins were also detected in the supernatant and the cell lysate **(Figure 24B, 24C)**. Universal E protein pentamers were detected

at approximately 55 kDa in the supernatant and cell lysate. Bands at approximately 37 kDa, 20 kDa, and 12 kDa were also detected in the cell lysate, which corresponds to the approximate sizes of E protein trimers, dimers, and monomers, respectively. Alternatively, the band at 55 kDa and 37 kDa may also be uncleaved E and M proteins **(Figure 24B)**. Universal M proteins were detected at approxamtely 22 kDa **(Figure 24C)**. The detection of the the universal E and M protein was expected, since their genetic sequences are the same as the SARS-CoV-2 E and M protein sequences as they are highly conserved among the three SARS betacoronaviruses. Overall, the presence of universal S, E and M proteins in the cell lysate and supernatant was promising, as it provides evidence that the universal VLPs are being assembled and released from the cell.

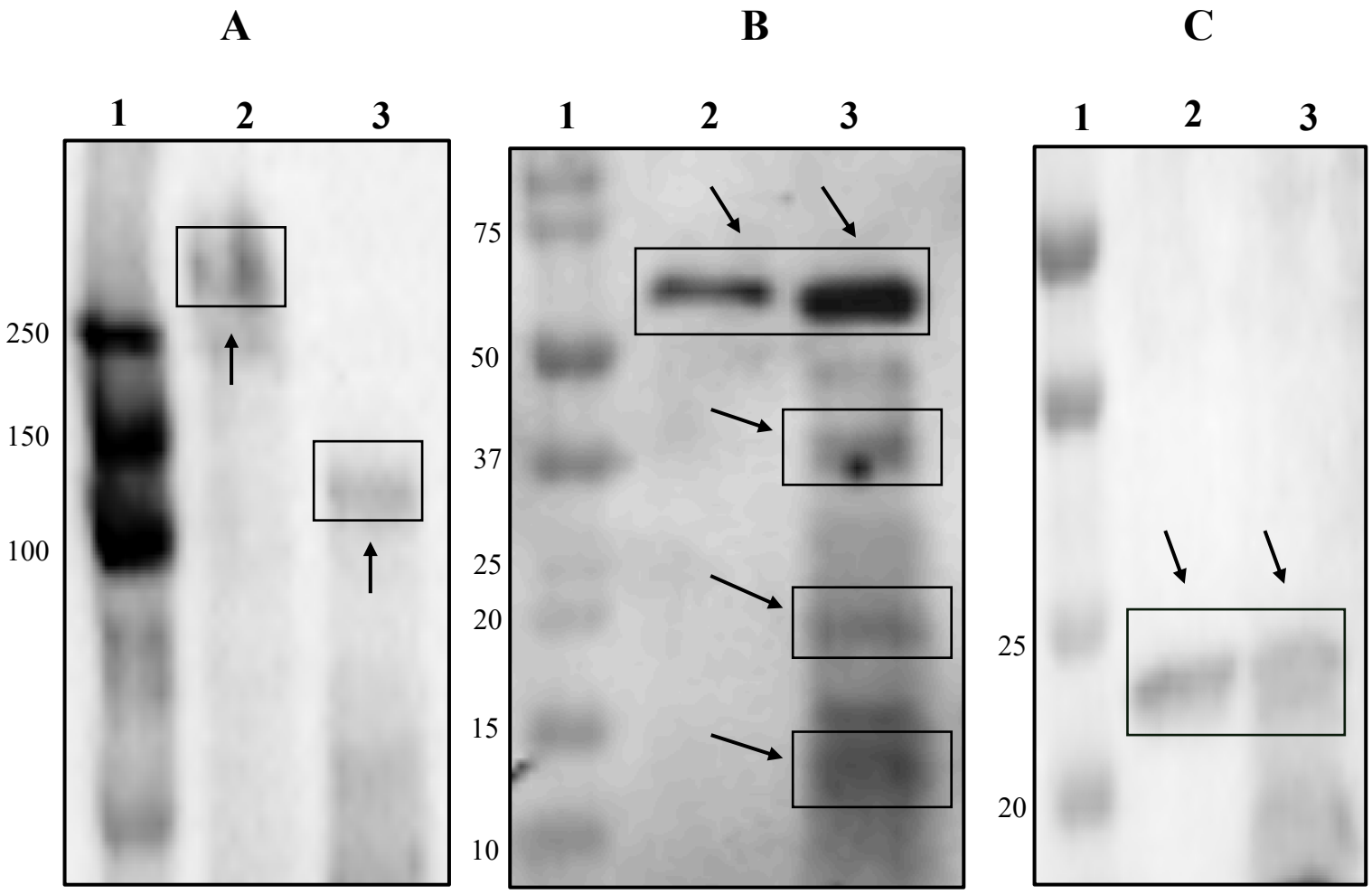

Figure 24: Western blot analysis to detect for universal SARS VLPs. (A) Universal spike protein. (B) Universal envelope protein. (C) Universal membrane protein. Lane 1, protein ladder; lane 2, supernatant; lane 3, cell lysate.

Chapter 5: Discussion

5.1 Simple glycosylation patterns from insect cells did not affect SARS-CoV-2 S protein trimerization

An insect cell line was chosen for VLP production as it provides a number of advantages, including high levels of recombinant protein production, post-translational modifications (PTMs), high levels of safety and scalability (Mi et al., 2021). However, it is known that insect cells are limited to high mannose glycosylation and do not have accurate PTMs as mammalian cells which could lead to improper assembly of VLPs (Mi et al., 2021). Protein glycosylation is critical due to their involvement in correct protein folding, directing cellular localization of proteins and protein function (Wu et al., 2010). In this work, S protein glycosylation is critical because this proper function of this glycoprotein allows for VLP release from the host cell into the supernatant. To assess whether S proteins are present in the supernatant, a western blot analysis was performed **(Figure 16)**. The bands >250 kDa seen in the supernatant suggests that spike trimers are present in the supernatant.

5.2 SARS-CoV-2 E and M protein can be simultaneously expressed under one promoter using a 2A self-cleaving peptide in *Sf9* insect cells

The production of SARS-CoV-2 VLPs and universal SARS betacoronavirus VLPs were performed using insect cell lines. The plasmid vector used was pFastBac Dual since it contained two strong promoters in polh and p10. Since the expression of 3 proteins were required (S, E and M), the two proteins allowing for VLP formation (E + M) inside the host cell were expressed

together by linking them with a 2A self-cleaving peptide sequence **(Appendix B)**. 2A self-cleaving peptides mediate an imperfect ribosomal skipping event during translation, allowing for the translation of two separate proteins under the same promoter (Y. Wang et al., 2015). Previous studies have shown that 2A self-cleaving peptides have proven effective for the co-expression of separate proteins under the same promoter, without interfering with protein activity and the expression of the second protein (C.-Y. Wu et al., 2019). In this study, the expression of S proteins is driven by the p10 promoter while the polh promoter drives the expression of E and M proteins. The E and M protein sequences were chosen to be the pair of sequences separated by the P2A peptide due to their smaller sizes and low amount required for virus assembly in comparison to the S protein. The molecular ratio of viral RNA for the S, E, and M proteins were determined to be 5:2:3 (Gourdelier et al., 2022). In addition, a study suggested that a low incorporation of E proteins into VLPs is critical to prevent the formation of vesicles containing only E proteins (Siu et al., 2008). When comparing the p10 and polh promoters, the expression of proteins driven by p10 reduces the expression of proteins driven by polh when both promoters are in the same construct (Sokolenko et al., 2012). Since the amount of S proteins required is high, its sequence was placed downstream of the p10 promoter.

Although many 2A self-cleaving peptides deriving from different viruses exist for use, such as P2A, T2A, E2A and F2A, the cleavage efficiency for P2A was shown to be the highest in insect cells and was therefore selected (Y. Wang et al., 2015). A study by Y. Wang et al., used a P2A peptide for the simultaneous expression of DsRed and EGFP genes. The results showed that RFP and GFP fluorescence was detected, suggesting that the use of P2A peptide allowed for the co-expression of two separate proteins under the same promoter. Furthermore, a past finding

indicated that the addition of a GSG spacer upstream of the P2A sequence resulted in a cleavage efficiency of 100% in *Sf9* cells (Y. Wang et al., 2015). Although an alternative approach is the use of three promoters to express the S, E and M proteins separately, incorporating 2A self-cleaving peptides can be advantageous as it leads to a smaller plasmid size which can lead to a higher transfection efficiency (Zhu et al., 2022). However, 2A self-cleaving peptides is not a perfect system and there are also limitations. For instance, the proteins being generated are not completely wildtype proteins due to additional peptide residues being left downstream or upstream of the ORF. The protein upstream of the 2A peptide will be completely attached to the 2A peptide except for the c-terminal proline, while the protein downstream of the 2A peptide is attached to a single proline at the N-terminus (Liu et al., 2017). Therefore, this can possibly lead to undesired biological effects. Furthermore, ribosomal skipping may not occur and lead to a fusion protein instead (Liu et al., 2017). Another possible outcome is successful skipping but ribosomal fall-off leading to discontinued translation of the protein downstream of the P2A peptide (Liu et al., 2017).

In this study, the E and M proteins were detected separately via western blot analysis, indicating that ribosomal skipping had occurred. Moreover, if ribosomal skipping did not occur, a fusion protein comprised of the E and M protein would result in a size of approximately 35 kDa which was not seen in the western blot analysis for the E and M protein. This further suggests that ribosomal skipping had likely occurred. Protein folding and function did not seem to be affected by the additional peptide residues as multiple bands can be seen in the western blot analysis for the E protein which indicates that E proteins had undergone oligomerization. Lastly, ribosomal fall-off did not seem to occur since the M protein was also detected. Furthermore, if

the M protein was not generated, the S, E, and M proteins would all be undetectable in the supernatant since E and M are required for VLP assembly and release into the supernatant.

5.3 Baculovirus Expression of SARS-CoV-2 S, E, and M Proteins form VLPs

The production of SARS VLPs in insect cell lines occurs in two steps: 1) the S, E, and M proteins self-assemble inside the host cell and 2) the VLP is released from the cell via exocytosis. To determine the presence of SARS VLPs, it was important to detect whether the S, E and M proteins are being produced and where they are located. Therefore, a western blot analysis was performed to detect for the presence of S, E and M proteins in the cell lysate and culture supernatant.

Although the S, E and M proteins were detected in the cell lysate, it is also important that they are detected in the supernatant since that is a strong indicator that the VLPs are being released into the supernatant. A study conducted by Plescia et al. (2020) showed that when the S protein was independently expressed, it was detectable in the cell lysate but not in the supernatant. The S protein is carried by the VLP after self-assembling inside the cell and becomes present in the supernatant after the VLP is released via exocytosis.

Furthermore, the M protein was not detectable in the cell lysate or supernatant when it was expressed alone (Plescia et al., 2020). This suggests that interactions between the M protein and other structural proteins such as S or E may be required for it to be detectable. In this study, the M protein was detectable in both the cell lysate and supernatant which suggests that the other structural proteins (S and E) are being expressed as well.

The E protein was detected in both the supernatant and the cell lysate. The band seen in the cell lysate was highly concentrated in comparison to the band in the supernatant. This is consistent with the finding that although the E protein is abundantly expressed inside the cell, only a small portion of it is actually incorporated into the virus particle which is released outside the cell (Venkatagopalan et al., 2015). The E protein contains a highly hydrophobic transmembrane domain (TMD) which allows it to oligomerize and form ion-channel proteins called 'viroporin' (Schoeman & Fielding, 2019). A past study focusing on synthetic peptides corresponding to the TMD of SARS-CoV E protein showed that these peptides can form dimers, trimers, and pentamers. With a monomeric size of 8-12 kDa, the band detected around 55 kDa **(Figure 17B)** most likely indicates E protein pentamers which would have an approximate size of 40-60 kDa. Similarly, the bands seen at approximately 20 and 22 kDa correspond to the size of E protein dimers at approximately 16-24 kDa.

Although the experiments discussed were conducted to determine whether there is a presence of SARS-CoV-2 VLPs, it is important to have a visual confirmation. TEM was performed for visual confirmation. The vesicle-like structures seen in **Figure 26** contain 'projections' on its outer surface, which may indicate either S proteins or GP64 proteins located on the outer membrane. These structures are consistent with the structures of SARS-CoV-2 VLPs. Furthermore, the expected size of SARS-CoV-2 VLPs are approximately 100 nm, which is the approximate size of the nanoparticles seen in the TEM. However, there are still uncertainties as the concentration of VLPs are not in accordance with what is seen in previous literatures. Images of SARS-CoV-2 VLPs via TEM seen in past studies appear to be clumped

together and contain a high concentration of particles. In contrast, the concentration of particles in this work is significantly low.

5.4 Purifying and characterizing SARS-CoV-2 VLPs is challenging due to contaminating baculoviruses

Though the IC-BEVS is widely used to produce VLPs, one of the major drawbacks is baculovirus contamination. VLPs and baculoviruses are similar in size and buoyant densities, resulting in challenges during the downstream processing of VLPs (Reiter et al., 2020). Although common separation techniques such as density gradient ultracentrifugation and size exclusion chromatography can potentially separate VLPs and baculoviruses, they are ineffective in efficiently separating the two (Reiter et al., 2020). Purification of enveloped VLPs presents even further challenges as it is known that both of them are produced concurrently and have similar physical and chemical characteristics (Fuenmayor et al., 2017). Unlike non-enveloped VLPs, enveloped VLPs are more complex because they acquire an outer membrane layer derived from the host cell (Dai et al., 2018). Using IC-BEVS means that the major envelope protein of baculoviruses, GP64, is also expressed. GP64 and S proteins are both glycoproteins that are localized on host cell-derived membranes. Since baculoviruses and enveloped VLPs are both released into the supernatant and carries host cell-derived membranes, both viral particles can potentially carry the GP64 and S proteins on their surfaces. This makes other purification techniques such as affinity chromatography ineffective.

In this study, iodixanol gradient ultracentrifugation was performed to semi-purify the VLPs. Sucrose gradient or cesium chloride gradient ultracentrifugation are commonly used

techniques; however, they are both time-consuming, labour intensive and not scalable (Liu et al., 2013). Furthermore, it is recommended that using a cesium chloride gradient should be avoided in the purification of VLPs as it can result in broken particles and add additional impurities in the downstream process (Millipore Sigma, 2016). Although density gradient ultracentrifugation is typically ineffective in separating VLPs and baculovirus particles, separation was observed in this work. This may be explained by the fact that unlike baculoviruses and some enveloped VLPs which bud out of the cell, SARS-CoV-2 VLPs are released from the cell via exocytosis (Lu et al., 2022). This means that the host cell-derived membrane carried by SARS-CoV-2 VLPs are different than the host-cell derived membrane carried by baculoviruses. Therefore, differences in their densities may have allowed separation to be possible.

While the S and M protein was detected after semi-purification, the E protein was not detected in any of the fractions (data not shown). This may be due to changes in temperature, shear forces and processes used during the purification process which can destroy the stability and integrity of the protein (Nooraei et al., 2021). Since the E protein is a very small protein (8-12 kDa), it may have easily been affected in comparison to the S and M proteins.

5.5 Structural proteins (S, E, M) produced from SARS betacoronavirus consensus sequences form universal VLPs

The use of S, E and M protein consensus sequences derived from SARS-CoV, MERS-CoV and SARS-CoV-2 to produce universal SARS betacoronavirus VLPs was the main goal of this study. However, one of the crucial steps in identifying whether VLP formation has occurred is determine whether the proteins are simply being expressed. In this work, SARS-CoV-2 S, E

and M proteins were detected via Western Blot analysis using SARS-CoV-2 anti-S, anti-E, and anti-M protein antibodies, respectively. This supports the hypothesis that the consensus sequences are able to generate the three structural proteins.

To detect the universal SARS betacoronavirus S, E and M proteins, SARS-CoV-2 anti-S, anti-E and anti-M protein antibodies were used to detect the universal SARS betacoronavirus S, E and M protein, respectively. This partially assessed the universality of the proteins and showed that SARS-CoV-2 antibodies are able to bind to them and is in support of this study's hypothesis. Since the 'universal' S, E, and M proteins were able to be detected by SARS-CoV-2 anti-S, anti-E, and anti-M antibodies, this indicates that the 'universal' proteins may have cross-protective potential against the three SARS betacoronaviruses.

Chapter 6: Conclusions and Future Steps

6.1 Production and Detection of SARS-CoV-2 VLPs

SARS-CoV-2 S, E, and M proteins were produced in insect cells using recombinant baculoviruses. Based on western blot analyses, the S, E, and M proteins were detected in the cell lysate which indicated that the proteins were successfully being produced. In addition, these proteins were also detected in the supernatant, which provided evidence that the proteins may have assembled into VLPs before exiting the cell via exocytosis. The 3 proteins assembled into structures that resembled SARS-CoV-2 VLPs, as shown in the TEM images. However, the concentration of particles was extremely low, indicating that there is most likely a low production yield of proteins or that the conditions during VLP production were not optimal. Therefore, further production and characterization work needs to be performed.

6.2 Downstream Processing of SARS-CoV-2 VLPs

The separation of SARS-CoV-2 VLPs and baculoviruses was observed. SARS-CoV-2 VLPs were semi-purified to remove contaminants via ultracentrifugation. Samples were ultracentrifuged using a 25% sucrose cushion followed by ultracentrifugation using an iodixanol density gradient. Twelve fractions were retrieved from top to bottom of the tube and each fraction were analyzed via western blot analysis to identify those that contained VLPs. Fraction 4 was found to contain the S and M proteins, along with GP64 proteins. However, the E protein was not detected in any fractions as its small size may have made it susceptible to harsh conditions during the purification process. An infectious assay (EPDA) was performed to

identify whether fraction 4 contained any infectious baculoviruses. The results showed no signs of cell infection when fraction 4 was added to insect cells, indicating an absence of infectious baculovirus particles. A SYBR green assay was also performed on fraction 4 to identify if defective baculovirus particles are present. The results showed no signs of baculovirus particles. Based on these results, fraction 4 was found to contain SARS-CoV-2 VLP particles without any contaminating baculoviruses. Furthermore, TEM imaging for fraction 4 showed vesicle-like structures resembling SARS-CoV-2 VLPs and no baculovirus particles. Although separation of VLPs and baculoviruses are known to be extremely difficult, the separation shown in this work may be due to differences in the host cell-derived membrane since SARS-CoV-2 VLPs are released from the cell via exocytosis whereas baculoviruses are released by budding out of the cell.

6.3 Production and Detection of Universal SARS Betacoronavirus VLPs

Recombinant baculoviruses expressing consensus sequences for SARS betacoronavirus S, E and M proteins produced universal SARS S, E, and M proteins. Similar to the characterization work for SARS-CoV-2 VLPs, the universal SARS S, E, and M proteins were detected in the cell lysate and supernatant after cell infection with recombinant baculoviruses. The presence of these proteins in the cell lysate supports the hypothesis that the consensus sequences generated for the S, E, and M proteins based on the three SARS betacoronaviruses can produce S, E, and M ‘synthetic consensus’ proteins using the IC-BEVS. Furthermore, the detection of these proteins in the supernatant provides evidence that VLP formation is likely since this is required for all three proteins to be present outside of the cell.

The 3 universal proteins were detected using antibodies against SARS-CoV-2, which indicates that binding of SARS-CoV-2 antibodies to these universal proteins had occurred. This finding was promising, as it partially assessed the universality of the proteins. In order to obtain more conclusive evidence that these VLPs are truly universal, further characterization work needs to be performed using SARS-CoV and MERS-CoV antibodies.

6.4 Future Steps

Although the results obtained in this work are promising, further purification and characterization work needs to be conducted for the SARS-CoV-2 VLPs and universal SARS VLPs. Vesicle-like structures can be seen via TEM imaging; however, further assessments of these particles are required. A potential approach in determining whether the S proteins are truly on these particles is to add anti-spike primary antibodies and using gold nanoparticles conjugated to its respective secondary antibody for visualization. Visualization of these gold nanoparticles on the vesicle-like structures can further confirm that the particles detected are truly VLPs. Subsequently, this approach can also be used to quantify these particles.

Similar to the experiments performed for the SARS-CoV-2 VLPs, the universal VLPs should also be semi-purified to determine which fractions may contain these VLPs. Analysis of fraction 4 should be performed to identify whether baculoviruses can be separated when semi-purifying the VLPs using iodixanol gradient ultracentrifugation.

Production and characterization work of SARS-CoV and MERS-CoV VLPs should also be performed. To test the universal VLPs, it is important to determine whether the universal S, E and M proteins can be detected using SARS-CoV and MERS-CoV anti-S, anti-E, and anti-M

protein antibodies, respectively. In addition, western blot analyses should be performed on SARS-CoV and MERS-CoV S, E, and M proteins using SARS-CoV-2 anti-S, anti-E, and anti-M antibodies to show that there is no cross-reactivity. This will provide evidence that the 'universal proteins' are truly universal and that the SARS-CoV-2 antibodies used are not simply cross-reactive with S, E, and M proteins belonging to all three betacoronaviruses.

Animal studies can also be conducted to produce 'universal' anti-S, anti-E, and anti-M antibodies. This can be accomplished by injecting the universal VLPs into a mouse model to antibodies against the universal SARS proteins. These 'universal' SARS antibodies can be used for further experiments. For instance, an ELISA can be performed by coating plates with SARS-CoV, MERS-CoV, and SARS-CoV-2 S proteins and determining whether the 'universal' anti-S antibodies can bind. This will allow the evaluation of its cross-reactivity against SARS-CoV, MERS-CoV, and SARS-CoV-2.

References

Abdelrahman, Z., Li, M., & Wang, X. (2020). Comparative Review of SARS-CoV-2, SARS-CoV, MERS-CoV, and Influenza A Respiratory Viruses. *Frontiers in Immunology*, *11*. https://doi.org/10.3389/fimmu.2020.552909

Ahmed, S. F., Quadeer, A. A., & McKay, M. R. (2020). Preliminary Identification of Potential Vaccine Targets for the COVID-19 Coronavirus (SARS-CoV-2) Based on SARS-CoV Immunological Studies. *Viruses*, *12*(3). https://doi.org/10.3390/v12030254

Alegria-Schaffer, A., Lodge, A., & Vattem, K. (2009). Chapter 33 Performing and Optimizing Western Blots with an Emphasis on Chemiluminescent Detection. In R. R. Burgess & M. P. Deutscher (Eds.), *Methods in Enzymology* (Vol. 463, pp. 573–599). Academic Press. https://doi.org/10.1016/S0076-6879(09)63033-0

Al-Qahtani, A. A. (2020). Severe Acute Respiratory Syndrome Coronavirus 2 (SARS-CoV-2): Emergence, history, basic and clinical aspects. *Saudi Journal of Biological Sciences*, *27*(10), 2531–2538. https://doi.org/10.1016/j.sjbs.2020.04.033

Araf, Y., Akter, F., Tang, Y., Fatemi, R., Parvez, Md. S. A., Zheng, C., & Hossain, Md. G. (2022). Omicron variant of SARS-CoV-2: Genomics, transmissibility, and responses to current COVID-19 vaccines. *Journal of Medical Virology*, *94*(5), 1825–1832. https://doi.org/10.1002/jmv.27588

Arvin, A. M., Fink, K., Schmid, M. A., Cathcart, A., Spreafico, R., Havenar-Daughton, C., Lanzavecchia, A., Corti, D., & Virgin, H. W. (2020). A perspective on potential

antibody-dependent enhancement of SARS-CoV-2. *Nature*, *584*(7821), 353–363. https://doi.org/10.1038/s41586-020-2538-8

Ashour, H. M., Elkhatib, W. F., Rahman, Md. M., & Elshabrawy, H. A. (2020). Insights into the Recent 2019 Novel Coronavirus (SARS-CoV-2) in Light of Past Human Coronavirus Outbreaks. *Pathogens*, *9*(3). https://doi.org/10.3390/pathogens9030186

Bachmann, M. F., & Zinkernagel, R. M. (1997). Neutralizing antiviral B cell responses. *Annual Review of Immunology*, *15*, 235–270. https://doi.org/10.1146/annurev.immunol.15.1.235

Bassetti, M., Vena, A., & Giacobbe, D. R. (2020). The novel Chinese coronavirus (2019-nCoV) infections: Challenges for fighting the storm. *European Journal of Clinical Investigation*, *50*(3). https://doi.org/10.1111/eci.13209

BCCDC. (2021). *COVID-19 Variants*. Retrieved April 29, 2021, from http://www.bccdc.ca/health-info/diseases-conditions/covid-19/about-covid-19/variants

Bender, A. T., Tzvetkov, E., Pereira, A., Wu, Y., Kasar, S., Przetak, M. M., Vlach, J., Niewold, T. B., Jensen, M. A., & Okitsu, S. L. (2020). TLR7 and TLR8 Differentially Activate the IRF and NF-κB Pathways in Specific Cell Types to Promote Inflammation. *ImmunoHorizons*, *4*(2), 93–107. https://doi.org/10.4049/immunohorizons.2000002

Bode, C., Zhao, G., Steinhagen, F., Kinjo, T., & Klinman, D. M. (2011). CpG DNA as a vaccine adjuvant. *Expert Review of Vaccines*, *10*(4), 499–511. https://doi.org/10.1586/erv.10.174

Brun, A., Bárcena, J., Blanco, E., Borrego, B., Dory, D., Escribano, J. M., Le Gall-Reculé, G., Ortego, J., & Dixon, L. K. (2011). Current strategies for subunit and genetic viral veterinary vaccine development. *Virus Research*, *157*(1), 1–12. https://doi.org/10.1016/j.virusres.2011.02.006

Buchholz, U. J., Bukreyev, A., Yang, L., Lamirande, E. W., Murphy, B. R., Subbarao, K., & Collins, P. L. (2004). Contributions of the structural proteins of severe acute respiratory syndrome coronavirus to protective immunity. *Proceedings of the National Academy of Sciences*, *101*(26), 9804–9809. https://doi.org/10.1073/pnas.0403492101

Contreras-Gómez, A., Sánchez-Mirón, A., García-Camacho, F., Molina-Grima, E., & Chisti, Y. (2014). Protein production using the baculovirus-insect cell expression system. *Biotechnology Progress*, *30*(1), 1–18. https://doi.org/10.1002/btpr.1842

Chan, J. F.-W., Kok, K.-H., Zhu, Z., Chu, H., To, K. K.-W., Yuan, S., & Yuen, K.-Y. (2020). Genomic characterization of the 2019 novel human-pathogenic coronavirus isolated from a patient with atypical pneumonia after visiting Wuhan. *Emerging Microbes & Infections*, *9*(1), 221–236. https://doi.org/10.1080/22221751.2020.1719902

Cherian, S., Potdar, V., Jadhav, S., Yadav, P., Gupta, N., Das, M., Das, S., Agarwal, A., Singh, S., Abraham, P., Panda, S., Mande, S., Swarup, R., Bhargava, B., Bhushan, R., Team, N. I. C., & Consortium, I. (2021). Convergent evolution of SARS-CoV-2 spike mutations, L452R, E484Q and P681R, in the second wave of COVID-19 in Maharashtra, India. *BioRxiv*, 2021.04.22.440932. https://doi.org/10.1101/2021.04.22.440932

Coleman, C. M., Liu, Y. V., Mu, H., Taylor, J. K., Massare, M., Flyer, D. C., Glenn, G. M., Smith, G. E., & Frieman, M. B. (2014). Purified coronavirus spike protein nanoparticles induce coronavirus neutralizing antibodies in mice. *Vaccine*, *32*(26), 3169–3174. https://doi.org/10.1016/j.vaccine.2014.04.016

Cui, J., Li, F., & Shi, Z.-L. (2019). Origin and evolution of pathogenic coronaviruses. *Nature Reviews. Microbiology*, *17*(3), 181–192. https://doi.org/10.1038/s41579-018-0118-9

CDC. (2021). *Coronavirus Disease 2019 (COVID-19)*. Centers for Disease Control and Prevention. https://www.cdc.gov/coronavirus/2019-ncov/science/science-briefs/scientific-brief-emerging-variants.html

Comas-Garcia, M., Colunga-Saucedo, M., & Rosales-Mendoza, S. (2020). The Role of Virus-Like Particles in Medical Biotechnology. *Molecular Pharmaceutics*, *17*(12), 4407–4420. https://doi.org/10.1021/acs.molpharmaceut.0c00828

Chen, H., Guo, J., Wang, C., Luo, F., Yu, X., Zhang, W., Li, J., Zhao, D., Xu, D., Gong, Q., Liao, J., Yang, H., Hou, W., & Zhang, Y. (2020). Clinical characteristics and intrauterine vertical transmission potential of COVID-19 infection in nine pregnant women: A retrospective review of medical records. *The Lancet*, *395*(10226), 809–815. https://doi.org/10.1016/S0140-6736(20)30360-3

Cimica, V., & Galarza, J. M. (2017). Adjuvant Formulations for Virus-Like Particle (VLP) Based Vaccines. *Clinical Immunology (Orlando, Fla.)*, *183*, 99–108. https://doi.org/10.1016/j.clim.2017.08.004

Dai, S., Wang, H., & Deng, F. (2018). Advances and challenges in enveloped virus-like particle (VLP)-based vaccines. Journal of Immunological Sciences, 2(2). https://www.immunologyresearchjournal.com/articles/advances-and-challenges-in-enveloped-viruslike-particle-vlpbased-vaccines.html

Dai, L., Zheng, T., Xu, K., Han, Y., Xu, L., Huang, E., An, Y., Cheng, Y., Li, S., Liu, M., Yang, M., Li, Y., Cheng, H., Yuan, Y., Zhang, W., Ke, C., Wong, G., Qi, J., Qin, C., … Gao, G. F. (2020). A Universal Design of Betacoronavirus Vaccines against COVID-19, MERS, and SARS. *Cell*, *182*(3), 722-733.e11. https://doi.org/10.1016/j.cell.2020.06.035

Daniels, R. W., Rossano, A. J., Macleod, G. T., & Ganetzky, B. (2014). Expression of Multiple Transgenes from a Single Construct Using Viral 2A Peptides in Drosophila. *PLoS ONE*, *9*(6). https://doi.org/10.1371/journal.pone.0100637

Dearlove, B., Lewitus, E., Bai, H., Li, Y., Reeves, D. B., Joyce, M. G., Scott, P. T., Amare, M. F., Vasan, S., Michael, N. L., Modjarrad, K., & Rolland, M. (2020). A SARS-CoV-2 vaccine candidate would likely match all currently circulating variants. *Proceedings of the National Academy of Sciences of the United States of America*, *117*(38), 23652–23662. https://doi.org/10.1073/pnas.2008281117

DeDiego, M. L., Álvarez, E., Almazán, F., Rejas, M. T., Lamirande, E., Roberts, A., Shieh, W.-J., Zaki, S. R., Subbarao, K., & Enjuanes, L. (2007). A Severe Acute Respiratory Syndrome Coronavirus That Lacks the E Gene Is Attenuated In Vitro and In Vivo. *Journal of Virology*, *81*(4), 1701–1713. https://doi.org/10.1128/JVI.01467-06

de Haan, C. A. M., & Rottier, P. J. M. (2005). Molecular Interactions in the Assembly of Coronaviruses. *Advances in Virus Research*, *64*, 165–230. https://doi.org/10.1016/S0065-3527(05)64006-7

Deschuyteneer, M., Elouahabi, A., Plainchamp, D., Plisnier, M., Soete, D., Corazza, Y., Lockman, L., Giannini, S., & Deschamps, M. (2010). Molecular and structural characterization of the L1 virus-like particles that are used as vaccine antigens in Cervarix™, the AS04-adjuvanted HPV-16 and -18 cervical cancer vaccine. *Human Vaccines*, *6*(5), 407–419. https://doi.org/10.4161/hv.6.5.11023

Donaldson, B., Lateef, Z., Walker, G. F., Young, S. L., & Ward, V. K. (2018). Virus-like particle vaccines: Immunology and formulation for clinical translation. *Expert Review of Vaccines*, *17*(9), 833–849. https://doi.org/10.1080/14760584.2018.1516552

Eden, W. van, Zee, R. van der, Kooten, P. van, Berlo, S. E., Cobelens, P. M., Kavelaars, A., Heijnen, C. J., Prakken, B., Roord, S., & Albani, S. (2002). Balancing the immune system: Th1 and Th2. *Annals of the Rheumatic Diseases*, *61*(suppl 2), ii25–ii28. https://doi.org/10.1136/ard.61.suppl_2.ii25

Estrada, L. D., & Schultz-Cherry, S. (2019). Development of a Universal Influenza Vaccine. *Journal of Immunology (Baltimore, Md.: 1950)*, *202*(2), 392–398. https://doi.org/10.4049/jimmunol.1801054

Fan, Y., Li, X., Zhang, L., Wan, S., Zhang, L., & Zhou, F. (2022). SARS-CoV-2 Omicron variant: Recent progress and future perspectives. *Signal Transduction and Targeted Therapy*, *7*(1), 1–11. https://doi.org/10.1038/s41392-022-00997-x

FDA (2021). COVID-19 Vaccines. *FDA*. https://www.fda.gov/emergency-preparedness-and-response/coronavirus-disease-2019-covid-19/covid-19-vaccines

Fuenmayor, J., Gòdia, F., & Cervera, L. (2017). Production of virus-like particles for vaccines. *New Biotechnology*, *39*, 174–180. https://doi.org/10.1016/j.nbt.2017.07.010

Firestone, M. J., Lorentz, A. J., Meyer, S., Wang, X., Como-Sabetti, K., Vetter, S., Smith, K., Holzbauer, S., Beaudoin, A., Garfin, J., Ehresmann, K., Danila, R., & Lynfield, R. (2021). First Identified Cases of SARS-CoV-2 Variant P.1 in the United States—Minnesota, January 2021. *Morbidity and Mortality Weekly Report*, *70*(10), 346–347. https://doi.org/10.15585/mmwr.mm7010e1

Fehr, A. R., & Perlman, S. (2015). Coronaviruses: An Overview of Their Replication and Pathogenesis. *Coronaviruses*, *1282*, 1–23. https://doi.org/10.1007/978-1-4939-2438-7_1

Galloway, S. E., Paul, P., MacCannell, D. R., Johansson, M. A., Brooks, J. T., MacNeil, A., Slayton, R. B., Tong, S., Silk, B. J., Armstrong, G. L., Biggerstaff, M., & Dugan, V. G. (2021). Emergence of SARS-CoV-2 B.1.1.7 Lineage—United States, December 29, 2020–January 12, 2021. *Morbidity and Mortality Weekly Report*, *70*(3), 95–99. https://doi.org/10.15585/mmwr.mm7003e2

García-Sastre, A., & Mena, I. (2013). Novel vaccine strategies against emerging viruses. *Current Opinion in Virology*, *3*(2), 210–216. https://doi.org/10.1016/j.coviro.2013.02.001

Gourdelier, M., Swain, J., Arone, C., Mouttou, A., Bracquemond, D., Merida, P., Saffarian, S., Lyonnais, S., Favard, C., & Muriaux, D. (2022). Optimized production and fluorescent labeling of SARS-CoV-2 virus-like particles. *Scientific Reports*, *12*(1), Article 1. https://doi.org/10.1038/s41598-022-18681-z

Grunwald, T., & Ulbert, S. (2015). Improvement of DNA vaccination by adjuvants and sophisticated delivery devices: Vaccine-platforms for the battle against infectious diseases. *Clinical and Experimental Vaccine Research*, *4*(1), 1–10. https://doi.org/10.7774/cevr.2015.4.1.1

Gupta, T., & Gupta, S. K. (2020). Potential adjuvants for the development of a SARS-CoV-2 vaccine based on experimental results from similar coronaviruses. *International Immunopharmacology*, *86*, 106717. https://doi.org/10.1016/j.intimp.2020.106717

Hamad, M. (2011). Universal vaccines: Shifting to one for many or shooting too high too soon! *APMIS*, *119*(9), 565–573. https://doi.org/10.1111/j.1600-0463.2011.02776.x

Hamming, I., Timens, W., Bulthuis, M., Lely, A., Navis, G., & van Goor, H. (2004). Tissue distribution of ACE2 protein, the functional receptor for SARS coronavirus. A first step in understanding SARS pathogenesis. *The Journal of Pathology*, *203*(2), 631–637. https://doi.org/10.1002/path.1570

Hartenian, E., Nandakumar, D., Lari, A., Ly, M., Tucker, J. M., & Glaunsinger, B. A. (2020). The molecular virology of coronaviruses. *The Journal of Biological Chemistry*, *295*(37), 12910–12934. https://doi.org/10.1074/jbc.REV120.013930

Health Canada. (2021). *COVID-19 Vaccines: Authorized vaccines*. https://www.canada.ca/en/health-canada/services/drugs-health-products/covid19-industry/drugs-vaccines-treatments/vaccines.html

Hellfritzsch, M., & Scherließ, R. (2019). Mucosal Vaccination via the Respiratory Tract. *Pharmaceutics*, *11*(8), 375. https://doi.org/10.3390/pharmaceutics11080375

Hitchman, R. B., Locanto, E., Possee, R. D., & King, L. A. (2011). Optimizing the baculovirus expression vector system. *Methods (San Diego, Calif.)*, *55*(1), 52–57. https://doi.org/10.1016/j.ymeth.2011.06.011

Hitchman, R. B., Possee, R. D., & King, L. A. (2009). Baculovirus expression systems for recombinant protein production in insect cells. *Recent Patents on Biotechnology*, *3*(1), 46–54. https://doi.org/10.2174/187220809787172669

Ho, Y., Lin, P.-H., Liu, C. Y. Y., Lee, S.-P., & Chao, Y.-C. (2004). Assembly of human severe acute respiratory syndrome coronavirus-like particles. *Biochemical and Biophysical Research Communications*, *318*(4), 833–838. https://doi.org/10.1016/j.bbrc.2004.04.111

Hoffmann, M., Kleine-Weber, H., & Pöhlmann, S. (2020). A Multibasic Cleavage Site in the Spike Protein of SARS-CoV-2 Is Essential for Infection of Human Lung Cells. *Molecular Cell*, *78*(4), 779-784.e5. https://doi.org/10.1016/j.molcel.2020.04.022

Honda-Okubo, Y., Barnard, D., Ong, C. H., Peng, B.-H., Tseng, C.-T. K., & Petrovsky, N. (2015). Severe Acute Respiratory Syndrome-Associated Coronavirus Vaccines Formulated with Delta Inulin Adjuvants Provide Enhanced Protection while Ameliorating Lung Eosinophilic Immunopathology. *Journal of Virology*, *89*(6), 2995–3007. https://doi.org/10.1128/JVI.02980-14

Hou, Y. J., Chiba, S., Halfmann, P., Ehre, C., Kuroda, M., Dinnon, K. H., Leist, S. R., Schäfer, A., Nakajima, N., Takahashi, K., Lee, R. E., Mascenik, T. M., Graham, R., Edwards, C. E., Tse, L. V., Okuda, K., Markmann, A. J., Bartelt, L., Silva, A. de, … Baric, R. S. (2020). SARS-CoV-2 D614G variant exhibits efficient replication ex vivo and transmission in vivo. *Science*, *370*(6523), 1464–1468. https://doi.org/10.1126/science.abe8499

Hu, T., Liu, Y., Zhao, M., Zhuang, Q., Xu, L., & He, Q. (2020). A comparison of COVID-19, SARS and MERS. *PeerJ*, *8*. https://doi.org/10.7717/peerj.9725

Huhti, L., Blazevic, V., Nurminen, K., Koho, T., Hytönen, V. P., & Vesikari, T. (2010). A comparison of methods for purification and concentration of norovirus GII-4 capsid virus-like particles. *Archives of Virology*, *155*(11), 1855–1858. https://doi.org/10.1007/s00705-010-0768-z

Ikeda, M., Hamajima, R., & Kobayashi, M. (2015). Baculoviruses: Diversity, evolution and manipulation of insects. *Entomological Science*, *18*(1), 1–20. https://doi.org/10.1111/ens.12105

Invitrogen Life Technologies. (2015). Bac-to-Bac Baculovirus Expression System. https://tools.thermofisher.com/content/sfs/manuals/bactobac_man.pdf

Iwasaki, A., & Omer, S. B. (2020). Why and How Vaccines Work. *Cell*, *183*(2), 290–295. https://doi.org/10.1016/j.cell.2020.09.040

Jaimes, J. A., Millet, J. K., & Whittaker, G. R. (2020a). Proteolytic Cleavage of the SARS-CoV-2 Spike Protein and the Role of the Novel S1/S2 Site. *IScience*, *23*(6), 101212. https://doi.org/10.1016/j.isci.2020.101212

Jaimes, J. A., André, N. M., Chappie, J. S., Millet, J. K., & Whittaker, G. R. (2020b). Phylogenetic Analysis and Structural Modeling of SARS-CoV-2 Spike Protein Reveals an Evolutionary Distinct and Proteolytically Sensitive Activation Loop. *Journal of Molecular Biology*, *432*(10), 3309–3325. https://doi.org/10.1016/j.jmb.2020.04.009

Jarvis, D. L. (2009). Chapter 14 Baculovirus–Insect Cell Expression Systems. In R. R. Burgess & M. P. Deutscher (Eds.), *Methods in Enzymology* (Vol. 463, pp. 191–222). Academic Press. https://doi.org/10.1016/S0076-6879(09)63014-7

Jehle, J. A., Blissard, G. W., Bonning, B. C., Cory, J. S., Herniou, E. A., Rohrmann, G. F., Theilmann, D. A., Thiem, S. M., & Vlak, J. M. (2006). On the classification and nomenclature of baculoviruses: A proposal for revision. *Archives of Virology*, *151*(7), 1257–1266. https://doi.org/10.1007/s00705-006-0763-6

Johnson, B. A., Xie, X., Bailey, A. L., Kalveram, B., Lokugamage, K. G., Muruato, A., Zou, J., Zhang, X., Juelich, T., Smith, J. K., Zhang, L., Bopp, N., Schindewolf, C., Vu, M., Vanderheiden, A., Winkler, E. S., Swetnam, D., Plante, J. A., Aguilar, P., … Menachery, V. D. (2021). Loss of furin cleavage site attenuates SARS-CoV-2 pathogenesis. *Nature*, *591*(7849), 293–299. https://doi.org/10.1038/s41586-021-03237-4

Karthik, K., Senthilkumar, T. M. A., Udhayavel, S., & Raj, G. D. (n.d.). Role of antibody-dependent enhancement (ADE) in the virulence of SARS-CoV-2 and its mitigation strategies for the development of vaccines and immunotherapies to counter COVID-19. *Human Vaccines & Immunotherapeutics*, 1–6. https://doi.org/10.1080/21645515.2020.1796425

Kelly, B. J., King, L. A., & Possee, R. D. (2007). Introduction to baculovirus molecular biology. *Methods in Molecular Biology (Clifton, N.J.)*, *388*, 25–54. https://doi.org/10.1007/978-1-59745-457-5_2

Khan, S., Nakajima, R., Jain, A., Assis, R. R. de, Jasinskas, A., Obiero, J. M., Adenaiye, O., Tai, S., Hong, F., Milton, D. K., Davies, H., Felgner, P. L., & Group, P. S. (2020). Analysis of Serologic Cross-Reactivity Between Common Human Coronaviruses and SARS-CoV-2 Using Coronavirus Antigen Microarray. *BioRxiv*, 2020.03.24.006544. https://doi.org/10.1101/2020.03.24.006544

Kim, S. J., Yao, Z., Marsh, M. C., Eckert, D. M., Kay, M. S., Lyakisheva, A., Pasic, M., Bansal, A., Birnboim, C., Jha, P., Galipeau, Y., Langlois, M.-A., Delgado, J. C., Elgort, M. G., Campbell, R. A., Middleton, E. A., Stagljar, I., & Owen, S. C. (2022). Homogeneous surrogate virus neutralization assay to rapidly assess neutralization activity of anti-SARS-

CoV-2 antibodies. *Nature Communications*, *13*(1), Article 1. https://doi.org/10.1038/s41467-022-31300-9

Klimek, L., Kündig, T., Kramer, M. F., Guethoff, S., Jensen-Jarolim, E., Schmidt-Weber, C. B., Palomares, O., Mohsen, M. O., Jakob, T., & Bachmann, M. (2018). Virus-like particles (VLP) in prophylaxis and immunotherapy of allergic diseases. *Allergo Journal International*, *27*(8), 245–255. https://doi.org/10.1007/s40629-018-0074-y

Koday, M. T., Leonard, J. A., Munson, P., Forero, A., Koday, M., Bratt, D. L., Fuller, J. T., Murnane, R., Qin, S., Reinhart, T. A., Duus, K., Messaoudi, I., Hartman, A. L., Stefano-Cole, K., Morrison, J., Katze, M. G., & Fuller, D. H. (2017). Multigenic DNA vaccine induces protective cross-reactive T cell responses against heterologous influenza virus in nonhuman primates. *PLOS ONE*, *12*(12), e0189780. https://doi.org/10.1371/journal.pone.0189780

Kost, T. A., & Kemp, C. W. (2016). Fundamentals of Baculovirus Expression and Applications. *Advances in Experimental Medicine and Biology*, *896*, 187–197. https://doi.org/10.1007/978-3-319-27216-0_12

Krammer, F. (2020). SARS-CoV-2 vaccines in development. *Nature*, *586*(7830), 516–527. https://doi.org/10.1038/s41586-020-2798-3

Kumar, A., Meldgaard, T. S., & Bertholet, S. (2018). Novel Platforms for the Development of a Universal Influenza Vaccine. *Frontiers in Immunology*, *9*, 600. https://doi.org/10.3389/fimmu.2018.00600

Kumar, S., Thambiraja, T. S., Karuppanan, K., & Subramaniam, G. (2022A). Omicron and Delta variant of SARS-CoV-2: A comparative computational study of spike protein. *Journal of Medical Virology*, *94*(4), 1641–1649. https://doi.org/10.1002/jmv.27526

Kumar, S., Karuppanan, K., & Subramaniam, G. (2022B). Omicron (BA.1) and sub-variants (BA.1.1, BA.2, and BA.3) of SARS-CoV-2 spike infectivity and pathogenicity: A comparative sequence and structural-based computational assessment. *Journal of Medical Virology*, *94*(10), 4780–4791. https://doi.org/10.1002/jmv.27927

Larkin, M. A., Blackshields, G., Brown, N. P., Chenna, R., McGettigan, P. A., McWilliam, H., Valentin, F., Wallace, I. M., Wilm, A., Lopez, R., Thompson, J. D., Gibson, T. J., & Higgins, D. G. (2007). Clustal W and Clustal X version 2.0. *Bioinformatics*, *23*(21), 2947–2948. https://doi.org/10.1093/bioinformatics/btm404

Lauring, A. S., & Hodcroft, E. B. (2021). Genetic Variants of SARS-CoV-2-What Do They Mean? *JAMA*, *325*(6), 529–531. https://doi.org/10.1001/jama.2020.27124

Lee, N.-H., Lee, J.-A., Park, S.-Y., Song, C.-S., Choi, I.-S., & Lee, J.-B. (2012). A review of vaccine development and research for industry animals in Korea. *Clinical and Experimental Vaccine Research*, *1*(1), 18–34. https://doi.org/10.7774/cevr.2012.1.1.18

Lee, S., & Nguyen, M. T. (2015). Recent Advances of Vaccine Adjuvants for Infectious Diseases. *Immune Network*, *15*(2), 51–57. https://doi.org/10.4110/in.2015.15.2.51

Lee, W. S., Wheatley, A. K., Kent, S. J., & DeKosky, B. J. (2020). Antibody-dependent enhancement and SARS-CoV-2 vaccines and therapies. *Nature Microbiology*, *5*(10), 1185–1191. https://doi.org/10.1038/s41564-020-00789-5

Li, Y.-D., Chi, W.-Y., Su, J.-H., Ferrall, L., Hung, C.-F., & Wu, T.-C. (2020). Coronavirus vaccine development: From SARS and MERS to COVID-19. *Journal of Biomedical Science*, *27*(1), 104. https://doi.org/10.1186/s12929-020-00695-2

Li, Y., Zhang, Z., Yang, L., Lian, X., Xie, Y., Li, S., Xin, S., Cao, P., & Lu, J. (2020). The MERS-CoV Receptor DPP4 as a Candidate Binding Target of the SARS-CoV-2 Spike. *IScience*, *23*(6), 101160. https://doi.org/10.1016/j.isci.2020.101160

Liang, Z., Zhu, H., Wang, X., Jing, B., Li, Z., Xia, X., Sun, H., Yang, Y., Zhang, W., Shi, L., Zeng, H., & Sun, B. (2020). Adjuvants for Coronavirus Vaccines. *Frontiers in Immunology*, *11*. https://doi.org/10.3389/fimmu.2020.589833

Liljas, L. (2013). Consensus Sequences. In S. Maloy & K. Hughes (Eds.), *Brenner's Encyclopedia of Genetics (Second Edition)* (pp. 163–164). Academic Press. https://doi.org/10.1016/B978-0-12-374984-0.00325-9

Lipman, N. S., Jackson, L. R., Trudel, L. J., & Weis-Garcia, F. (2005). Monoclonal Versus Polyclonal Antibodies: Distinguishing Characteristics, Applications, and Information Resources. *ILAR Journal*, *46*(3), 258–268. https://doi.org/10.1093/ilar.46.3.258

Liu, F., Wu, X., Li, L., Liu, Z., & Wang, Z. (2013). Use of baculovirus expression system for generation of virus-like particles: Successes and challenges. *Protein Expression and Purification*, *90*(2), 104–116. https://doi.org/10.1016/j.pep.2013.05.009

Liu, Z., Chen, O., Wall, J. B. J., Zheng, M., Zhou, Y., Wang, L., Ruth Vaseghi, H., Qian, L., & Liu, J. (2017). Systematic comparison of 2A peptides for cloning multi-genes in a polycistronic vector. *Scientific Reports*, *7*(1), Article 1. https://doi.org/10.1038/s41598-017-02460-2

Liu, L., Wei, Q., Lin, Q., Fang, J., Wang, H., Kwok, H., Tang, H., Nishiura, K., Peng, J., Tan, Z., Wu, T., Cheung, K.-W., Chan, K.-H., Alvarez, X., Qin, C., Lackner, A., Perlman, S., Yuen, K.-Y., & Chen, Z. (2019). Anti–spike IgG causes severe acute lung injury by skewing macrophage responses during acute SARS-CoV infection. *JCI Insight*, *4*(4). https://doi.org/10.1172/jci.insight.123158

Lu, W., Zhao, Z., Huang, Y.-W., & Wang, B. (2022). Review: A systematic review of virus-like particles of coronavirus: Assembly, generation, chimerism and their application in basic research and in the clinic. *International Journal of Biological Macromolecules*, *200*, 487–497. https://doi.org/10.1016/j.ijbiomac.2022.01.108

Luckow, V. A., Lee, S. C., Barry, G. F., & Olins, P. O. (1993). Efficient generation of infectious recombinant baculoviruses by site-specific transposon-mediated insertion of foreign genes into a baculovirus genome propagated in Escherichia coli. *Journal of Virology*, *67*(8), 4566–4579.

Maldonado, L. L., Bertelli, A. M., & Kamenetzky, L. (2021). Molecular features similarities between SARS-CoV-2, SARS, MERS and key human genes could favour the viral infections and trigger collateral effects. *Scientific Reports*, *11*(1), 4108. https://doi.org/10.1038/s41598-021-83595-1

McKinnon, K. M. (2018). Flow Cytometry: An Overview. *Current Protocols in Immunology*, *120*, 5.1.1-5.1.11. https://doi.org/10.1002/cpim.40

McMillan, C. L. D., Young, P. R., Watterson, D., & Chappell, K. J. (2021). The Next Generation of Influenza Vaccines: Towards a Universal Solution. *Vaccines*, *9*(1). https://doi.org/10.3390/vaccines9010026

Mi, Y., Xie, T., Zhu, B., Tan, J., Li, X., Luo, Y., Li, F., Niu, H., Han, J., Lv, W., & Wang, J. (2021). Production of SARS-CoV-2 virus-like particles in insect cells. *BioRxiv*, 2021.01.30.428979. https://doi.org/10.1101/2021.01.30.428979

Millipore Sigma. (2016). *Generic Processes of Virus-Like Particle (VLP) Based Vaccine Manufacturing.* https://www.emdmillipore.com/Web-CA-Site/en_CA/-/CAD/ShowDocument-File?ProductSKU=MM_NF-C7631&DocumentId=201701.075.ProNet&DocumentUID=42572493&DocumentType=TI&Language=EN&Country=NF&Origin=PDP

Mistry, P., Barmania, F., Mellet, J., Peta, K., Strydom, A., Viljoen, I. M., James, W., Gordon, S., & Pepper, M. S. (2022). SARS-CoV-2 Variants, Vaccines, and Host Immunity. *Frontiers in Immunology*, *12*, 809244. https://doi.org/10.3389/fimmu.2021.809244

Mortola, E., & Roy, P. (2004). Efficient assembly and release of SARS coronavirus-like particles by a heterologous expression system. *Febs Letters*, *576*(1–2), 174–178. https://doi.org/10.1016/j.febslet.2004.09.009

Mohsen, M. O., Zha, L., Cabral-Miranda, G., & Bachmann, M. F. (2017). Major findings and recent advances in virus–like particle (VLP)-based vaccines. *Seminars in Immunology*, *34*, 123–132. https://doi.org/10.1016/j.smim.2017.08.014

Mousavizadeh, L., & Ghasemi, S. (2020). Genotype and phenotype of COVID-19: Their roles in pathogenesis. *Journal of Microbiology, Immunology, and Infection*. https://doi.org/10.1016/j.jmii.2020.03.022

Nabel, G. J. (2013). Designing Tomorrow's Vaccines. *The New England Journal of Medicine*, *368*(6), 551–560. https://doi.org/10.1056/NEJMra1204186

Nachbagauer, R., & Krammer, F. (2017). Universal influenza virus vaccines and therapeutic antibodies. *Clinical Microbiology and Infection : The Official Publication of the European Society of Clinical Microbiology and Infectious Diseases*, *23*(4), 222–228. https://doi.org/10.1016/j.cmi.2017.02.009

Naskalska, A., & Pyrć, K. (2015). Virus Like Particles as Immunogens and Universal Nanocarriers. *Polish Journal of Microbiology*, *64*(1), 3–13.

Naqvi, A. A. T., Fatima, K., Mohammad, T., Fatima, U., Singh, I. K., Singh, A., Atif, S. M., Hariprasad, G., Hasan, G. M., & Hassan, Md. I. (2020). Insights into SARS-CoV-2 genome, structure, evolution, pathogenesis and therapies: Structural genomics approach. *Biochimica et Biophysica Acta. Molecular Basis of Disease*, *1866*(10), 165878. https://doi.org/10.1016/j.bbadis.2020.165878

Nelson, P. N., Westwood, Olwyn. M., Jefferis, R., Goodall, M., & Hay, F. C. (1997). Characterisation of anti-IgG monoclonal antibody A57H by epitope mapping. *Biochemical Society Transactions*, *25*(2), 373S-373S. https://doi.org/10.1042/bst025373s

Neuman, B. W., Kiss, G., Kunding, A. H., Bhella, D., Baksh, M. F., Connelly, S., Droese, B., Klaus, J. P., Makino, S., Sawicki, S. G., Siddell, S. G., Stamou, D. G., Wilson, I. A., Kuhn, P., & Buchmeier, M. J. (2011). A structural analysis of M protein in coronavirus assembly and morphology. *Journal of Structural Biology*, *174*(1), 11–22. https://doi.org/10.1016/j.jsb.2010.11.021

Nicola, M., Alsafi, Z., Sohrabi, C., Kerwan, A., Al-Jabir, A., Iosifidis, C., Agha, M., & Agha, R. (2020). The socio-economic implications of the coronavirus pandemic (COVID-19): A

review. *International Journal of Surgery (London, England)*, *78*, 185–193. https://doi.org/10.1016/j.ijsu.2020.04.018

Nieto-Torres, J. L., DeDiego, M. L., Álvarez, E., Jiménez-Guardeño, J. M., Regla-Nava, J. A., Llorente, M., Kremer, L., Shuo, S., & Enjuanes, L. (2011). Subcellular location and topology of severe acute respiratory syndrome coronavirus envelope protein. *Virology*, *415*(2), 69–82. https://doi.org/10.1016/j.virol.2011.03.029

Nooraei, S., Bahrulolum, H., Hoseini, Z. S., Katalani, C., Hajizade, A., Easton, A. J., & Ahmadian, G. (2021). Virus-like particles: Preparation, immunogenicity and their roles as nanovaccines and drug nanocarriers. *Journal of Nanobiotechnology*, *19*(1), 59. https://doi.org/10.1186/s12951-021-00806-7

Örd, M., Faustova, I., & Loog, M. (2020). The sequence at Spike S1/S2 site enables cleavage by furin and phospho-regulation in SARS-CoV2 but not in SARS-CoV1 or MERS-CoV. *Scientific Reports*, *10*(1), 16944. https://doi.org/10.1038/s41598-020-74101-0

Ou, X., Liu, Y., Lei, X., Li, P., Mi, D., Ren, L., Guo, L., Guo, R., Chen, T., Hu, J., Xiang, Z., Mu, Z., Chen, X., Chen, J., Hu, K., Jin, Q., Wang, J., & Qian, Z. (2020). Characterization of spike glycoprotein of SARS-CoV-2 on virus entry and its immune cross-reactivity with SARS-CoV. *Nature Communications*, *11*(1), 1620. https://doi.org/10.1038/s41467-020-15562-9

Ou, X., Zheng, W., Shan, Y., Mu, Z., Dominguez, S. R., Holmes, K. V., & Qian, Z. (2016). Identification of the Fusion Peptide-Containing Region in Betacoronavirus Spike Glycoproteins. *Journal of Virology*, *90*(12), 5586–5600. https://doi.org/10.1128/JVI.00015-16

Padron-Regalado, E. (2020). Vaccines for SARS-CoV-2: Lessons from Other Coronavirus Strains. *Infectious Diseases and Therapy*, 1–20. https://doi.org/10.1007/s40121-020-00300-x

Petersen, E., Koopmans, M., Go, U., Hamer, D. H., Petrosillo, N., Castelli, F., Storgaard, M., Khalili, S. A., & Simonsen, L. (2020). Comparing SARS-CoV-2 with SARS-CoV and influenza pandemics. *The Lancet Infectious Diseases*, *20*(9), e238–e244. https://doi.org/10.1016/S1473-3099(20)30484-9

Pica, N., & Palese, P. (2013). Toward a Universal Influenza Virus Vaccine: Prospects and Challenges. *Annual Review of Medicine*, *64*(1), 189–202. https://doi.org/10.1146/annurev-med-120611-145115

Plescia, C. B., David, E. A., Patra, D., Sengupta, R., Amiar, S., Su, Y., & Stahelin, R. V. (2021). SARS-CoV-2 viral budding and entry can be modeled using BSL-2 level virus-like particles. *The Journal of Biological Chemistry*, *296*, 100103. https://doi.org/10.1074/jbc.RA120.016148

Qian, C., Liu, X., Xu, Q., Wang, Z., Chen, J., Li, T., Zheng, Q., Yu, H., Gu, Y., Li, S., & Xia, N. (2020). Recent Progress on the Versatility of Virus-Like Particles. *Vaccines*, *8*(1). https://doi.org/10.3390/vaccines8010139

Raoult, D., Zumla, A., Locatelli, F., Ippolito, G., & Kroemer, G. (n.d.). Coronavirus infections: Epidemiological, clinical and immunological features and hypotheses. *Cell Stress*, *4*(4), 66–75. https://doi.org/10.15698/cst2020.04.216

Rauch, S., Jasny, E., Schmidt, K. E., & Petsch, B. (2018). New Vaccine Technologies to Combat Outbreak Situations. *Frontiers in Immunology*, *9*. https://doi.org/10.3389/fimmu.2018.01963

Reiter, K., Pereira Aguilar, P., Grammelhofer, D., Joseph, J., Steppert, P., & Jungbauer, A. (2020). Separation of influenza virus-like particles from baculovirus by polymer-grafted anion exchanger. *Journal of Separation Science*, *43*(12), 2270–2278. https://doi.org/10.1002/jssc.201901215

Rodriguez, V. A., Belaich, M. N., & Ghiringhelli, P. D. (2012). Baculoviruses: Members of Integrated Pest Management Strategies. *Integrated Pest Management and Pest Control - Current and Future Tactics*. https://doi.org/10.5772/32779

Roldão, A., Mellado, M. C. M., Castilho, L. R., Carrondo, M. J. T., & Alves, P. M. (2010). Virus-like particles in vaccine development. *Expert Review of Vaccines*, *9*(10), 1149–1176. https://doi.org/10.1586/erv.10.115

Rossi, G. A., Sacco, O., Mancino, E., Cristiani, L., & Midulla, F. (2020). Differences and similarities between SARS-CoV and SARS-CoV-2: Spike receptor-binding domain recognition and host cell infection with support of cellular serine proteases. *Infection*, *48*(5), 665–669. https://doi.org/10.1007/s15010-020-01486-5

Ryu, W.-S. (2017). Chapter 2—Virus Structure. In W.-S. Ryu (Ed.), *Molecular Virology of Human Pathogenic Viruses* (pp. 21–29). Academic Press. https://doi.org/10.1016/B978-0-12-800838-6.00002-3

Satarker, S., & Nampoothiri, M. (2020). Structural Proteins in Severe Acute Respiratory Syndrome Coronavirus-2. Archives of Medical Research, 51(6), 482–491. https://doi.org/10.1016/j.arcmed.2020.05.012

Sautto, G. A., Kirchenbaum, G. A., & Ross, T. M. (2018). Towards a universal influenza vaccine: Different approaches for one goal. *Virology Journal*, *15*(1), 17. https://doi.org/10.1186/s12985-017-0918-y

Shah, V. K., Firmal, P., Alam, A., Ganguly, D., & Chattopadhyay, S. (2020). Overview of Immune Response During SARS-CoV-2 Infection: Lessons From the Past. *Frontiers in Immunology*, *11*. https://doi.org/10.3389/fimmu.2020.01949

Shang, H., Garretson, T. A., Kumar, C. M. S., Dieter, R. F., & Cheng, X.-W. (2017). Improved pFastBac™ donor plasmid vectors for higher protein production using the Bac-to-Bac® baculovirus expression vector system. *Journal of Biotechnology*, *255*, 37–46. https://doi.org/10.1016/j.jbiotec.2017.06.397

Shang, J., Wan, Y., Luo, C., Ye, G., Geng, Q., Auerbach, A., & Li, F. (2020). Cell entry mechanisms of SARS-CoV-2. *Proceedings of the National Academy of Sciences*, *117*(21), 11727–11734. https://doi.org/10.1073/pnas.2003138117

Shen, C. F., Meghrous, J., & Kamen, A. (2002). Quantitation of baculovirus particles by flow cytometry. *Journal of Virological Methods*, *105*(2), 321–330. https://doi.org/10.1016/S0166-0934(02)00128-3

Smith, G. E., Fraser, M. J., & Summers, M. D. (1983). Molecular Engineering of the Autographa californica Nuclear Polyhedrosis Virus Genome: Deletion Mutations Within the

Polyhedrin Gene. *Journal of Virology*, *46*(2), 584–593. https://doi.org/10.1128/JVI.46.2.584-593.1983

Sokolenko, S., George, S., Wagner, A., Tuladhar, A., Andrich, J. M. S., & Aucoin, M. G. (2012). Co-expression vs. co-infection using baculovirus expression vectors in insect cell culture: Benefits and drawbacks. *Biotechnology Advances*, *30*(3), 766–781. https://doi.org/10.1016/j.biotechadv.2012.01.009

Srinivasan, S., Cui, H., Gao, Z., Liu, M., Lu, S., Mkandawire, W., Narykov, O., Sun, M., & Korkin, D. (2020). Structural Genomics of SARS-CoV-2 Indicates Evolutionary Conserved Functional Regions of Viral Proteins. *Viruses*, *12*(4). https://doi.org/10.3390/v12040360

Steppert, P., Burgstaller, D., Klausberger, M., Tover, A., Berger, E., & Jungbauer, A. (2017). Quantification and characterization of virus-like particles by size-exclusion chromatography and nanoparticle tracking analysis. *Journal of Chromatography A*, *1487*, 89–99. https://doi.org/10.1016/j.chroma.2016.12.085

Sun, W., Luo, T., Liu, W., & Li, J. (2020). Progress in the Development of Universal Influenza Vaccines. *Viruses*, *12*(9). https://doi.org/10.3390/v12091033

Sullivan, E., Sung, P.-Y., Wu, W., Berry, N., Kempster, S., Ferguson, D., Almond, N., Jones, I. M., & Roy, P. (2022). SARS-CoV-2 Virus-like Particles Produced by a Single Recombinant Baculovirus Generate Anti-S Antibody and Protect against Variant Challenge. *Viruses*, *14*(5), 914. https://doi.org/10.3390/v14050914

Swann, H., Sharma, A., Preece, B., Peterson, A., Eldridge, C., Belnap, D. M., Vershinin, M., & Saffarian, S. (2020). Minimal system for assembly of SARS-CoV-2 virus like particles. *Scientific Reports*, *10*(1), 21877. https://doi.org/10.1038/s41598-020-78656-w

Tang, J. W., Toovey, O. T. R., Harvey, K. N., & Hui, D. D. S. (2021). Introduction of the South African SARS-CoV-2 variant 501Y.V2 into the UK. *The Journal of Infection*. https://doi.org/10.1016/j.jinf.2021.01.007

Tau, G., & Rothman, P. (1999). Biologic functions of the IFN-γ receptors. *Allergy*, *54*(12), 1233–1251. https://doi.org/10.1034/j.1398-9995.1999.00099.x

Thompson, C. M., Petiot, E., Mullick, A., Aucoin, M. G., Henry, O., & Kamen, A. A. (2015). Critical assessment of influenza VLP production in Sf9 and HEK293 expression systems. *BMC Biotechnology*, *15*(1), 31. https://doi.org/10.1186/s12896-015-0152-x

Thompson, C. M., Aucoin, M. G., & Kamen, A. A. (2016). Production of Virus-Like Particles for Vaccination. *Methods in Molecular Biology (Clifton, N.J.)*, *1350*, 299–315. https://doi.org/10.1007/978-1-4939-3043-2_14

To, K. K. W., Hung, I. F. N., Chan, J. F. W., & Yuen, K.-Y. (2013). From SARS coronavirus to novel animal and human coronaviruses. *Journal of Thoracic Disease*, *5*(Suppl 2), S103–S108. https://doi.org/10.3978/j.issn.2072-1439.2013.06.02

Umakanthan, S., Sahu, P., Ranade, A. V., Bukelo, M. M., Rao, J. S., Abrahao-Machado, L. F., Dahal, S., Kumar, H., & Kv, D. (2020). Origin, transmission, diagnosis, and management of coronavirus disease 2019 (COVID-19). *Postgraduate Medical Journal*, *96*(1142), 753–758. https://doi.org/10.1136/postgradmedj-2020-138234

Valencia, I., Peiró, C., Lorenzo, Ó., Sánchez-Ferrer, C. F., Eckel, J., & Romacho, T. (2020). DPP4 and ACE2 in Diabetes and COVID-19: Therapeutic Targets for Cardiovascular Complications? *Frontiers in Pharmacology*, *11*. https://doi.org/10.3389/fphar.2020.01161

Van Oers, M. M. (2011). Opportunities and challenges for the baculovirus expression system. *Journal of Invertebrate Pathology*, *107*, S3–S15. https://doi.org/10.1016/j.jip.2011.05.001

Vaughn, J. L., Goodwin, R. H., Tompkins, G. J., & McCawley, P. (1977). The establishment of two cell lines from the insect Spodoptera frugiperda (Lepidoptera; Noctuidae). *In Vitro*, *13*(4), 213–217. https://doi.org/10.1007/BF02615077

Venkatagopalan, P., Daskalova, S. M., Lopez, L. A., Dolezal, K. A., & Hogue, B. G. (2015). Coronavirus envelope (E) protein remains at the site of assembly. Virology, 478, 75–85. https://doi.org/10.1016/j.virol.2015.02.005

Vieira, H. L. A., Estêvão, C., Roldão, A., Peixoto, C. C., Sousa, M. F. Q., Cruz, P. E., Carrondo, M. J. T., & Alves, P. M. (2005). Triple layered rotavirus VLP production: Kinetics of vector replication, mRNA stability and recombinant protein production. *Journal of Biotechnology*, *120*(1), 72–82. https://doi.org/10.1016/j.jbiotec.2005.03.026

Vogel, O. A., & Manicassamy, B. (2020). Broadly Protective Strategies Against Influenza Viruses: Universal Vaccines and Therapeutics. *Frontiers in Microbiology*, *11*. https://doi.org/10.3389/fmicb.2020.00135

Walls, A. C., Park, Y.-J., Tortorici, M. A., Wall, A., McGuire, A. T., & Veesler, D. (2020). Structure, Function, and Antigenicity of the SARS-CoV-2 Spike Glycoprotein. *Cell*, *181*(2), 281-292.e6. https://doi.org/10.1016/j.cell.2020.02.058

Wan, Y., Shang, J., Graham, R., Baric, R. S., & Li, F. (2020). Receptor Recognition by the Novel Coronavirus from Wuhan: An Analysis Based on Decade-Long Structural Studies of SARS Coronavirus. *Journal of Virology*, *94*(7). https://doi.org/10.1128/JVI.00127-20

Wang, C., Zheng, X., Gai, W., Zhao, Y., Wang, H., Wang, H., Feng, N., Chi, H., Qiu, B., Li, N., Wang, T., Gao, Y., Yang, S., & Xia, X. (2016). MERS-CoV virus-like particles produced in insect cells induce specific humoural and cellular imminity in rhesus macaques. *Oncotarget*, *8*(8), 12686–12694. https://doi.org/10.18632/oncotarget.8475

Wang, M.-Y., Zhao, R., Gao, L.-J., Gao, X.-F., Wang, D.-P., & Cao, J.-M. (2020a). SARS-CoV-2: Structure, Biology, and Structure-Based Therapeutics Development. *Frontiers in Cellular and Infection Microbiology*, *10*. https://doi.org/10.3389/fcimb.2020.587269

Wang, N., Shang, J., Jiang, S., & Du, L. (2020b). Subunit Vaccines Against Emerging Pathogenic Human Coronaviruses. *Frontiers in Microbiology*, *11*. https://doi.org/10.3389/fmicb.2020.00298

Wang, Y., Wang, F., Wang, R., Zhao, P., & Xia, Q. (2015). 2A self-cleaving peptide-based multi-gene expression system in the silkworm Bombyx mori. *Scientific Reports*, *5*. https://doi.org/10.1038/srep16273

World Health Organization. (2020). *Draft landscape and tracker of COVID-19 candidate vaccines*. Retrieved March 27, 2021, from https://www.who.int/publications/m/item/draft-landscape-of-covid-19-candidate-vaccines

World Health Organization. (2021a). *Archived: WHO Timeline - COVID-19*. Retrieved January 10, 2021, from https://www.who.int/news/item/27-04-2020-who-timeline---covid-19

World Health Organization. (2021b). *WHO Coronavirus Disease (COVID-19) Dashboard*. Retrieved January 20, 2021, from https://covid19.who.int

Wong, K. T., Peter, C. H., Greenfield, P. F., Reid, S., & Nielsen, L. K. (1996). Low multiplicity infection of insect cells with a recombinant baculovirus: The cell yield concept. *Biotechnology and Bioengineering*, *49*(6), 659–666. https://doi.org/10.1002/(SICI)1097-0290(19960320)49:6<659::AID-BIT7>3.0.CO;2-N

Wu, C.-Y., Yeh, Y.-C., Yang, Y.-C., Chou, C., Liu, M.-T., Wu, H.-S., Chan, J.-T., & Hsiao, P.-W. (2010). Mammalian Expression of Virus-Like Particles for Advanced Mimicry of Authentic Influenza Virus. *PLoS ONE*, *5*(3), e9784. https://doi.org/10.1371/journal.pone.0009784

Wu, C.-Y., Huang, C.-W., Nai, Y.-S., Chu, P.-Y., Wang, C.-H., & Ding, S.-T. (2019). A Newly Designed EGFP-2A Peptide Monocistronic Baculoviral Vector for Concatenating the Expression of Recombinant Proteins in Insect Cells. *Processes*, *7*(5), 291. https://doi.org/10.3390/pr7050291

Wu, P., Hao, X., Lau, E. H. Y., Wong, J. Y., Leung, K. S. M., Wu, J. T., Cowling, B. J., & Leung, G. M. (2020). Real-time tentative assessment of the epidemiological characteristics of novel coronavirus infections in Wuhan, China, as of 22 January 2020. *Eurosurveillance*, *25*(3). https://doi.org/10.2807/1560-7917.ES.2020.25.3.2000044

Wu, Y., & Zhao, S. (2021). Furin cleavage sites naturally occur in coronaviruses. *Stem Cell Research*, *50*, 102115. https://doi.org/10.1016/j.scr.2020.102115

Wu, Z., & McGoogan, J. M. (2020). Characteristics of and Important Lessons from the Coronavirus Disease 2019 (COVID-19) Outbreak in China: Summary of a Report of 72 314 Cases from the Chinese Center for Disease Control and Prevention. *JAMA*, *323*(13), 1239. https://doi.org/10.1001/jama.2020.2648

Xu, R., Shi, M., Li, J., Song, P., & Li, N. (2020). Construction of SARS-CoV-2 Virus-Like Particles by Mammalian Expression System. *Frontiers in Bioengineering and Biotechnology*, *8*. https://doi.org/10.3389/fbioe.2020.00862

Yan, R., Zhang, Y., Li, Y., Xia, L., Guo, Y., & Zhou, Q. (2020). Structural basis for the recognition of SARS-CoV-2 by full-length human ACE2. *Science*, *367*(6485), 1444–1448. https://doi.org/10.1126/science.abb2762

Yuan, Y., Cao, D., Zhang, Y., Ma, J., Qi, J., Wang, Q., Lu, G., Wu, Y., Yan, J., Shi, Y., Zhang, X., & Gao, G. F. (2017). Cryo-EM structures of MERS-CoV and SARS-CoV spike glycoproteins reveal the dynamic receptor binding domains. *Nature Communications*, *8*, 15092. https://doi.org/10.1038/ncomms15092

Zhang, A., Jin, H., Zhang, F., Ma, Z., Tu, Y., Ren, Z., Zhang, X., Zhu, K., & Wang, B. (2005). Effects of Multiple Copies of CpG on DNA Vaccination. *DNA and Cell Biology*, *24*(5), 292–298. https://doi.org/10.1089/dna.2005.24.292

Zhang, C., Maruggi, G., Shan, H., & Li, J. (2019). Advances in mRNA Vaccines for Infectious Diseases. *Frontiers in Immunology*, *10*. https://doi.org/10.3389/fimmu.2019.00594

Zhu, Z., Lian, X., Su, X., Wu, W., Marraro, G. A., & Zeng, Y. (2020). From SARS and MERS to COVID-19: A brief summary and comparison of severe acute respiratory infections

caused by three highly pathogenic human coronaviruses. *Respiratory Research*, *21*(1), 224. https://doi.org/10.1186/s12931-020-01479-w

Zhu, X., Ricci-Tam, C., & Sgro, A. E. (2022). *Self-cleaving 2A peptides allow for expression of multiple genes in Dictyostelium discoideum* (p. 2022.03.08.482734). bioRxiv. https://doi.org/10.1101/2022.03.08.482734

Appendices

Appendix A: *Sf9* Cell Infection Preliminary Data

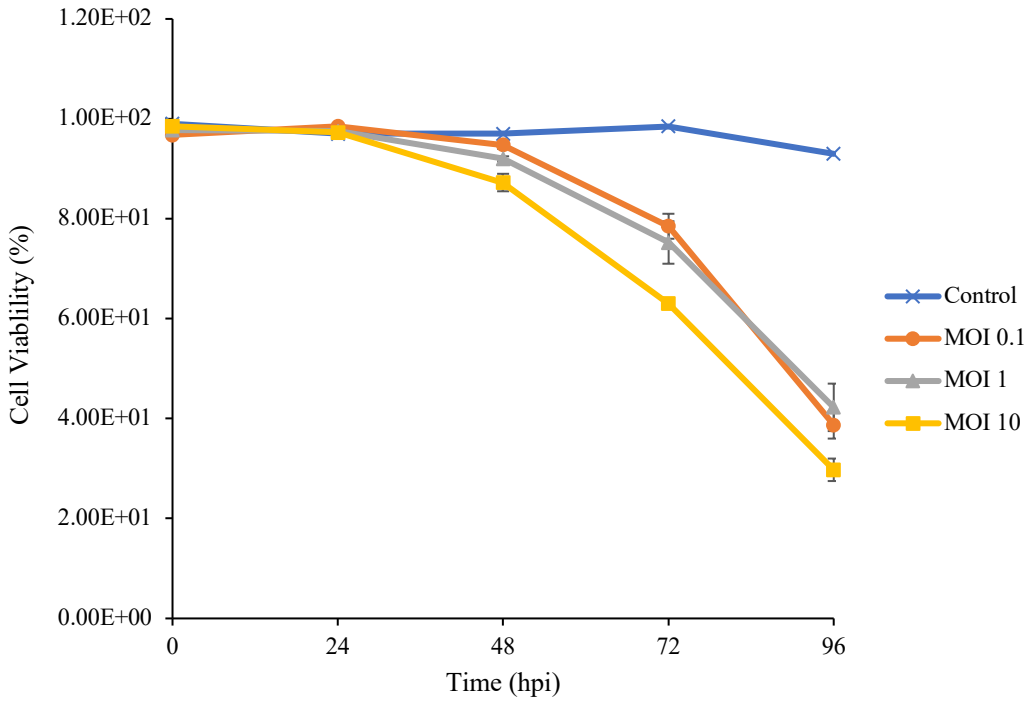

Figure AA-1: *Sf9* cell viability at 24, 48, and 72 hpi. *Sf9* cells were infected with mKOk baculoviruses at MOI 0.1, 1, and 10. Error bars represent the range of duplicate flasks.

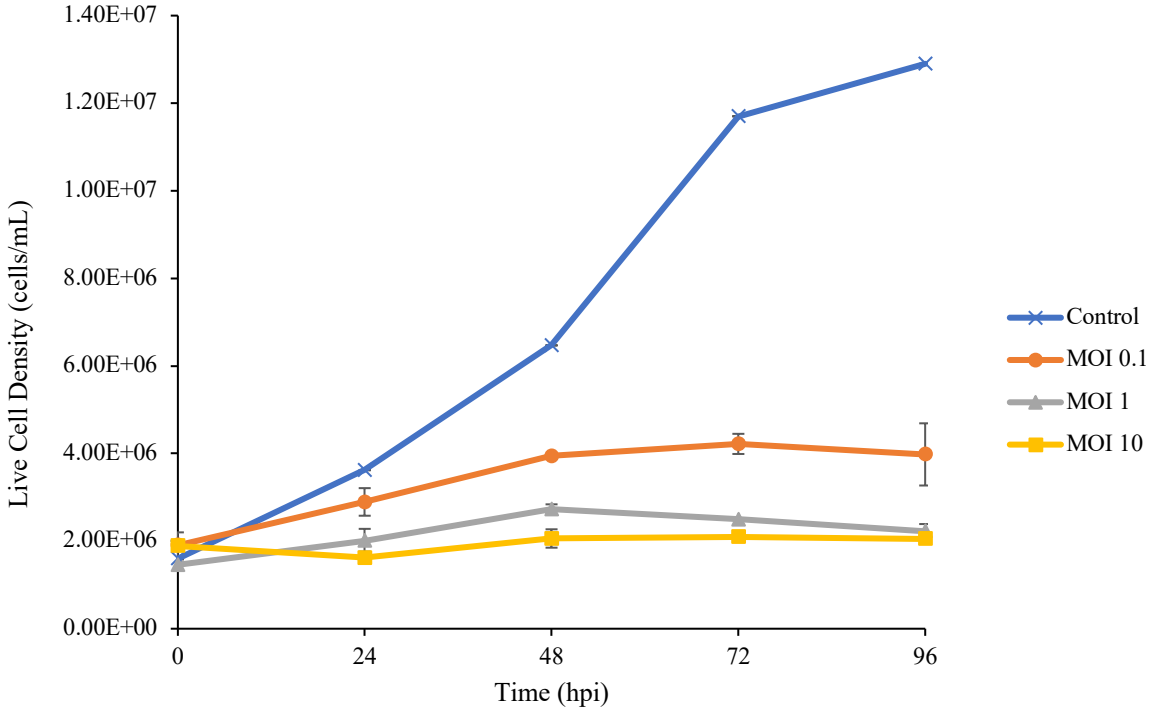

Figure AA-2: *Sf9* cell density at 24, 48, and 72 hpi. *Sf9* cells were infected with mKOk baculoviruses at MOI 0.1, 1, and 10. Error bars represent the range of duplicate flasks.

Appendix B: VLP Constructs

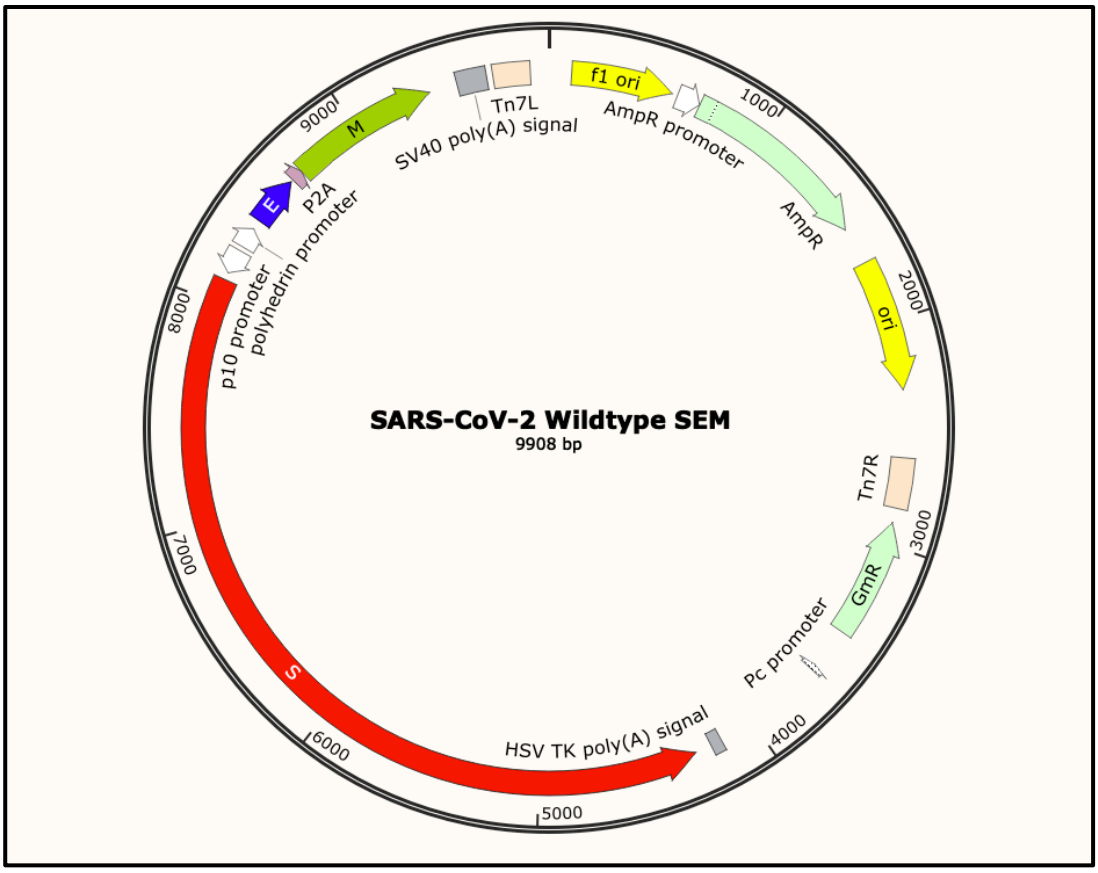

Figure AB-1: pFastBac Dual plasmid containing SARS-CoV-2 S, E and M protein sequences. S protein sequence located downstream of p10 promoter. E and M protein sequences located downstream of polyhedrin promoter and separated by a P2A self-cleaving peptide. Ordered from GenScript (USA).

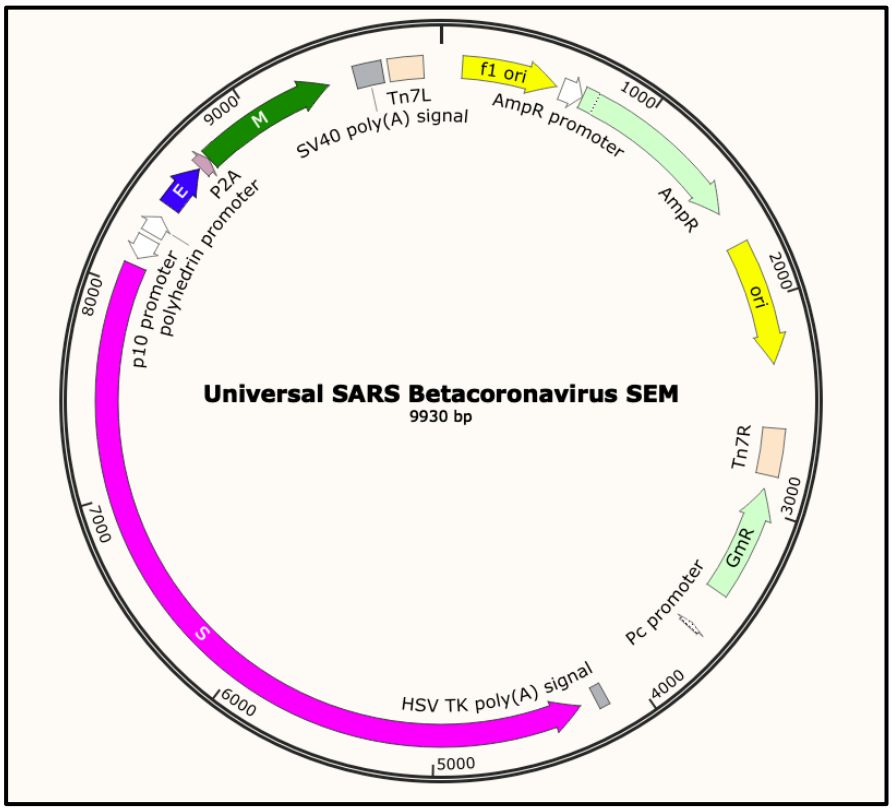

Figure AB-2: pFastBac Dual plasmid containing consensus sequences for S, E and M proteins based on SARS-CoV, MERS-CoV and SARS-CoV-2. Universal S protein sequence located downstream of p10 promoter. Universal E and M protein sequences located downstream of polyhedrin promoter and separated by a P2A self-cleaving peptide. Ordered from GenScript (USA).

Appendix C: Recombinant Bacmid Production

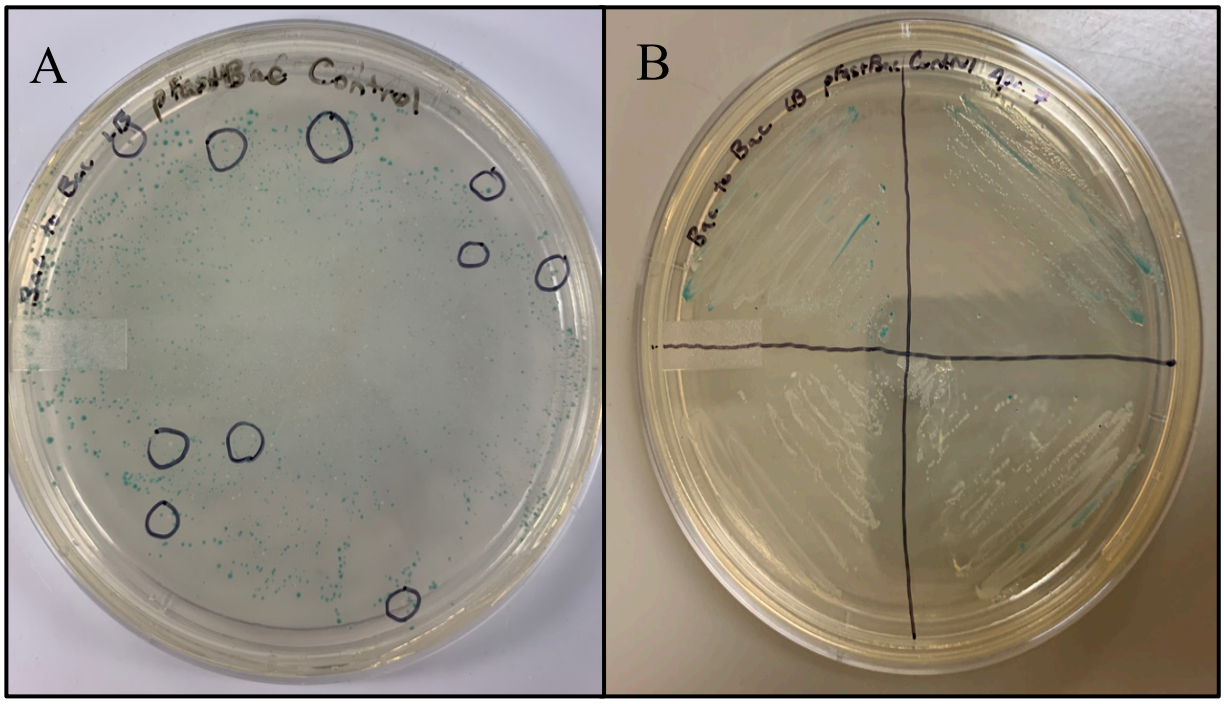

Figure AC-1: Plates containing transformed DH10Bac *E.coli* cells with SARS-CoV-2 wildtype SEM plasmid. (A) Plate used for blue-white screening. (B) Plate after restreaking white colonies. White colonies are isolated in the bottom left quadrant.

A B

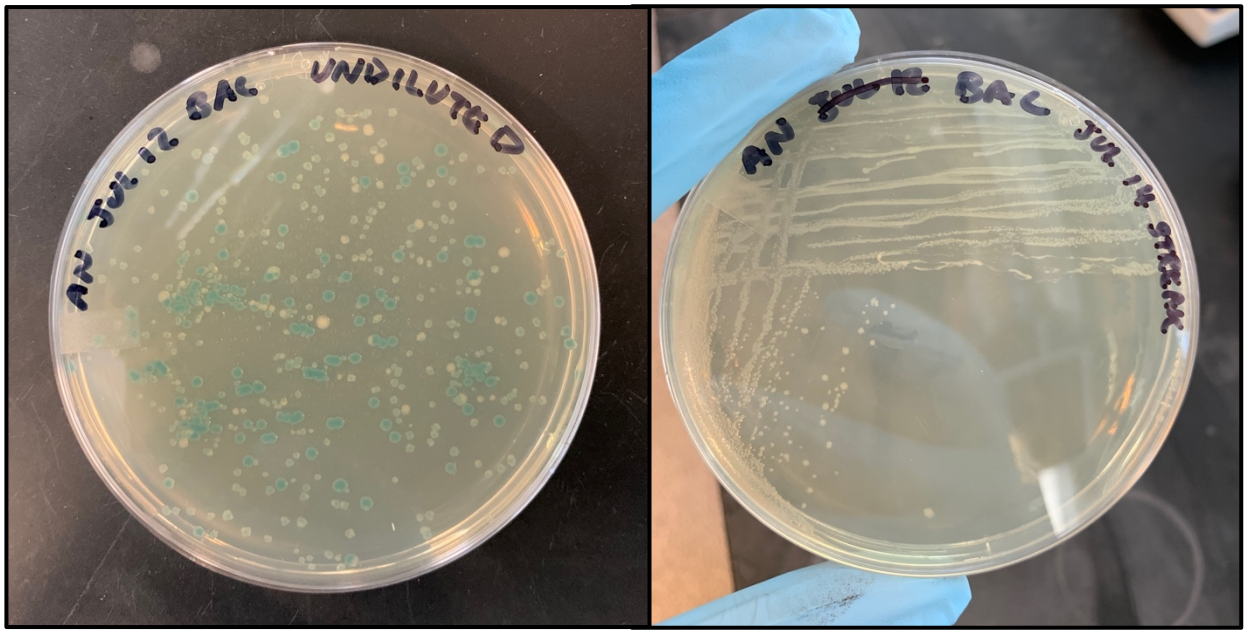

Figure AC-2: Plates containing transformed DH10Bac *E. coli* cells with universal SARS betacoronavirus SEM plasmid. (A) Plate used for blue-white screening. (B) Plate containing isolated white colonies.

Appendix D: VLP Production

Equation AD-1. Volume of virus required for infection calculation

$$Volume\ of\ virus\ (mL) = \frac{MOI\ (\frac{pfu}{mL}) * number\ of\ cells}{Virus\ Titer\ (\frac{pfu}{mL})}$$